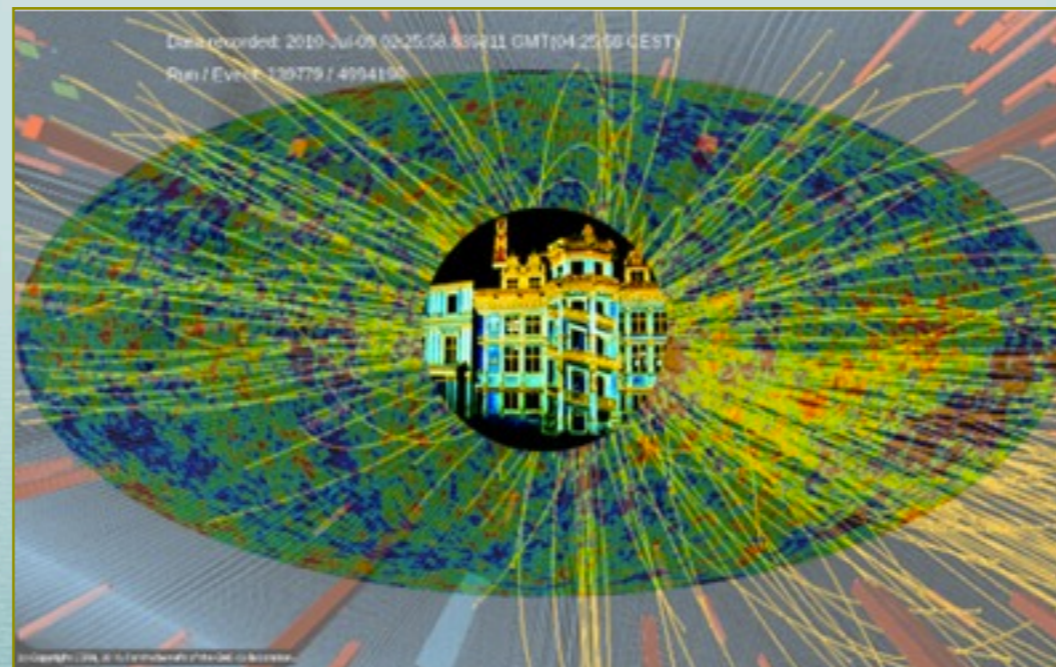


OBSERVATION OF COSMIC RAY ANISOTROPY ABOVE TEV ENERGIES IN ICECUBE

Simona Toscano *on behalf of the* **IceCube collaboration**

23rd Rencontres de Blois

*Particle Physics and
Cosmology*



*Château Royal de Blois
May 29 - June 3 2011*





Outline


- * The **IceCube** detector
- * Energy dependence of the **large scale anisotropy** (*paper in preparation*):
 - ▶ preliminary results at 20 and 400 TeV.
- * **Medium and small scale** structures (submitted to ApJ, **arXiv:1105.2326**):
 - ▶ analysis
 - ▶ results
- * Conclusions


Bartol Research Inst, Univ of Delaware, USA
 University of Alaska Anchorage, USA
 Pennsylvania State University, USA
University of Wisconsin-Madison, USA
 University of Wisconsin-River Falls, USA
 LBNL, Berkeley, USA
 UC Berkeley, USA
 UC Irvine, USA

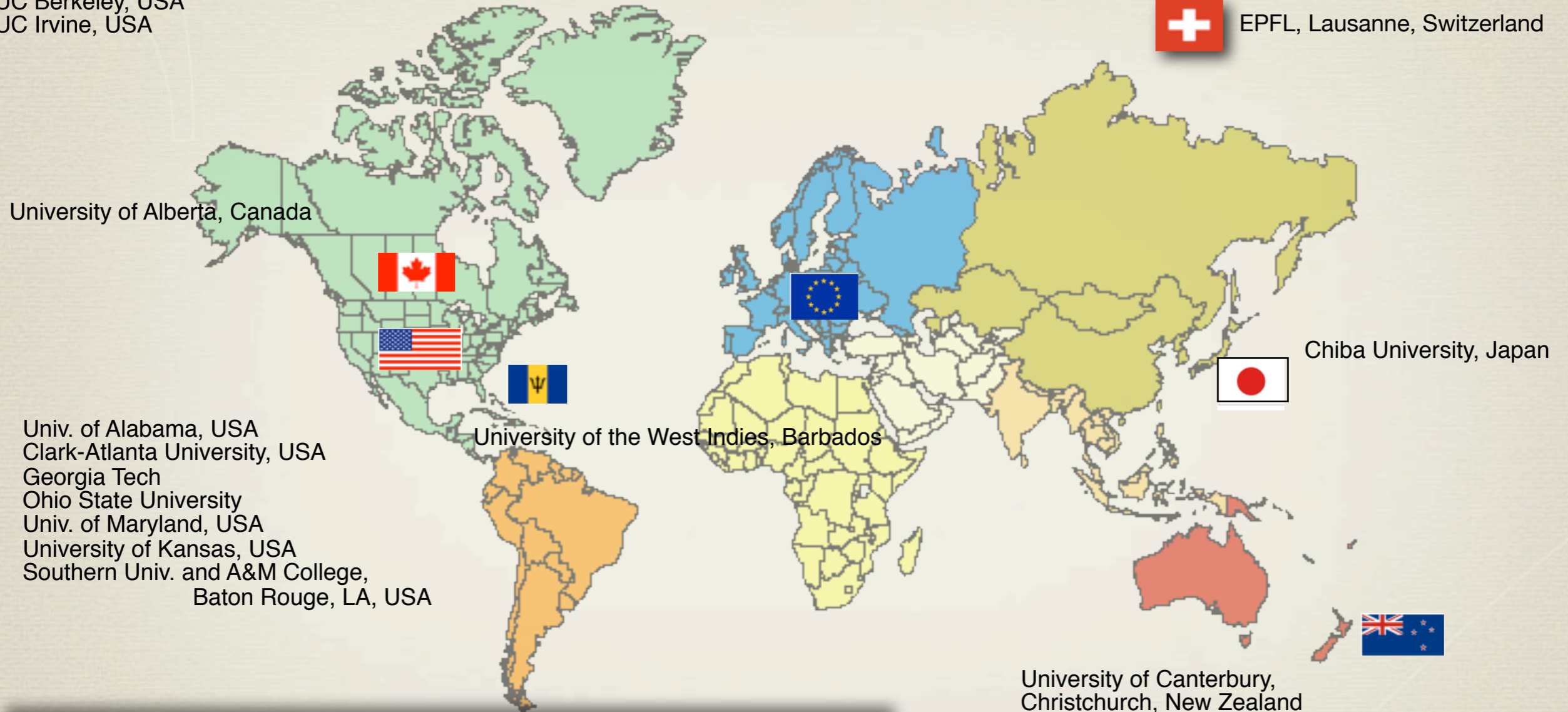
 Universität Mainz, Germany
 DESY Zeuthen, Germany
 Universität Wuppertal, Germany
 Universität Dortmund, Germany
 Humboldt Universität, Germany
 TWTH Aachen, Germany
 Universität Bonn, Germany
 Ruhr-Universität, Bochum, Germany
 MPI, Heidelberg, Germany

 Uppsala Universitet, Sweden
 Stockholm Universitet, Sweden

 Imperial College, London, UK
 University of Oxford, UK

 Université Libre de Bruxelles, Belgium
 Vrije Universiteit Brussel, Belgium
 Université de Mons, Belgium
 Universiteit Gent, Belgium

 EPFL, Lausanne, Switzerland



IceCube Collaboration

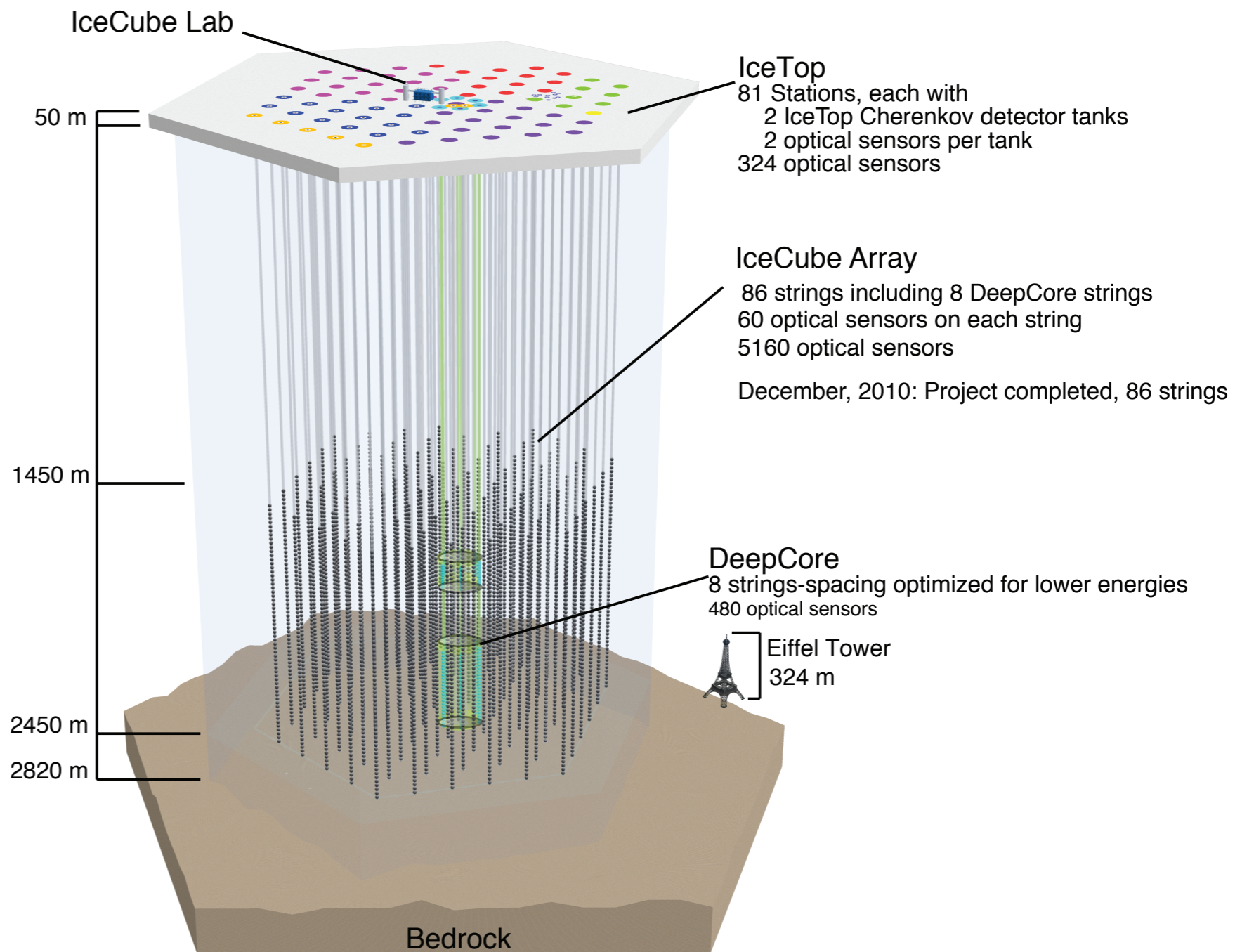
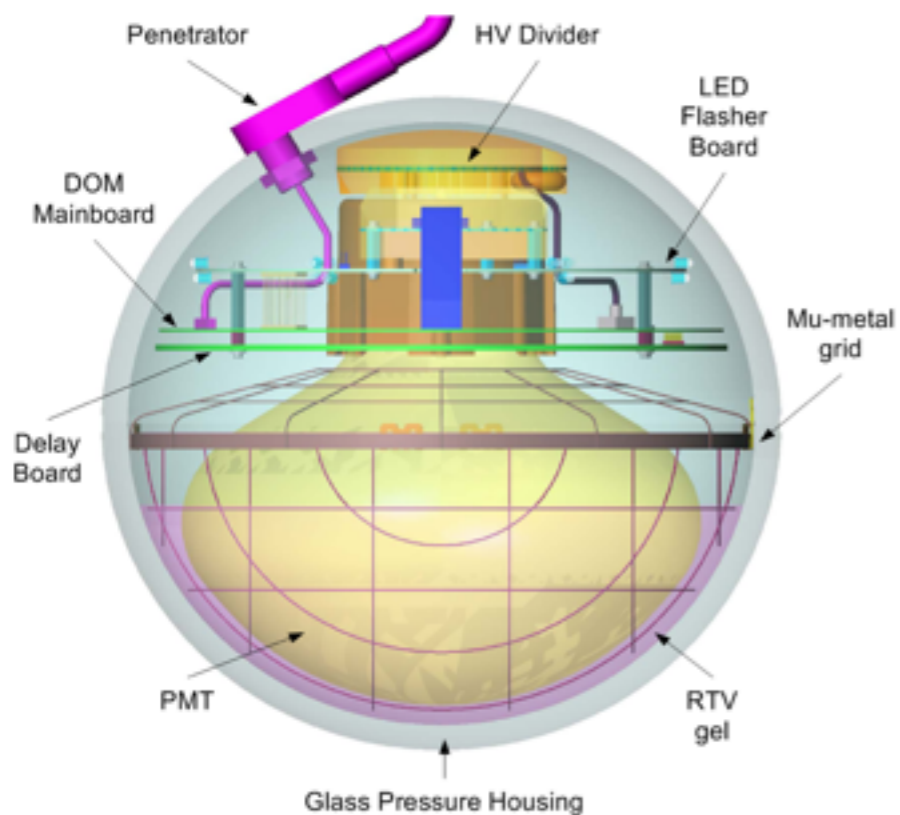
10 countries
36 institutions
~260 collaborators

The IceCube detector

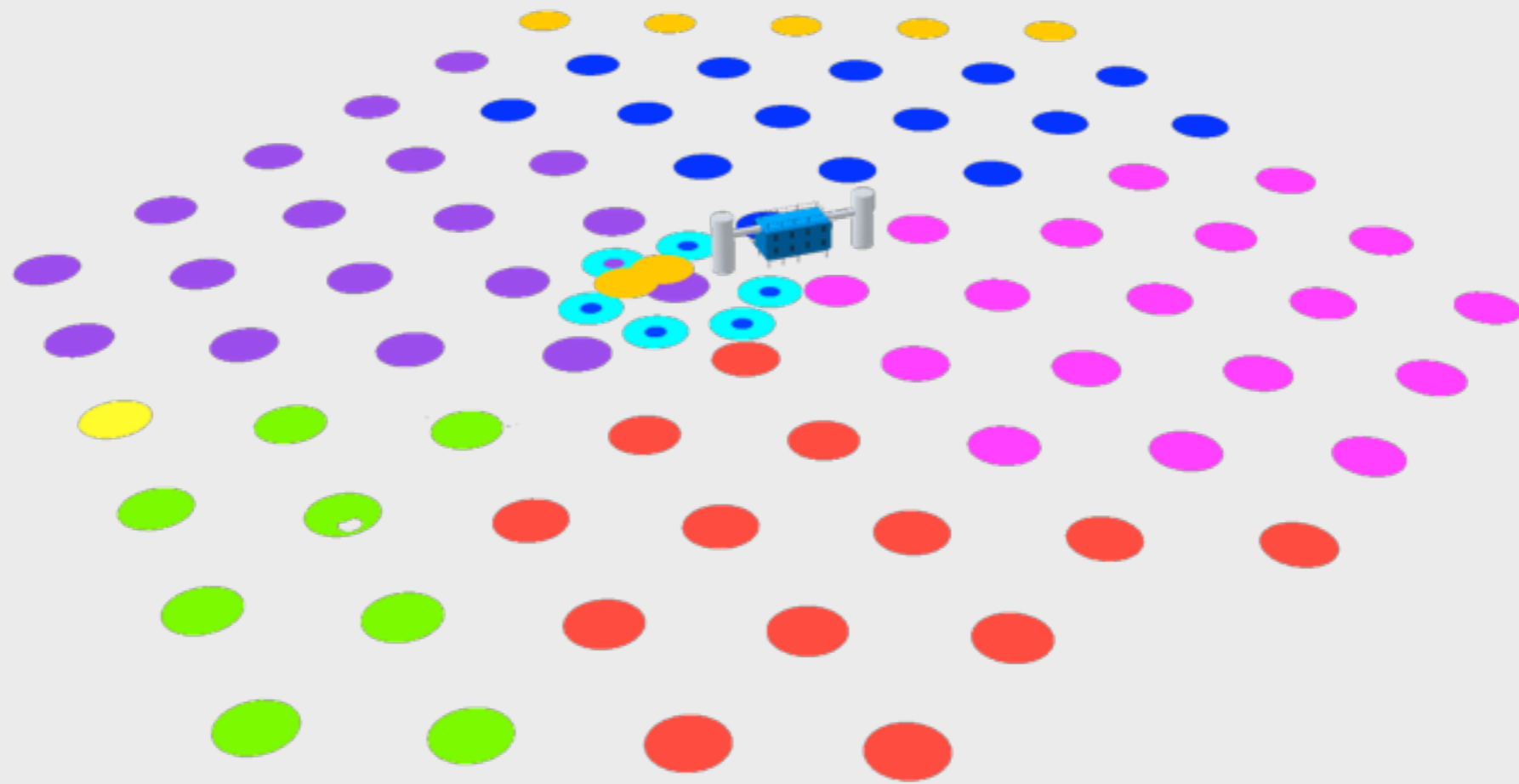
IceCube is a km³-scale neutrino detector “frozen” into the South Pole ice.

- **86 strings**
- **5160 DOMs**
- **17 m vertical spacing**
- **125 m between strings**

Digital Optical Module

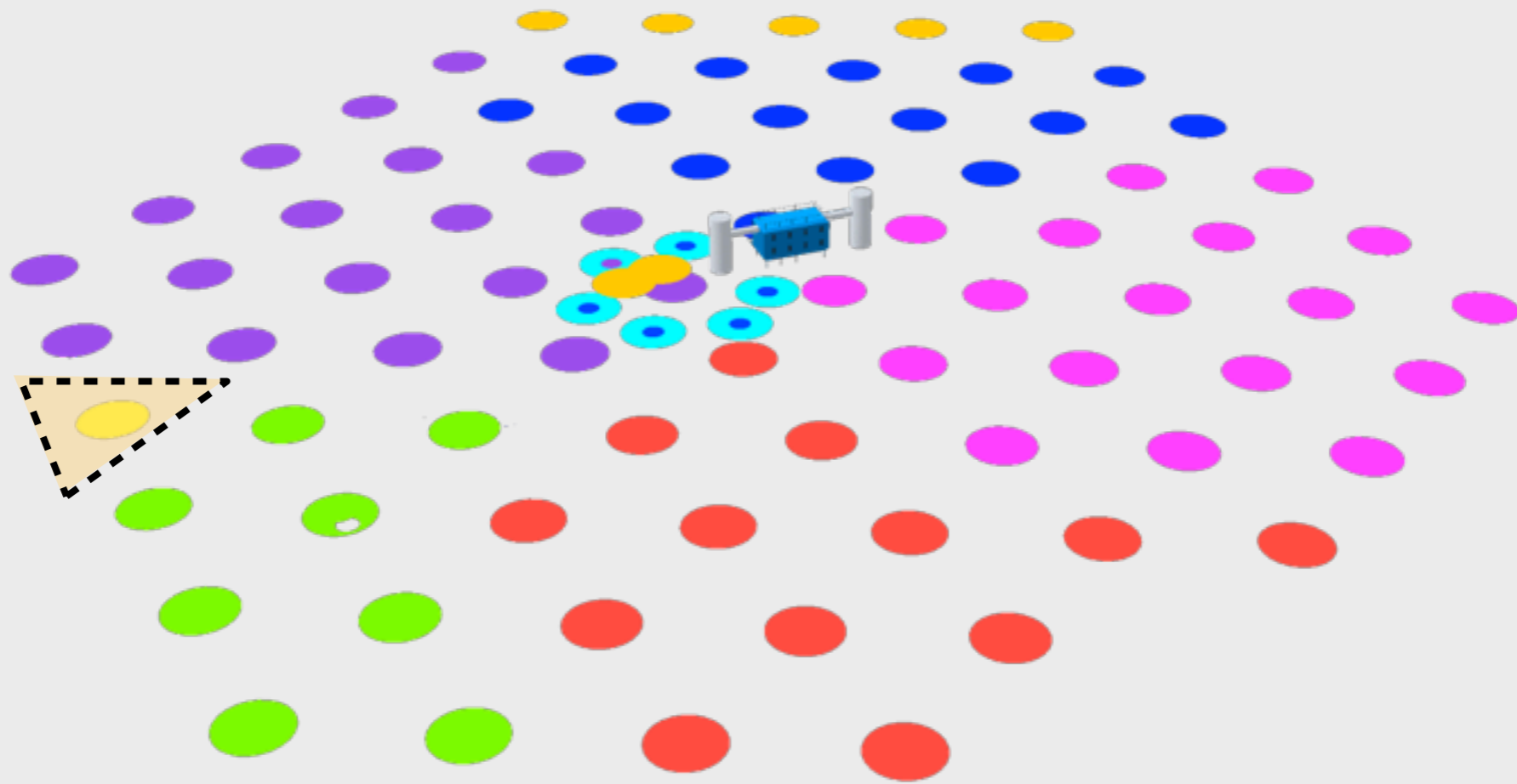


IceCube configurations

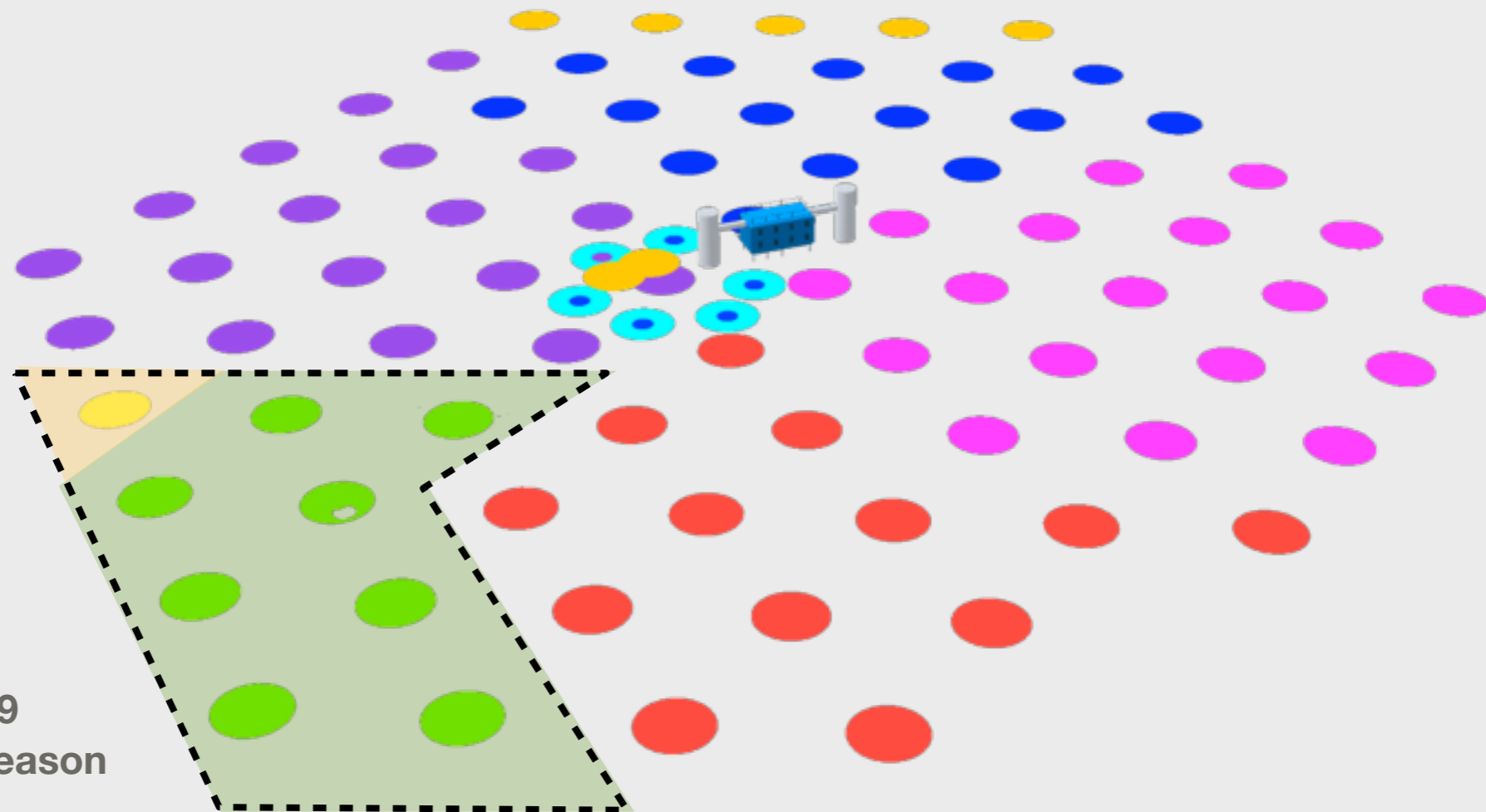


IceCube configurations

IC-1
05-06 Season

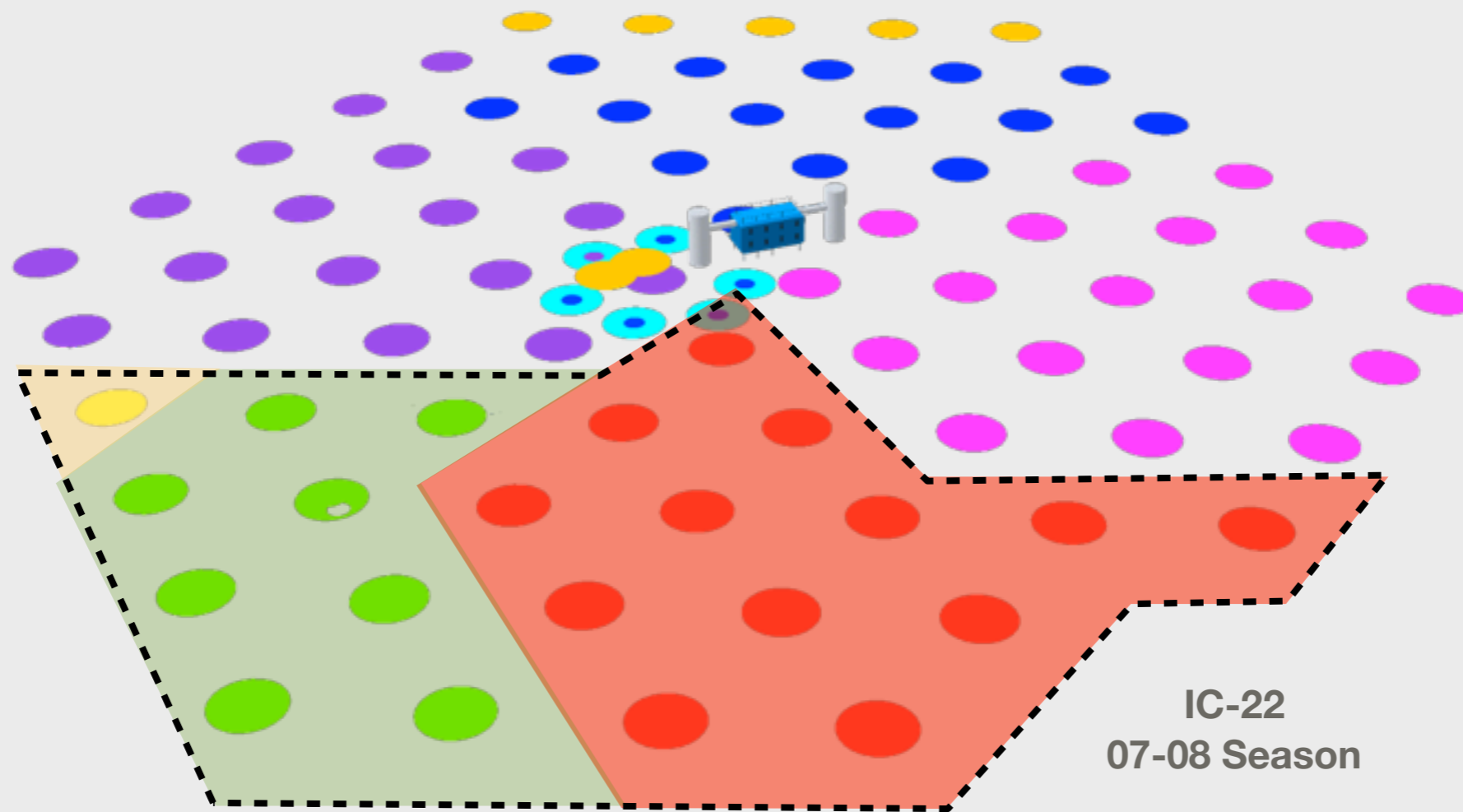


IceCube configurations

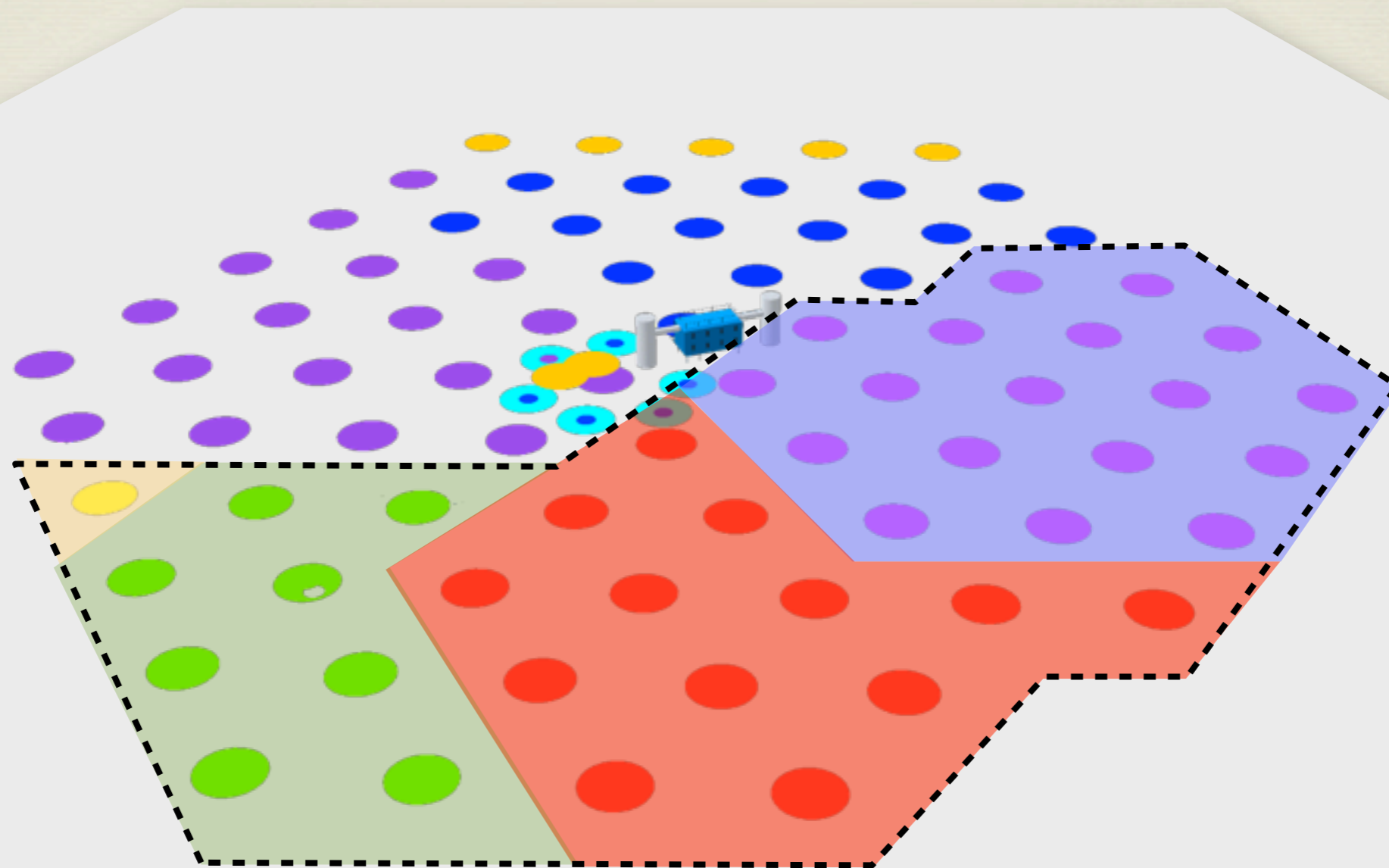


IC-9
06-07 Season

IceCube configurations



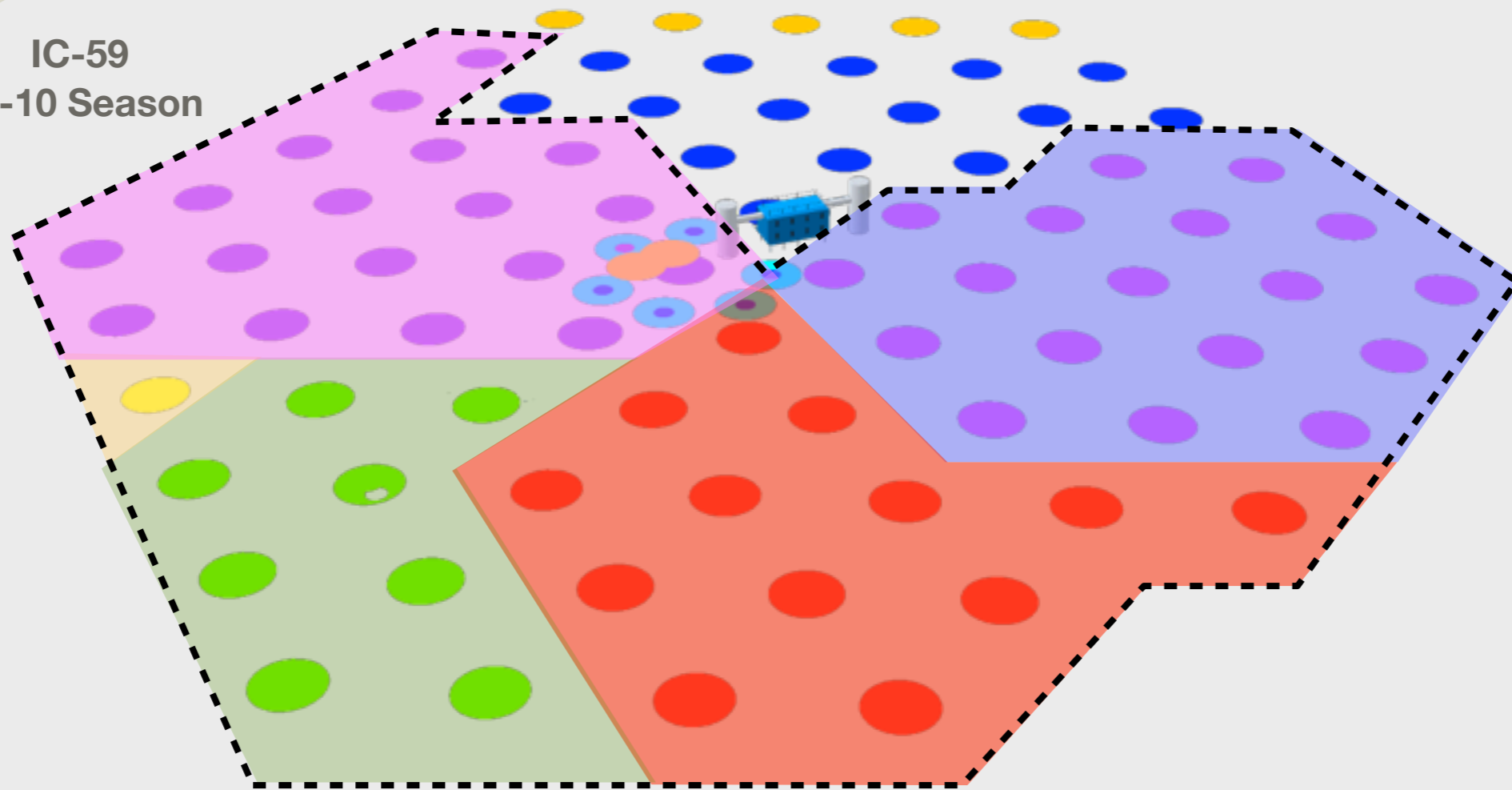
IceCube configurations



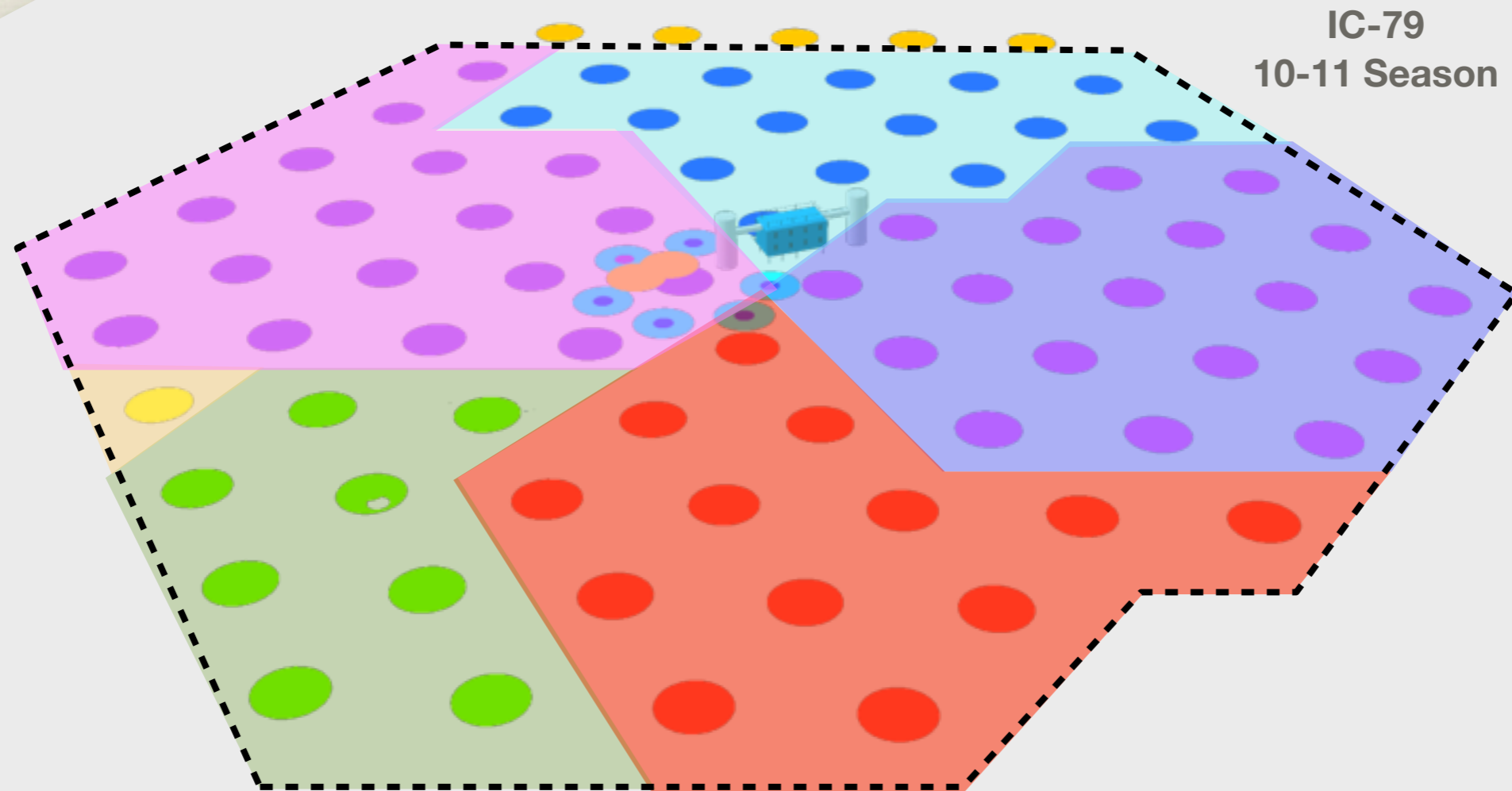
IC-40
08-09 Season

IceCube configurations

IC-59
09-10 Season

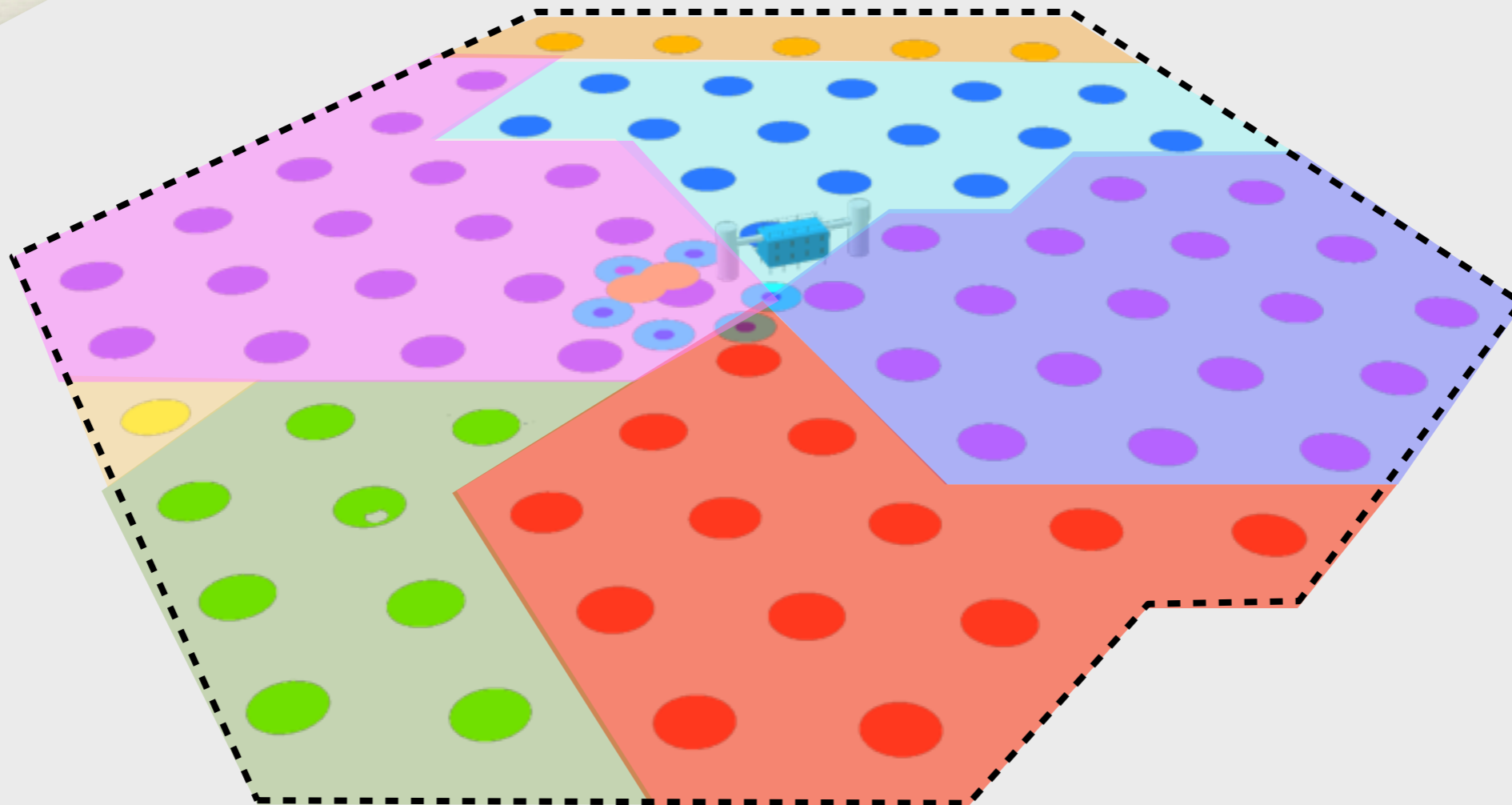


IceCube configurations



IceCube configurations

IC-86 2011...

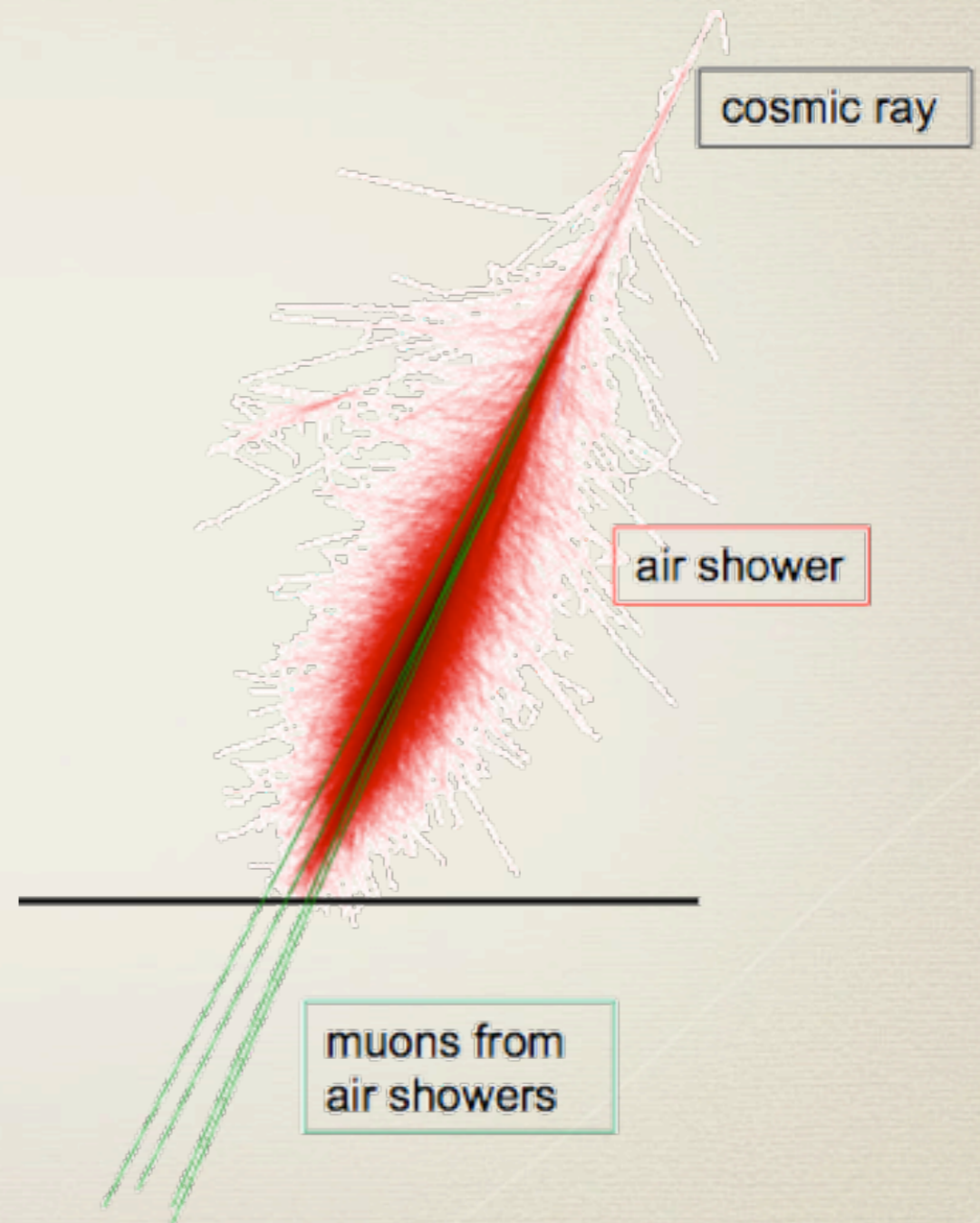


Construction finished on December 2010

Cosmic rays in IceCube

IceCube tries to identify cosmic ray sources by their neutrino signal, but it also allows for a study of the *cosmic ray flux* itself, as the detector is sensitive to *downward going muons* produced in cosmic ray air showers in the southern hemisphere.

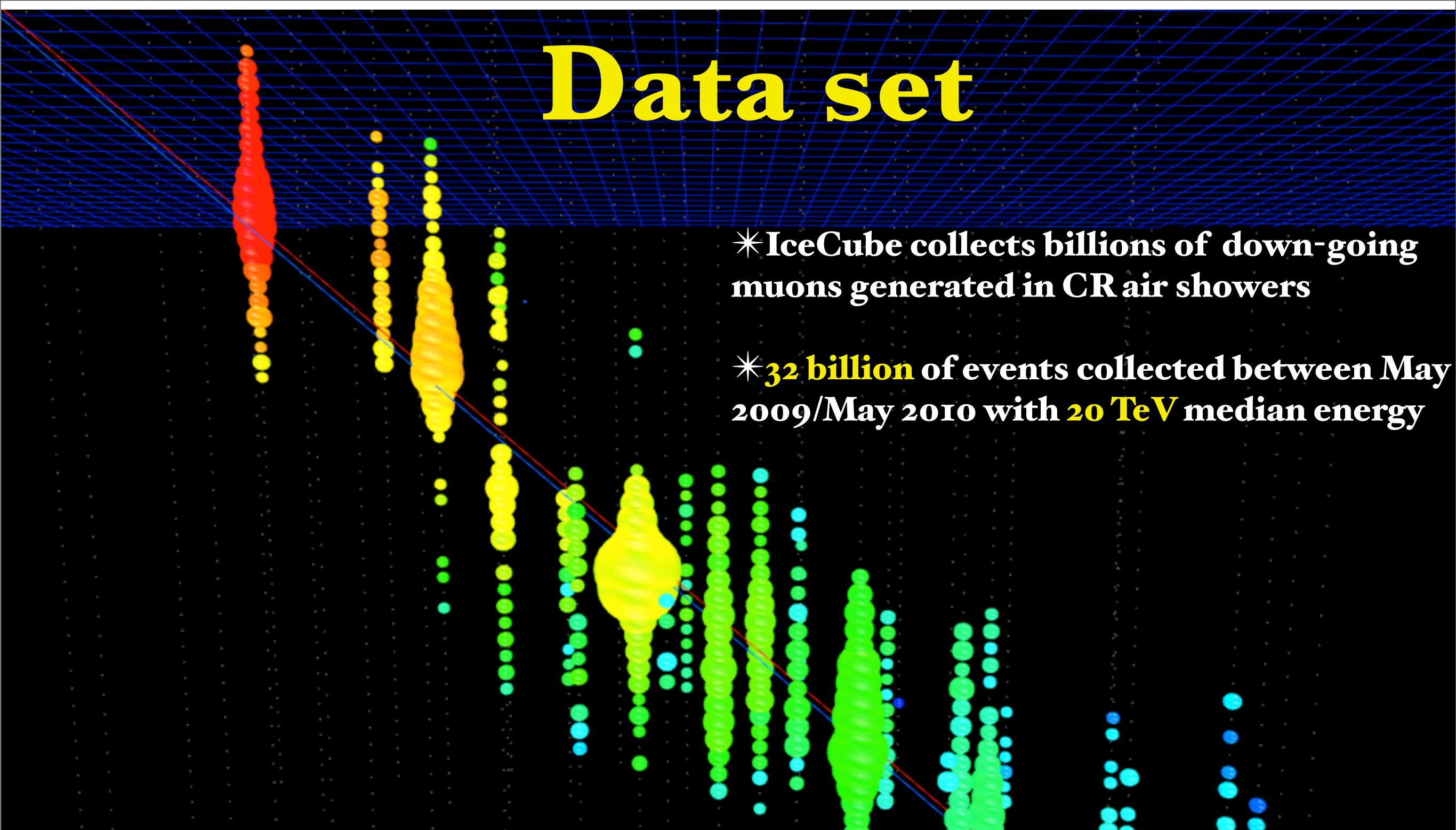
By detecting downgoing muons, IceCube can study the *arrival direction distribution of cosmic rays* in the energy range ~ 10 TeV to several 100 TeV and produce a cosmic ray sky map of the southern sky.



Data set

* IceCube collects billions of down-going muons generated in CR air showers

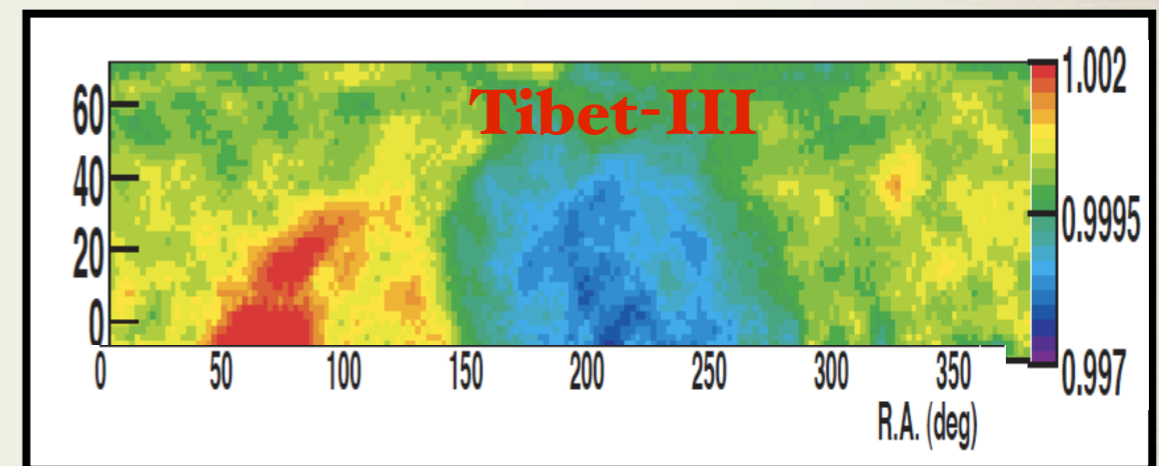
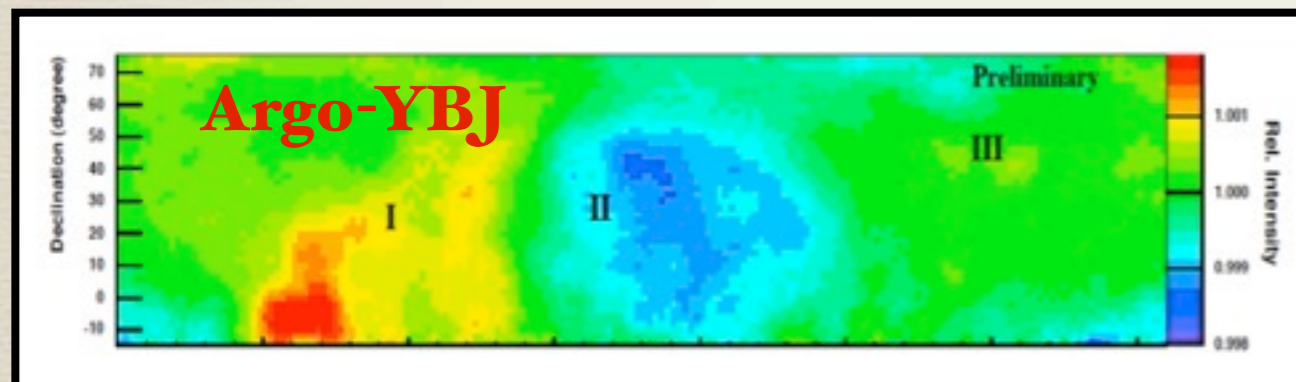
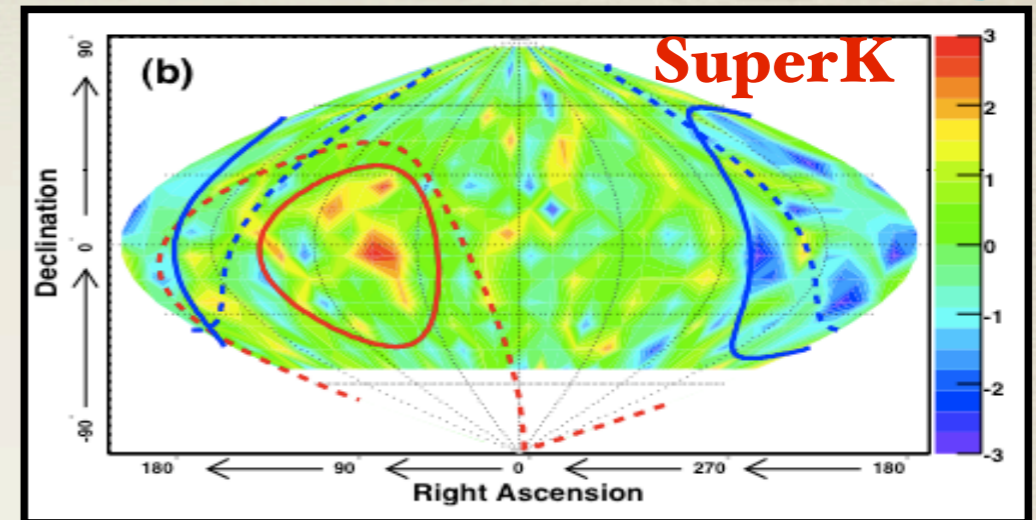
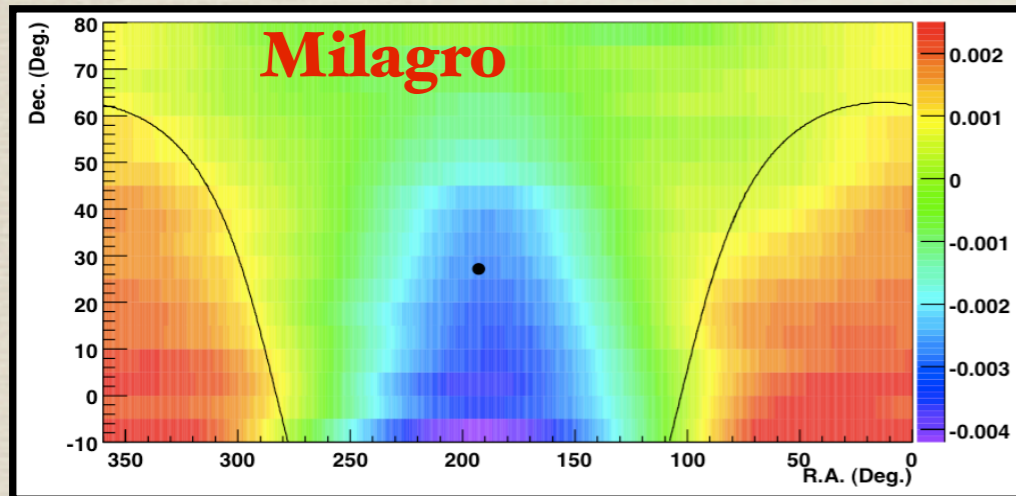
* **32 billion** of events collected between May 2009/May 2010 with **20 TeV** median energy



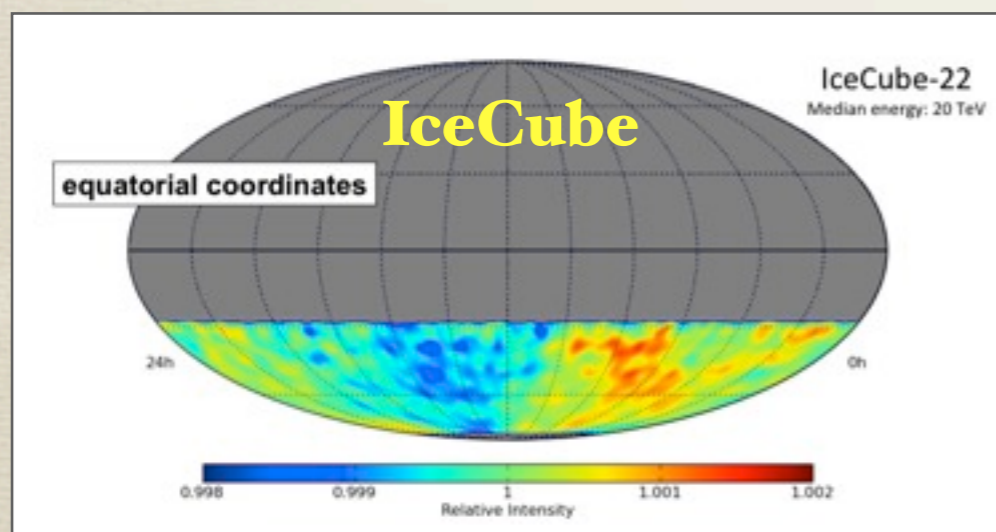
IceCube-59	Level 1 "Muon Filter"	DST
Live Time	96%	96%
Trigger rate	22 Hz	1.4 kHz
N_{events}	8.0×10^8	3.2×10^{10}
Angular resolution	$< 1^\circ$	3°
Energy resolution	$\Delta \log_{10}(E) = 0.3$	$\Delta \log_{10}(E) = 0.5$

Observation of the CRs large scale anisotropy

There have been several observations of *large-scale, part-per-mille anisotropy* in cosmic ray arrival directions between 0.1 and 100 TeV.



Northern Sky

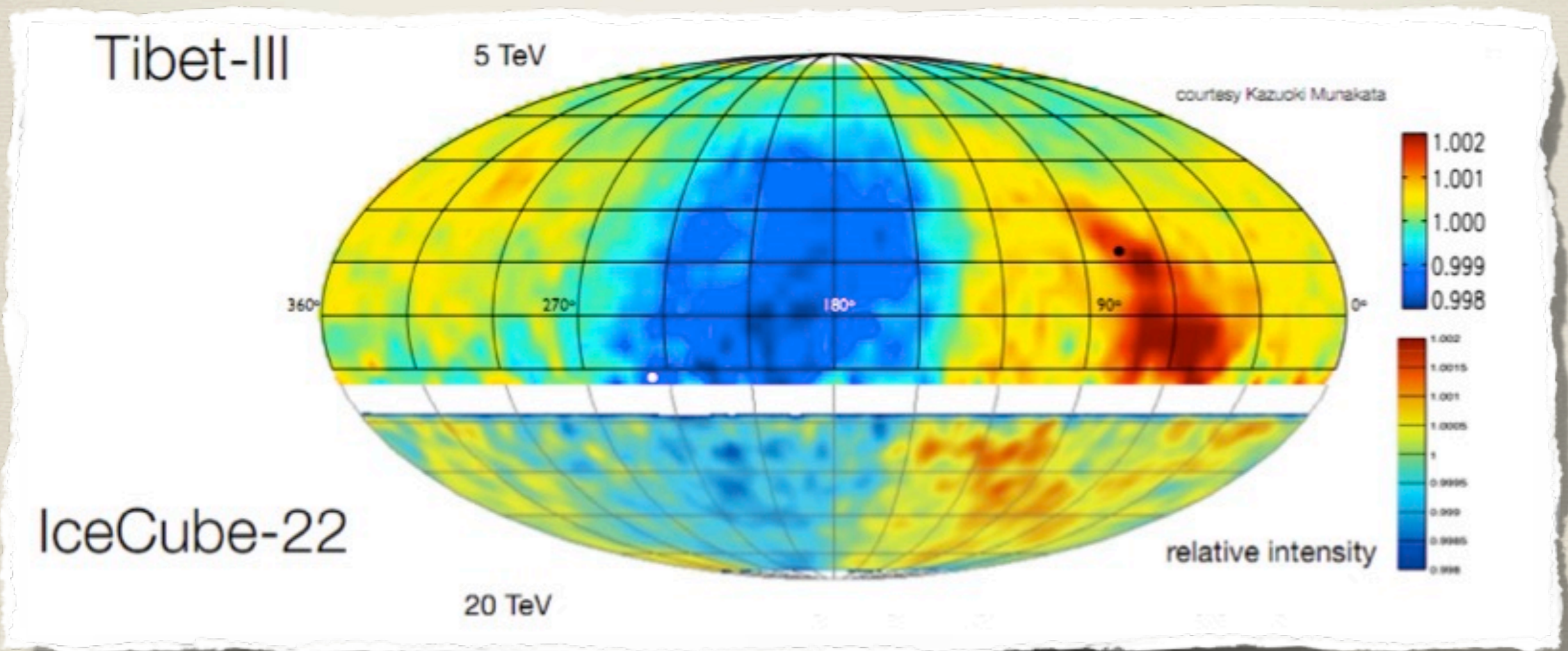


Southern Sky

Tibet ASy	M. Amenomori et al., <i>Astrophys. J.</i> 626 (2005) L29
SuperK	G. Guillian et al., <i>Phys. Rev. D</i> 75 (2007) 062003
Milagro	A. Abdo et al., <i>Astrophys. J.</i> 698 (2009) 2121
ARGO-YBJ	S. Vernetto, Proc. 31st ICRC, 2009
EAS-Top	M. Aglietta, <i>Astrophys. J.</i> 692 (2009) L130
IceCube	R. Abbasi <i>et al</i> , <i>Astrophys. J.</i> 718 (2010) L194

Large scale anisotropy

- * IceCube observed a large scale anisotropy at 10^{-3} level for the first time in the Southern Sky.
- * The anisotropy appears to be a continuation of large scale structures observed in the Northern Hemisphere.



Relative intensity of the cosmic ray event rate in equatorial coordinates: for each declination belt of width 3° , the plot shows the number of events relative to the average number of events in the belt.

Energy dependence of the anisotropy

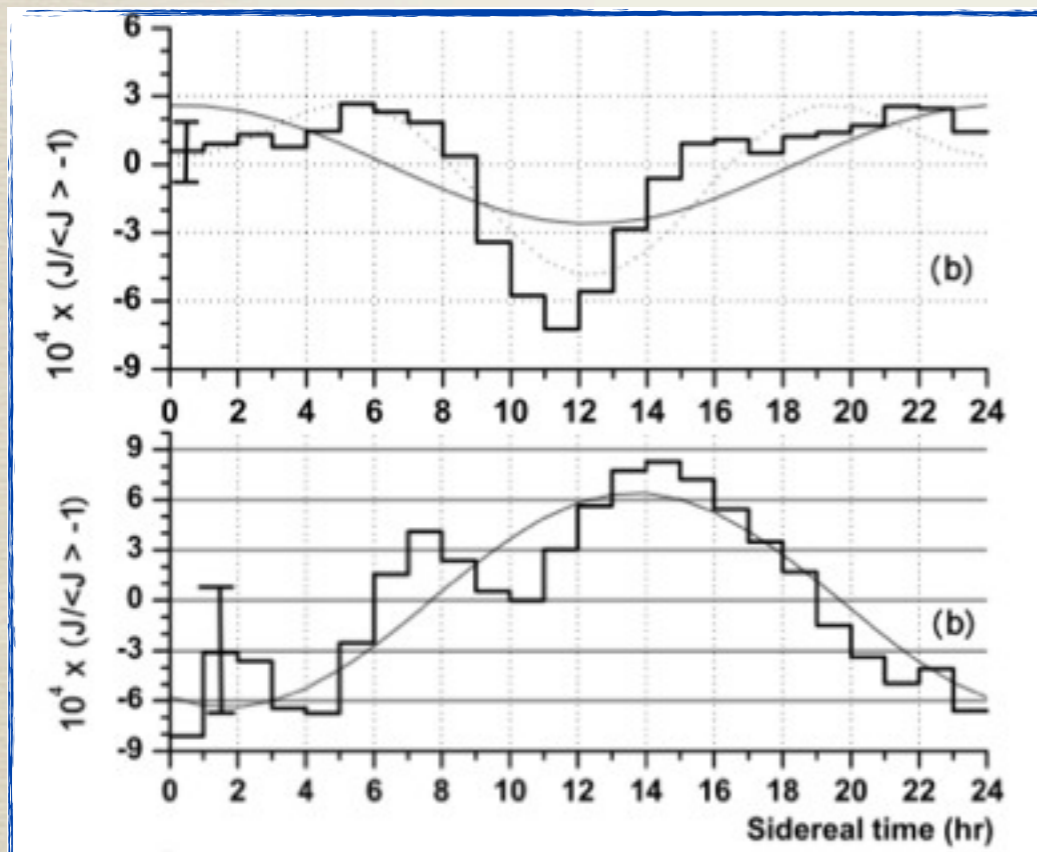
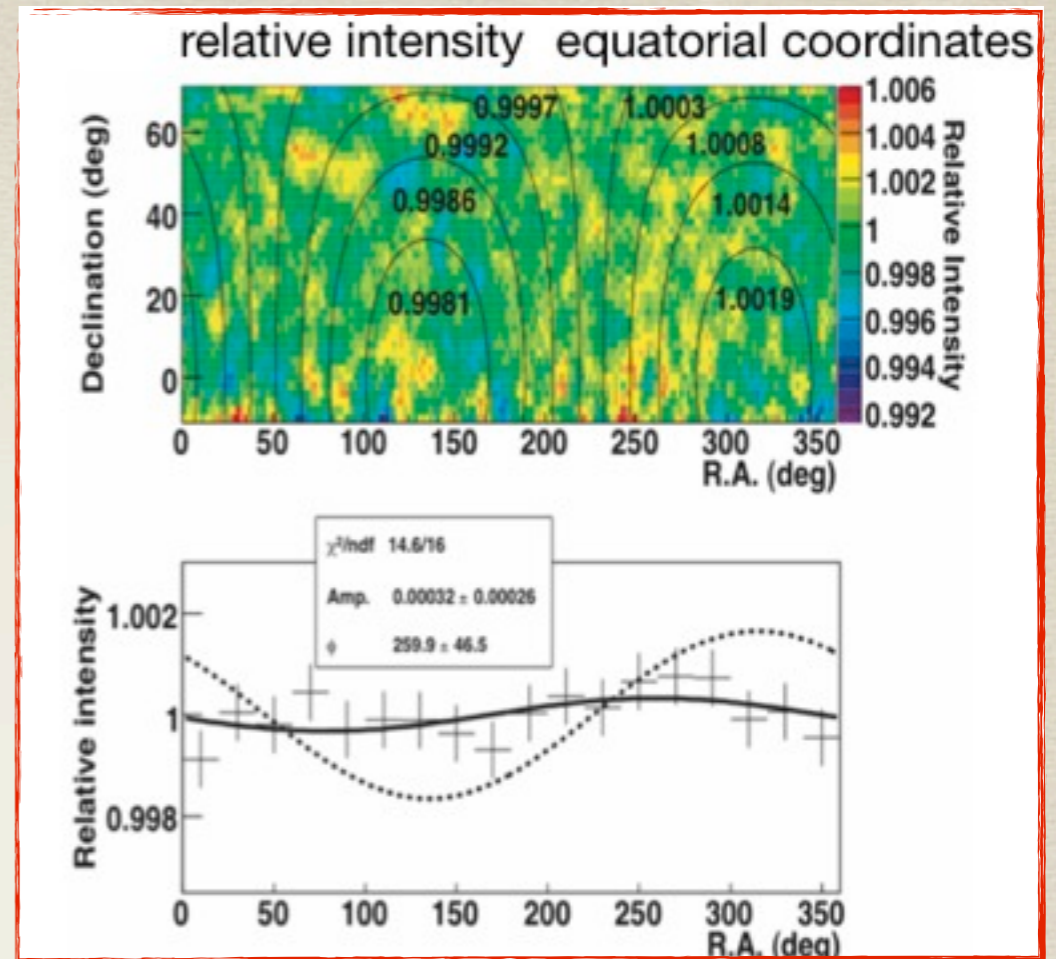
300 TeV

Tibet - III

Amenomori et al., Science Vol. 314, pp. 439, 2006

Amplitude: $(3.2 \pm 2.6) \times 10^{-4}$

consistent with **no anisotropy**



110 TeV

370 TeV

EAS-Top

Aglietta et al., ApJ 692, L130, 2009

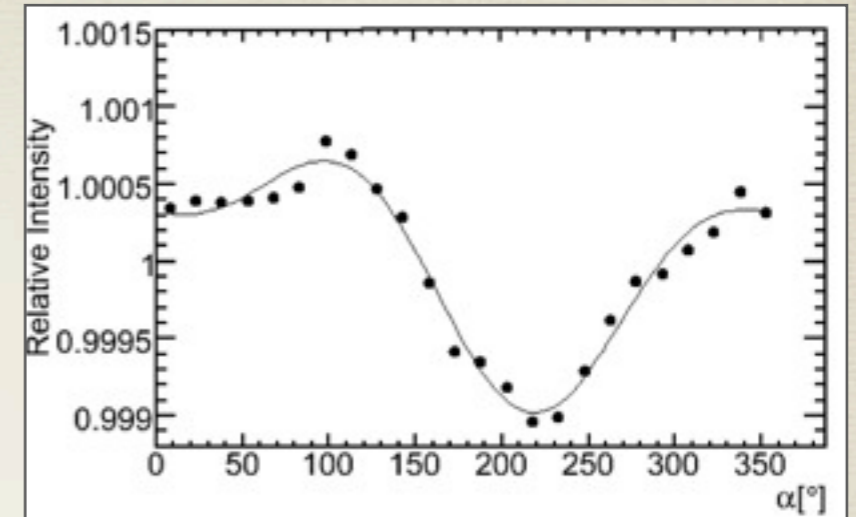
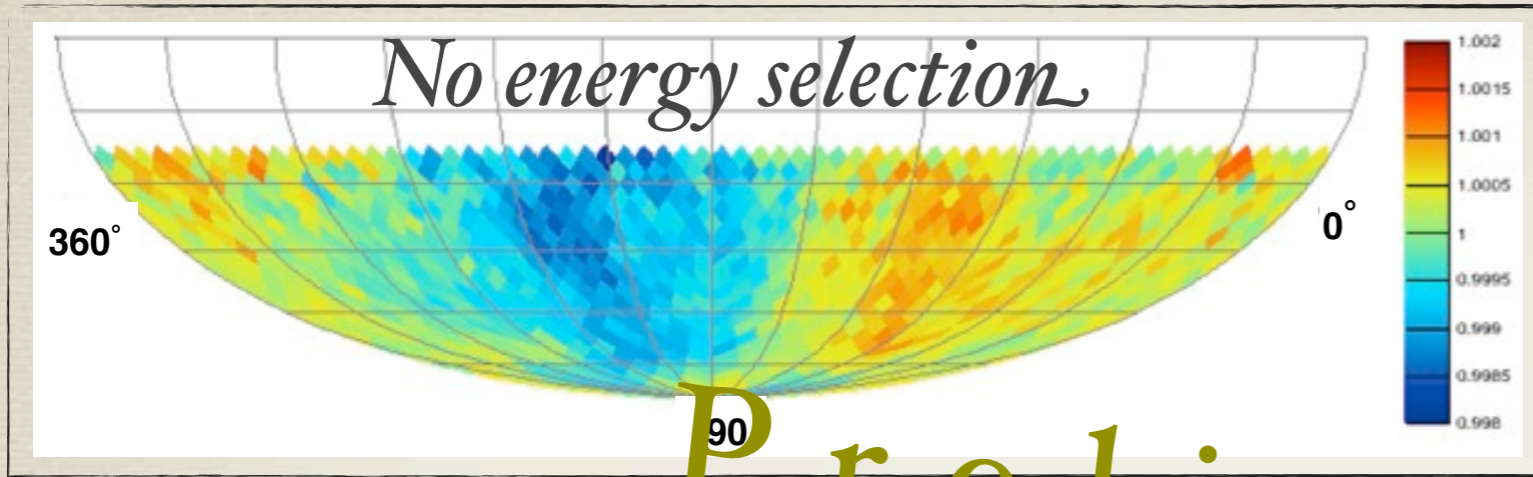
Amplitude (370 TeV): $(6.4 \pm 2.5) \times 10^{-4}$

low significance, still not conclusive.

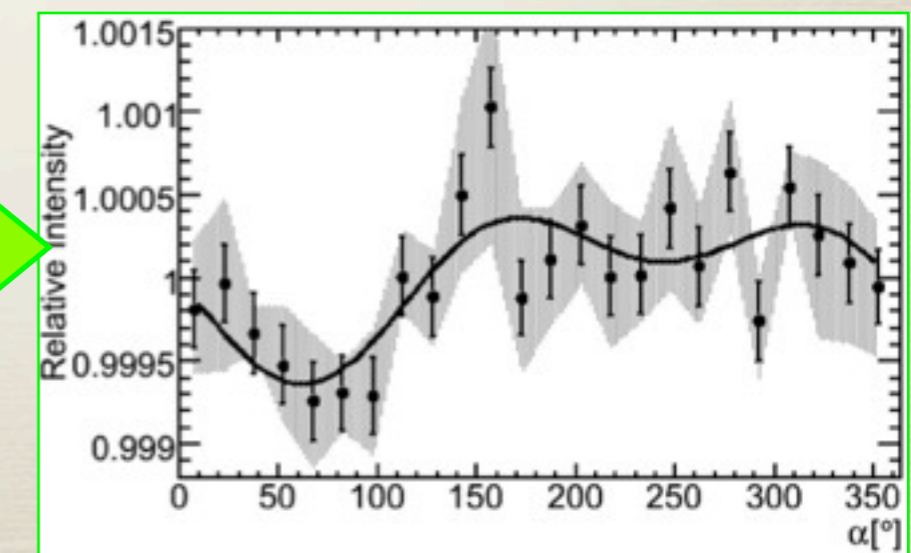
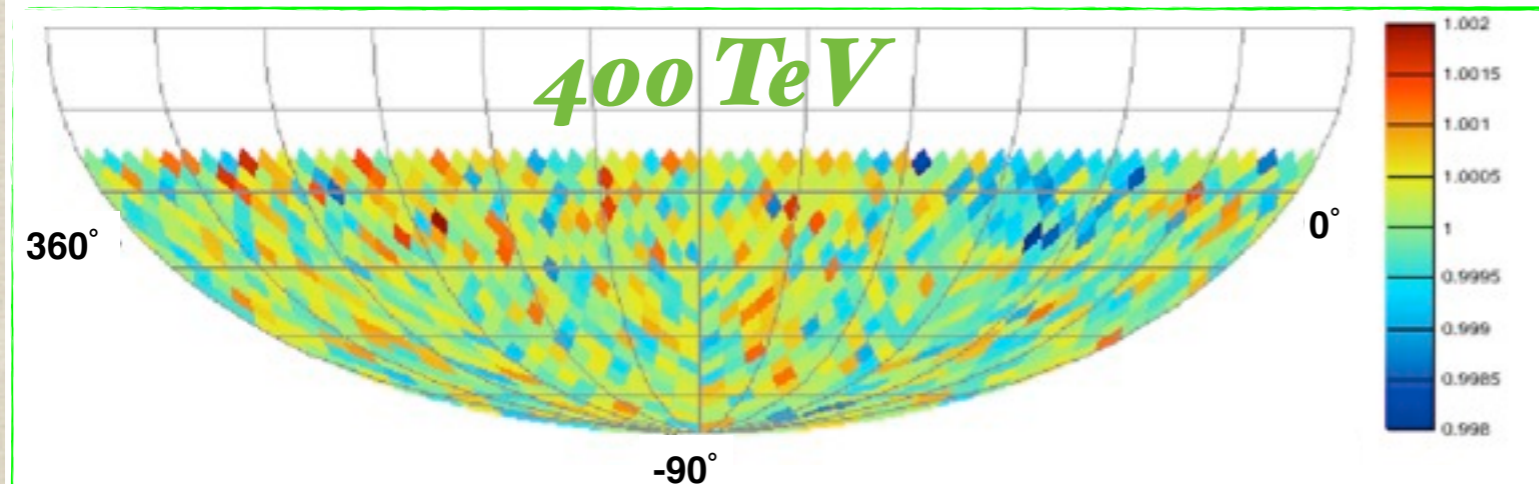
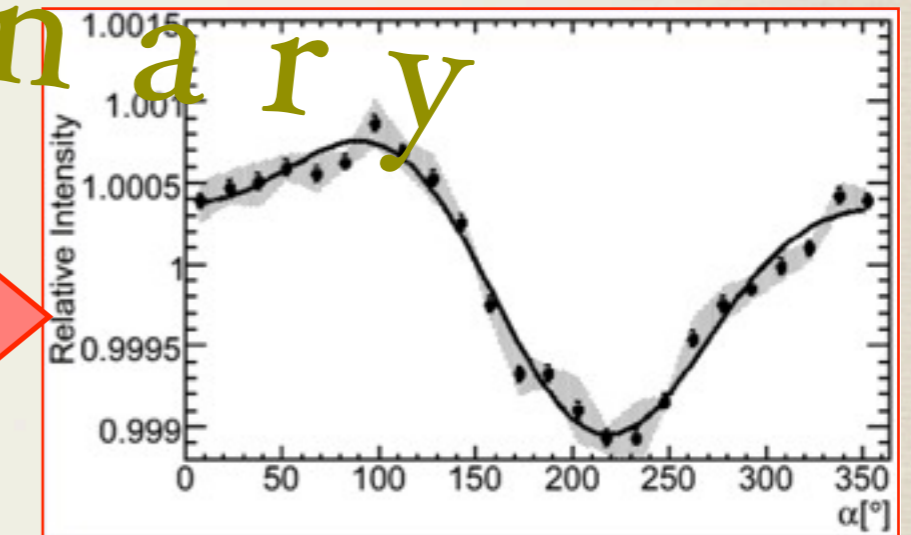
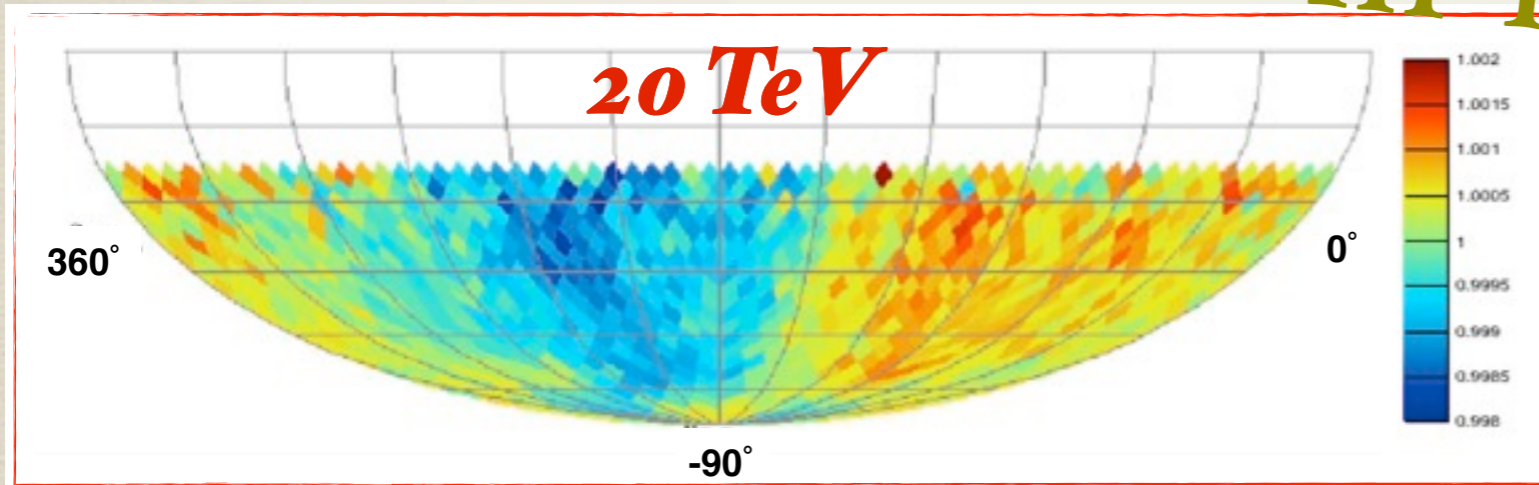
IO

Relative Intensity

Equatorial sky maps in HEALPix with $N_{\text{Side}} = 16$, $\text{pix resol} \sim 3^\circ$



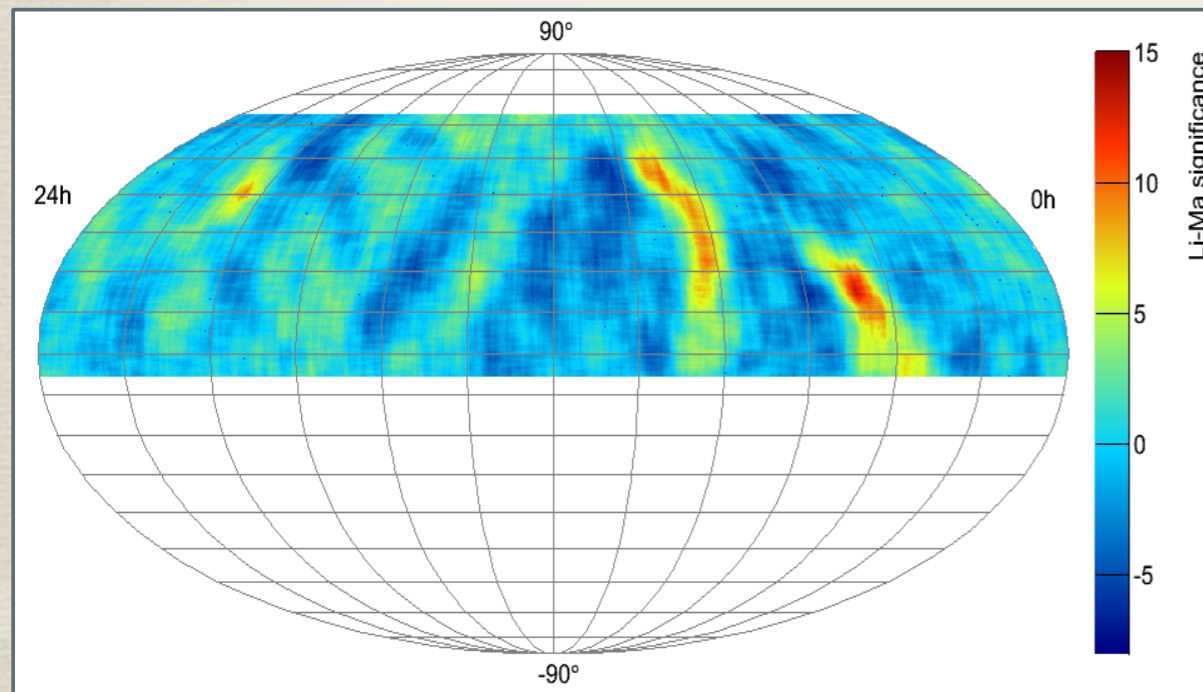
Preliminary



Small scale anisotropy

Several experiments have discovered anisotropies on scales of about 10°

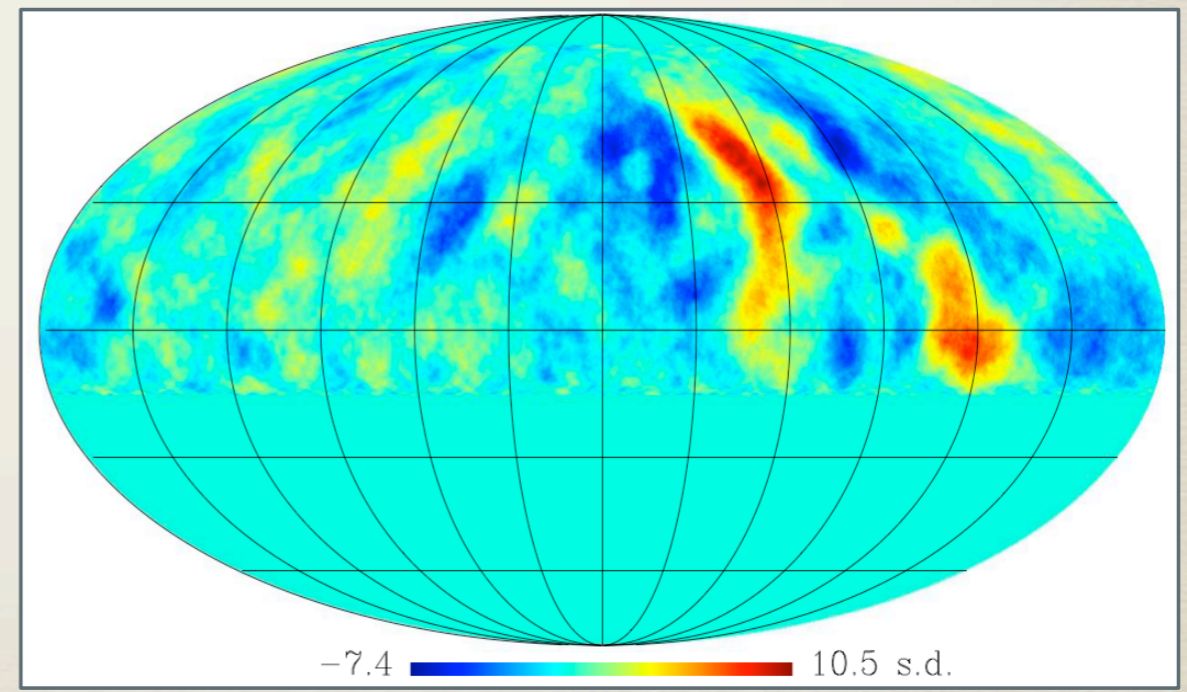
- * Milagro observes two localized regions with **significance $> 10\sigma$** in the total data set of $2.2 \cdot 10^{11}$ events recorded over 7 years. The “hot” regions have fractional excesses of order several times 10^{-4} relative to the background.
- * Same structures observed by ARGO-YBJ.



A. Abdo et al., PRL 101 (2008) 221101

Milagro

Median Energy: 1 TeV



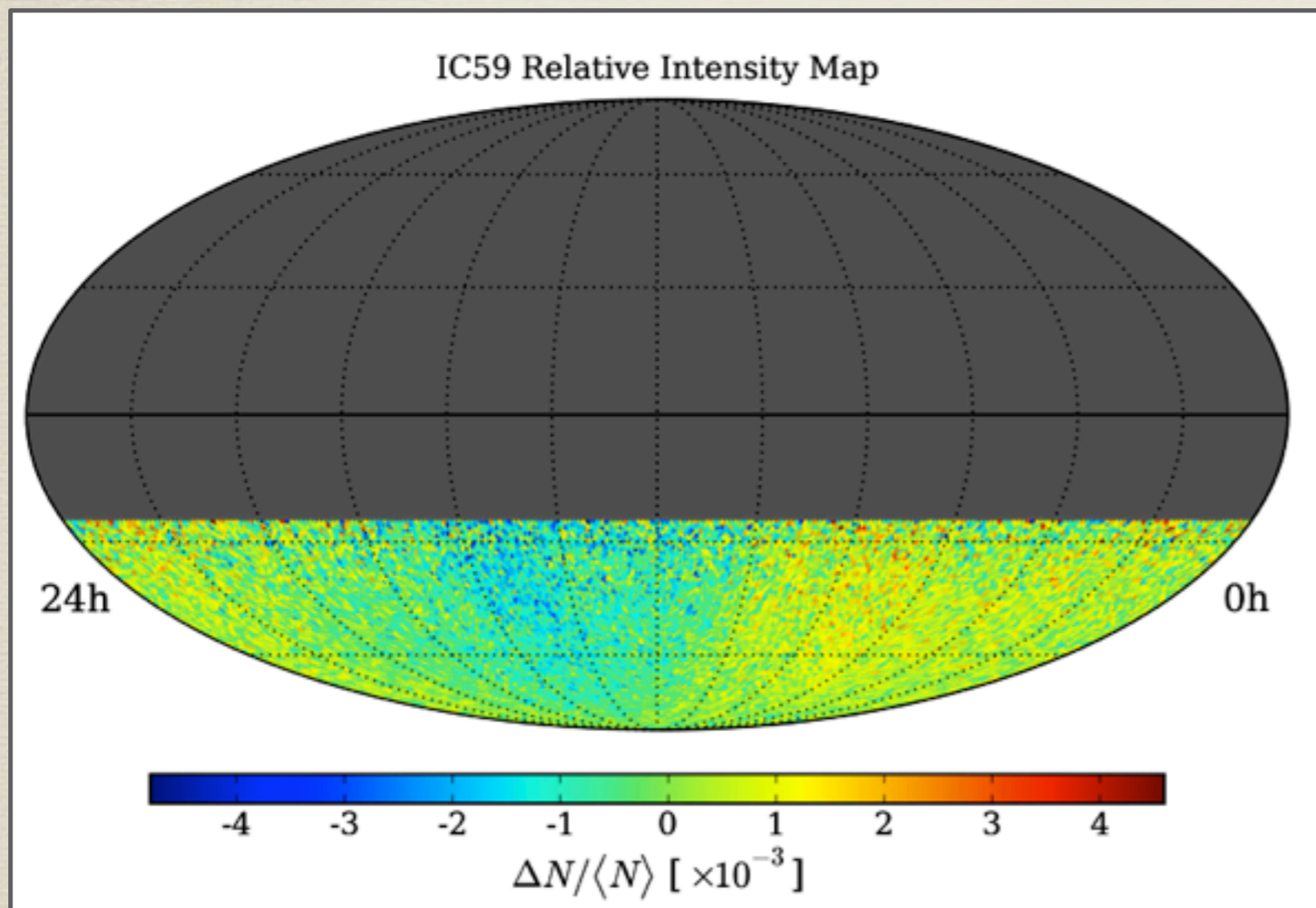
S. Vernetto, Proc. 31st ICRC, 2009

ARGO-YBJ

Median Energy: 2 TeV

Relative Intensity map

Equatorial sky maps in HEALPix: equal area pixel (size ~ 0.9°)



Sky map created using the background estimation technique from real data:

- N_i : number of data events in the i^{th} pixel.
- $\langle N_i \rangle$: expected number of events in an isotropic sky (time scrambling in 24 hr) in the i^{th} pixel.
- Relative Intensity:

$$\frac{\Delta N_i}{\langle N \rangle_i} = \frac{N_i(\alpha, \delta) - \langle N_i(\alpha, \delta) \rangle}{\langle N_i(\alpha, \delta) \rangle}$$

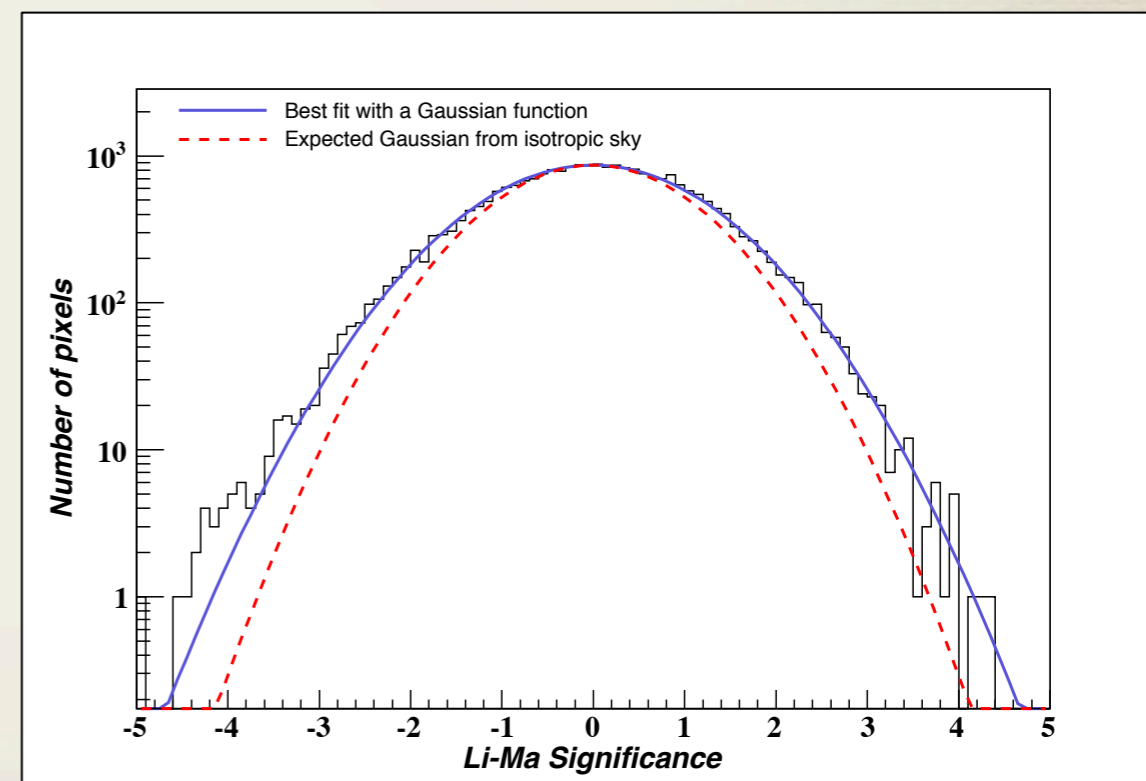
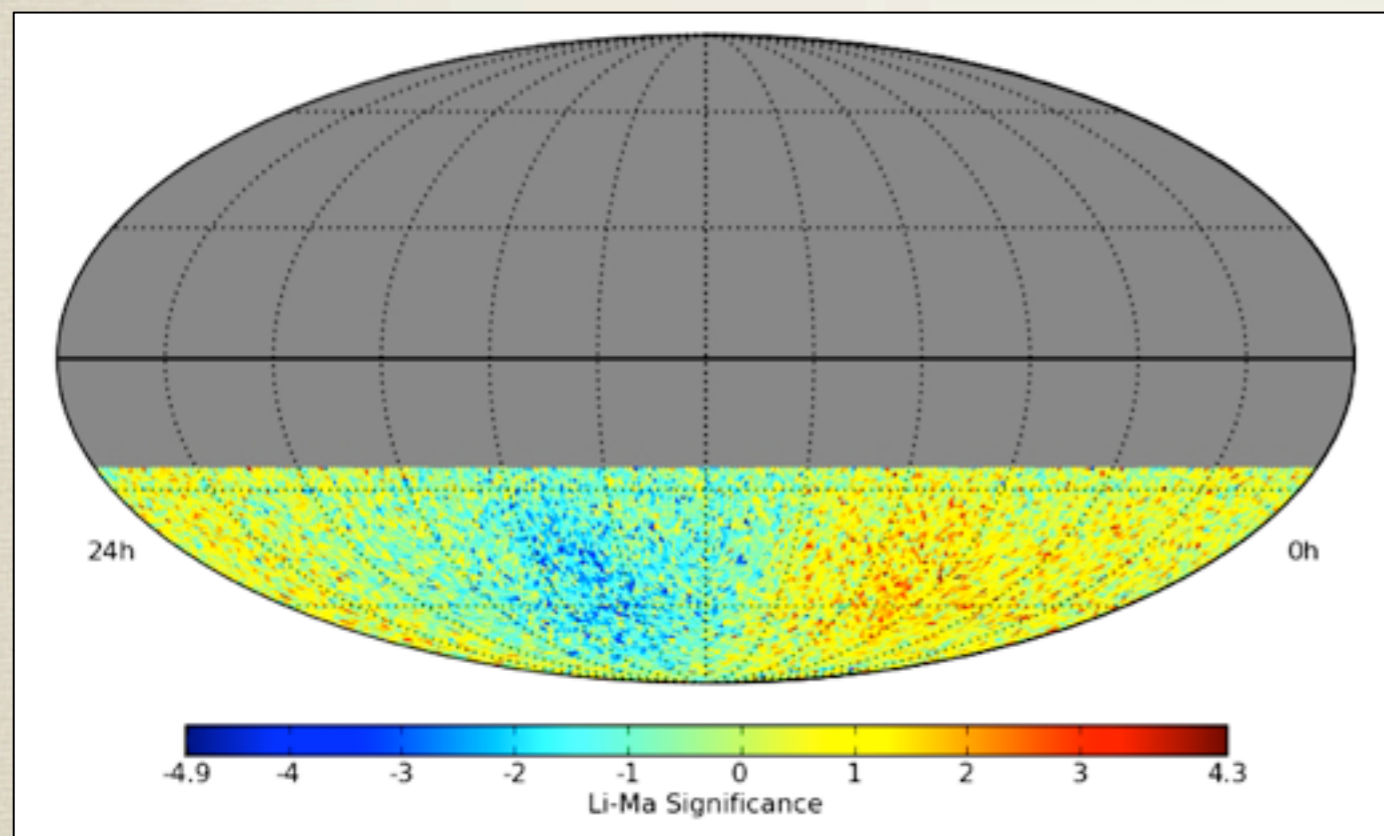
Relative intensity map is *not isotropic*. In IceCube-59, the *strong large scale structure* already observed in IceCube-22 data is visible in the “raw” data.

Significance map

Significance calculation:

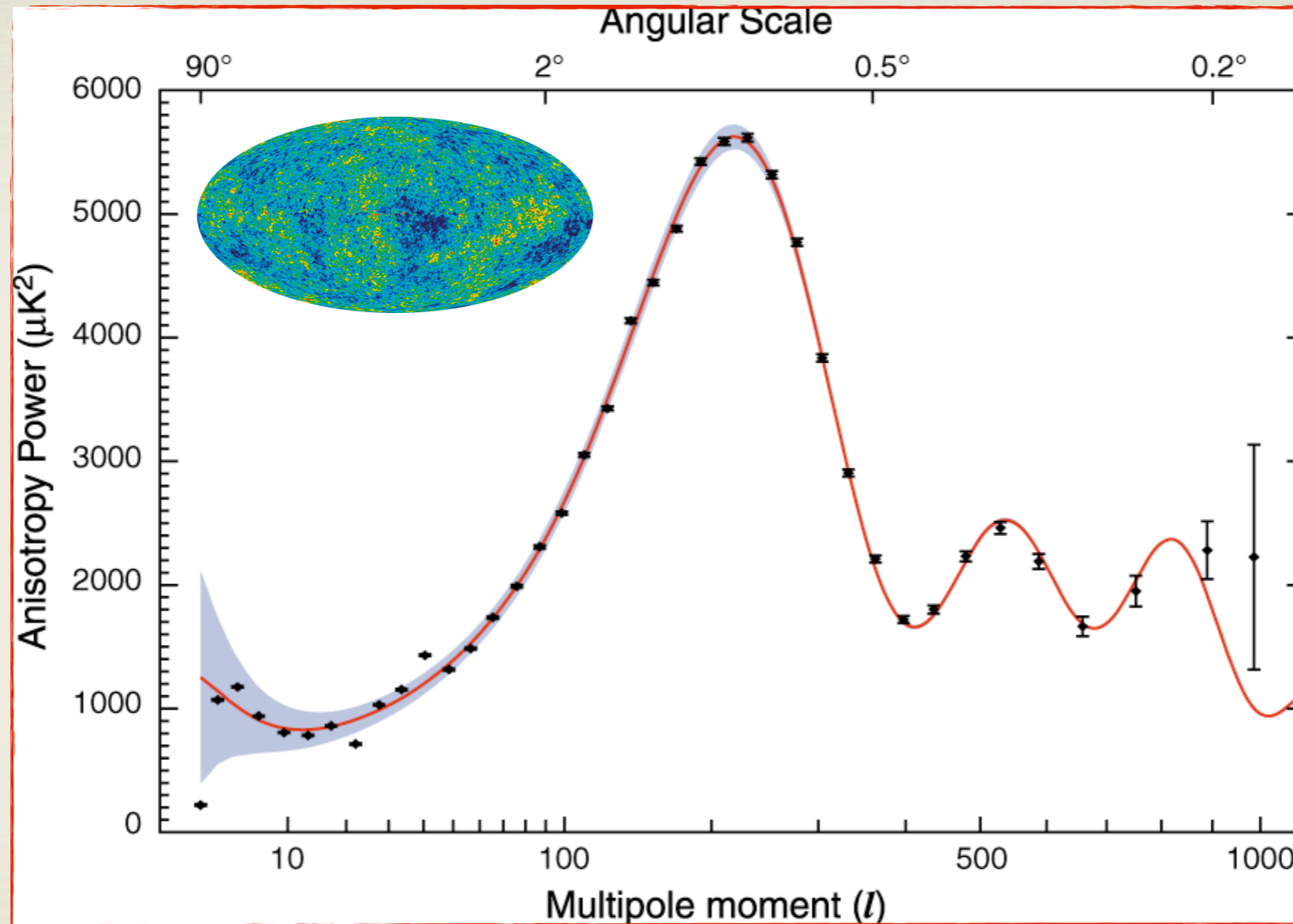
$$s = \sqrt{2} \left\{ N_{\text{on}} \ln \left[\frac{1 + \alpha}{\alpha} \left(\frac{N_{\text{on}}}{N_{\text{on}} + N_{\text{off}}} \right) \right] + N_{\text{off}} \ln \left[(1 + \alpha) \left(\frac{N_{\text{off}}}{N_{\text{on}} + N_{\text{off}}} \right) \right] \right\}^{1/2} \quad \alpha = 1/20$$

Li, T., & Ma, Y. 1983, ApJ, 272, 317



Power spectrum

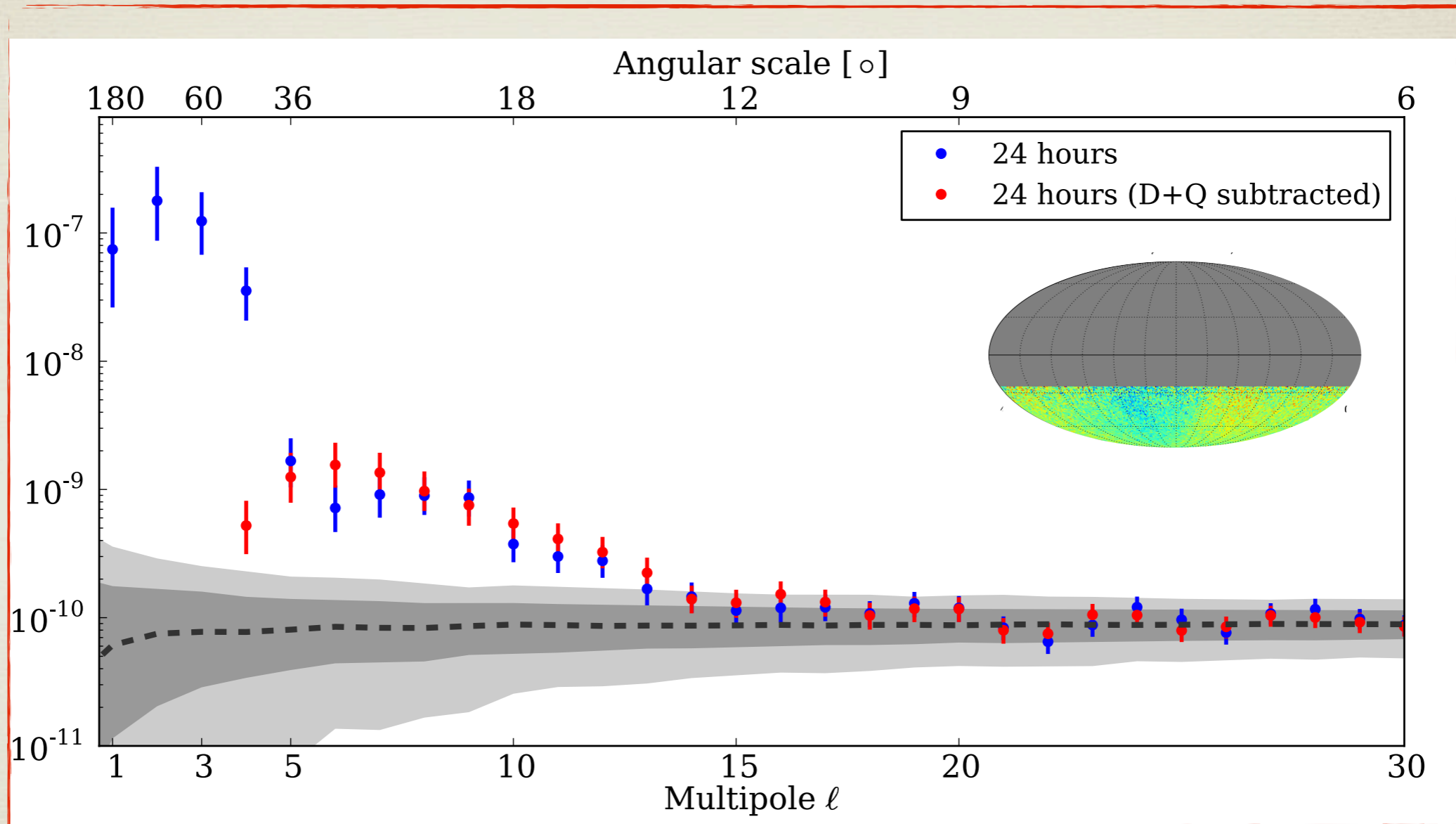
Angular size $\theta \sim \frac{180^\circ}{\ell}$



Multipole expansion: $\delta I(\mathbf{u}_i) = \sum_{\ell=1}^{\infty} \sum_{m=-\ell}^{\ell} a_{\ell m} Y_{\ell m}(\mathbf{u}_i)$ $C_{\ell} = \frac{1}{2\ell + 1} \sum_m |a_{\ell m}|^2$

Power spectrum

Angular size $\theta \sim \frac{180^\circ}{\ell}$



Multipole expansion:

$$\delta I(\mathbf{u}_i) = \sum_{\ell=1}^{\infty} \sum_{m=-\ell}^{\ell} a_{\ell m} Y_{\ell m}(\mathbf{u}_i) \quad C_{\ell} = \frac{1}{2\ell + 1} \sum_m |a_{\ell m}|^2$$

Dipole and quadrupole fit

$$\delta I(\alpha, \delta) = m_0$$

$$+ p_x \cos \delta \cos \alpha + p_y \cos \delta \sin \alpha + p_z \sin \delta$$

$$+ \frac{1}{2} Q_1 (3 \cos^2 \delta - 1) + Q_2 \sin 2\delta \cos \alpha + Q_3 \sin 2\delta \sin \alpha + Q_4 \cos^2 \delta \cos 2\alpha + Q_5 \cos^2 \delta \sin 2\alpha$$

monopole

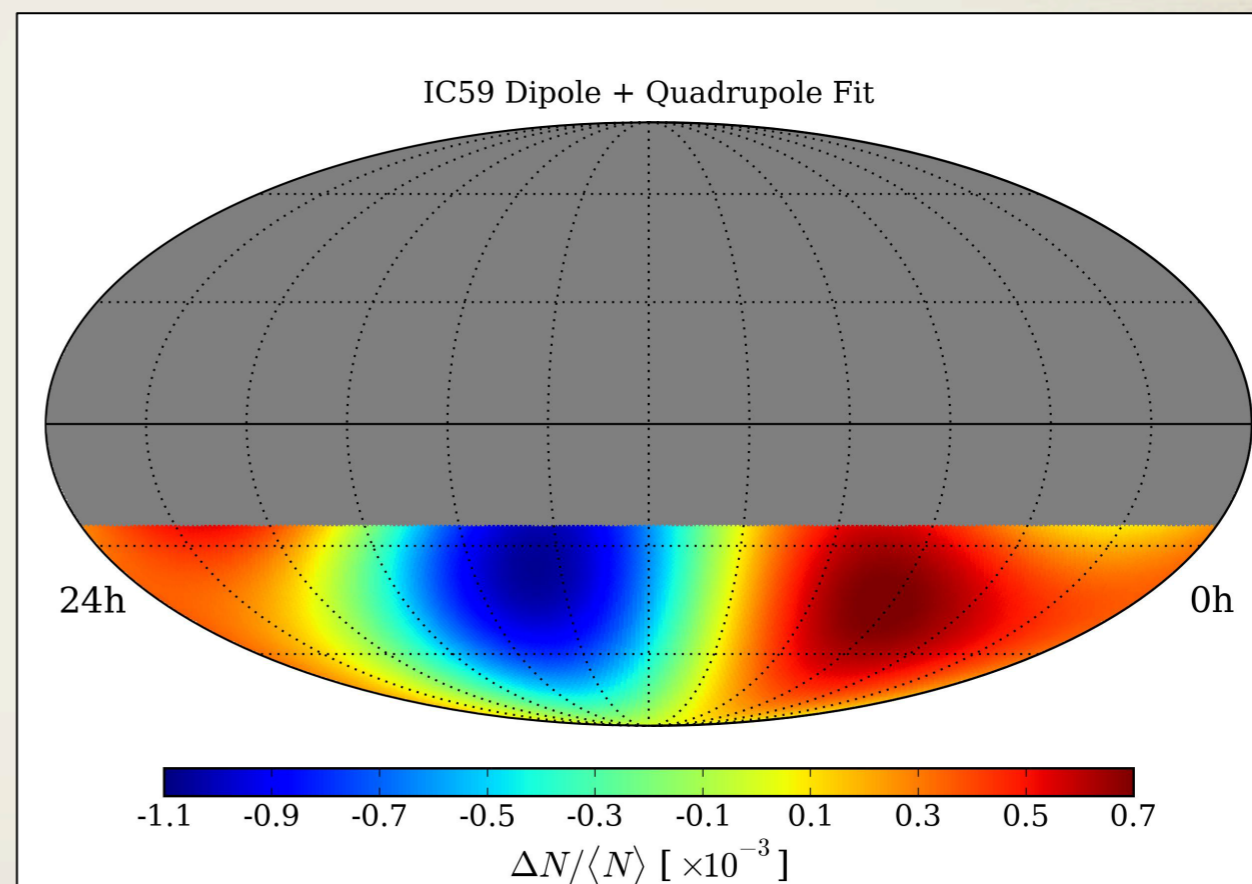
dipole

quadrupole

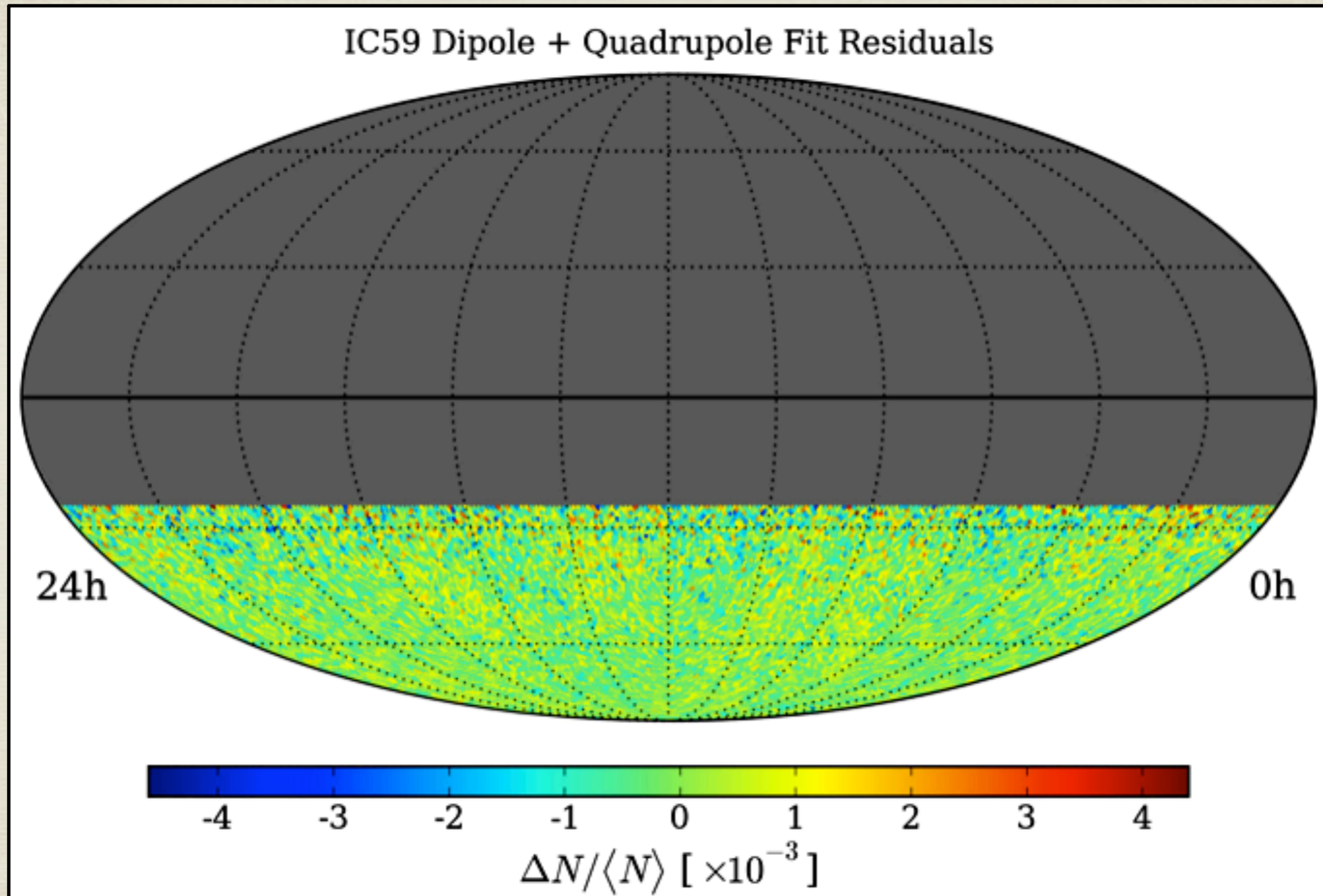
Coefficient	Fit Value
m_0	0.320 ± 2.264
p_x	2.435 ± 0.707
p_y	-3.856 ± 0.707
p_z	0.548 ± 3.872
Q_1	0.233 ± 1.702
Q_2	-2.949 ± 0.494
Q_3	-8.797 ± 0.494
Q_4	-2.148 ± 0.200
Q_5	-5.268 ± 0.200

$$\chi^2/\text{ndf} = 14743.4/14187$$

$$\text{Pr}(\chi^2|\text{ndf}) = 5.5 \times 10^{-4}$$



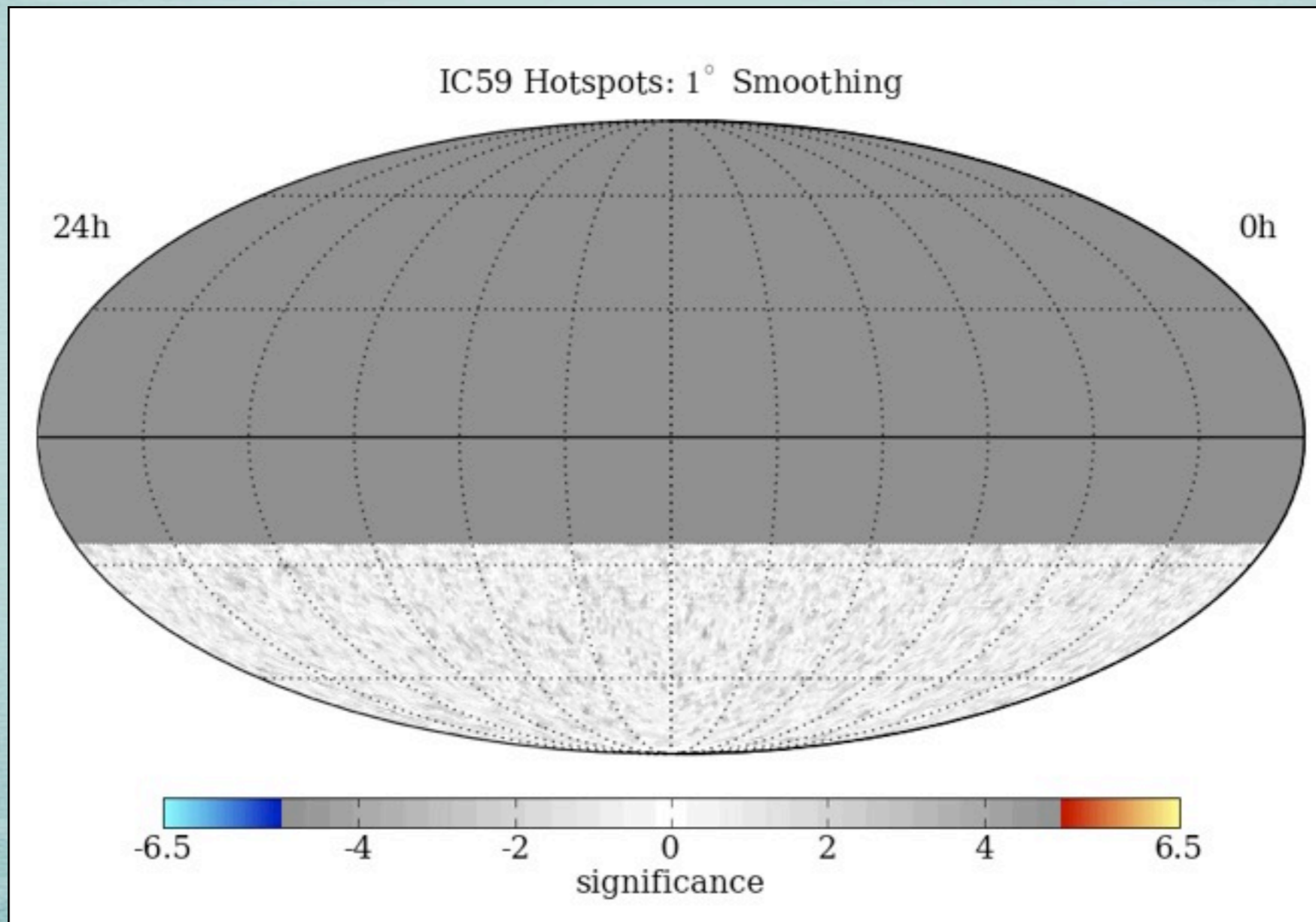
Residual map



No structures seem to be present: we need to smooth the map.

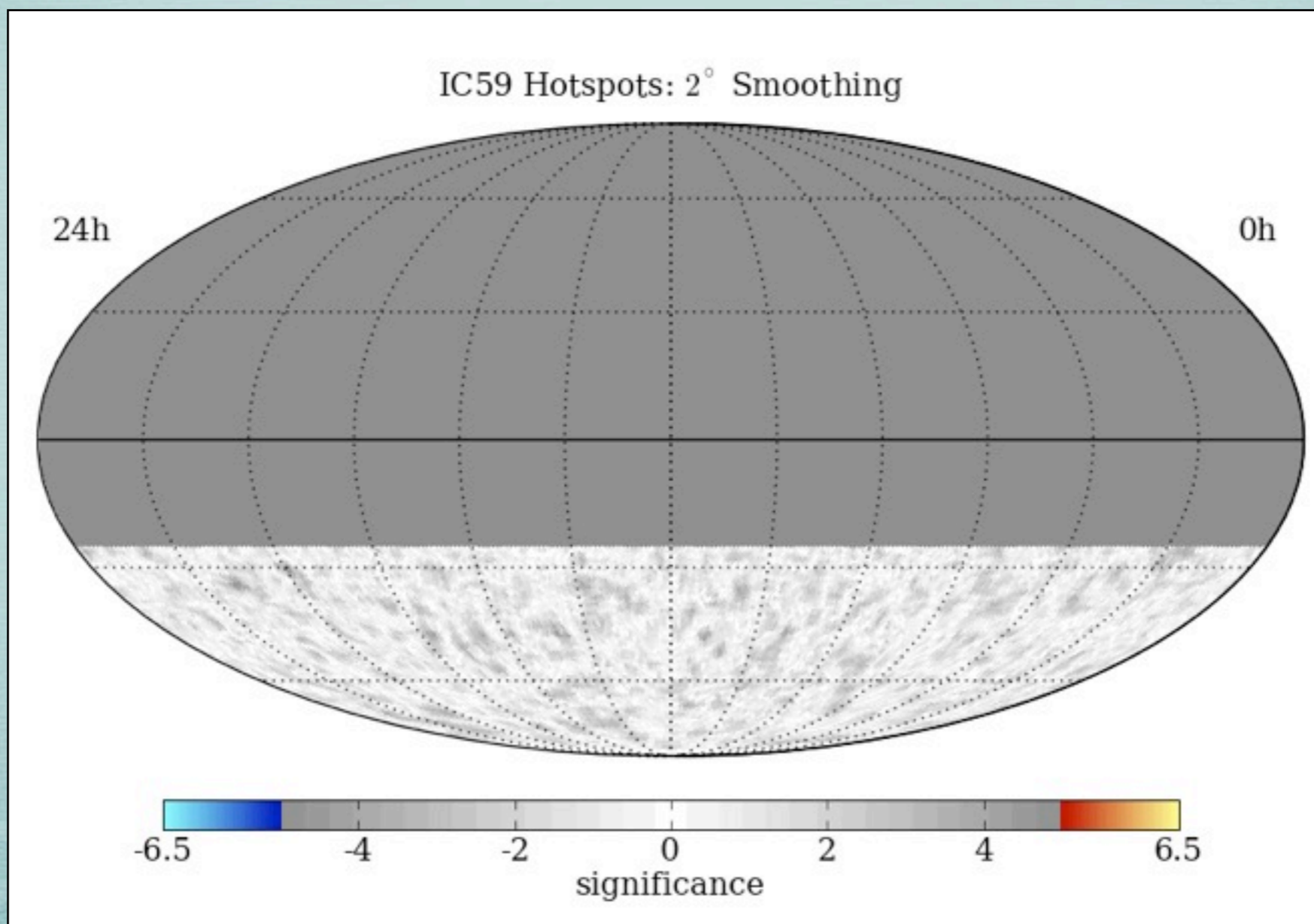
MAP SMOOTHING SCAN

Scan from 1 - 30° in smoothing
Different regions have different optimal angular smoothing
Significances are pre-trial



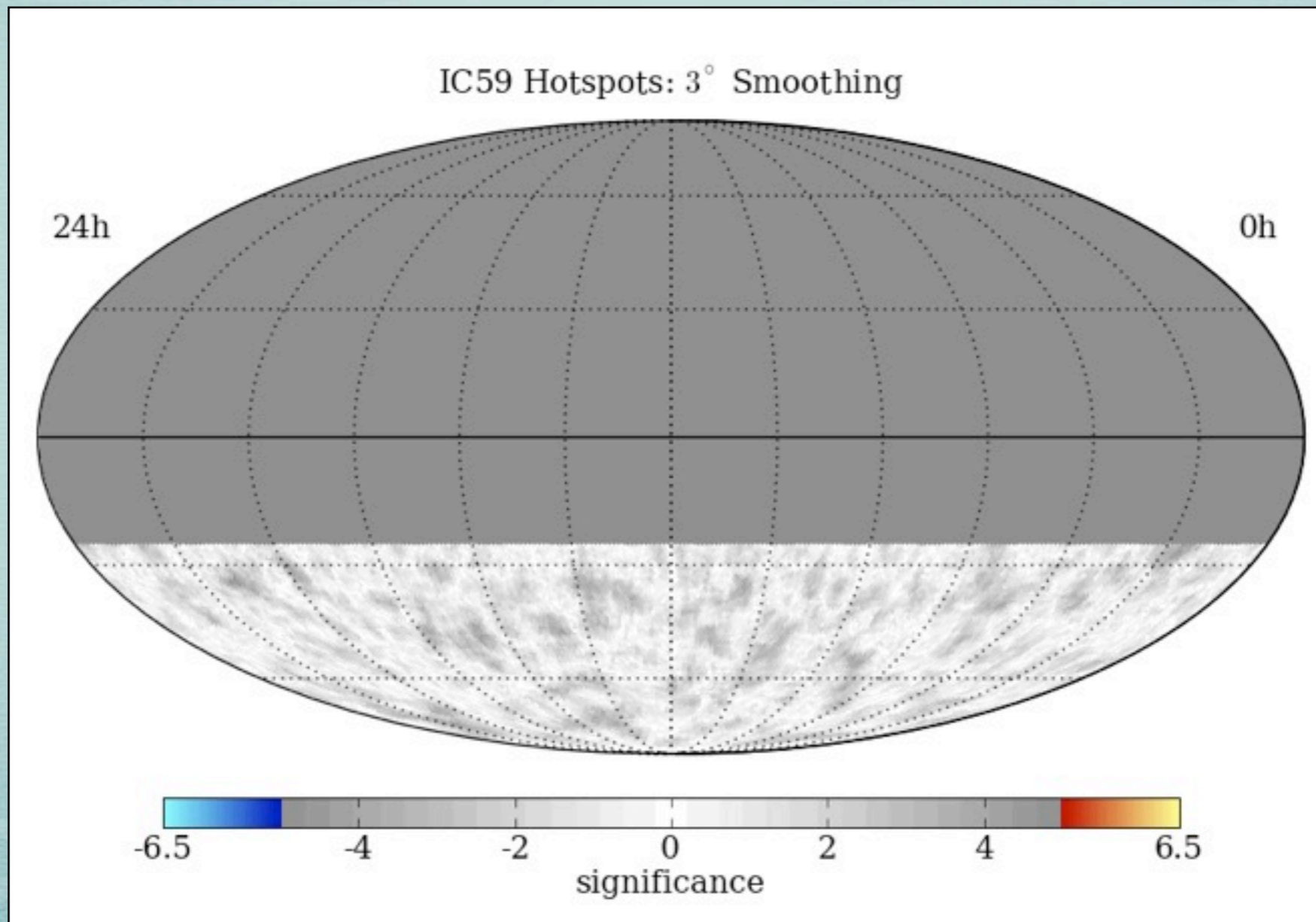
MAP SMOOTHING SCAN

Scan from 1 - 30° in smoothing
Different regions have different optimal angular smoothing
Significances are pre-trial



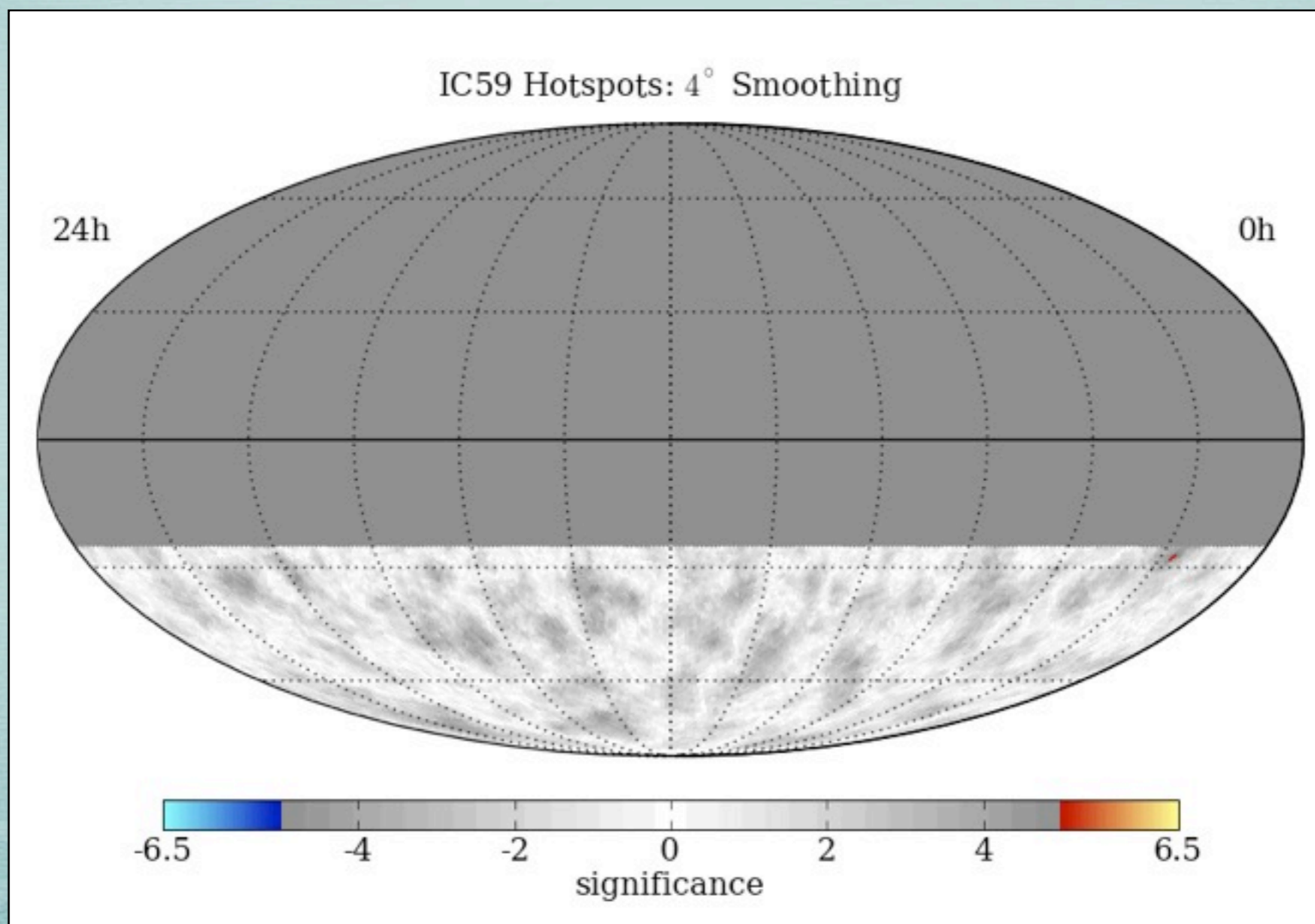
MAP SMOOTHING SCAN

Scan from 1 - 30° in smoothing
Different regions have different optimal angular smoothing
Significances are pre-trial



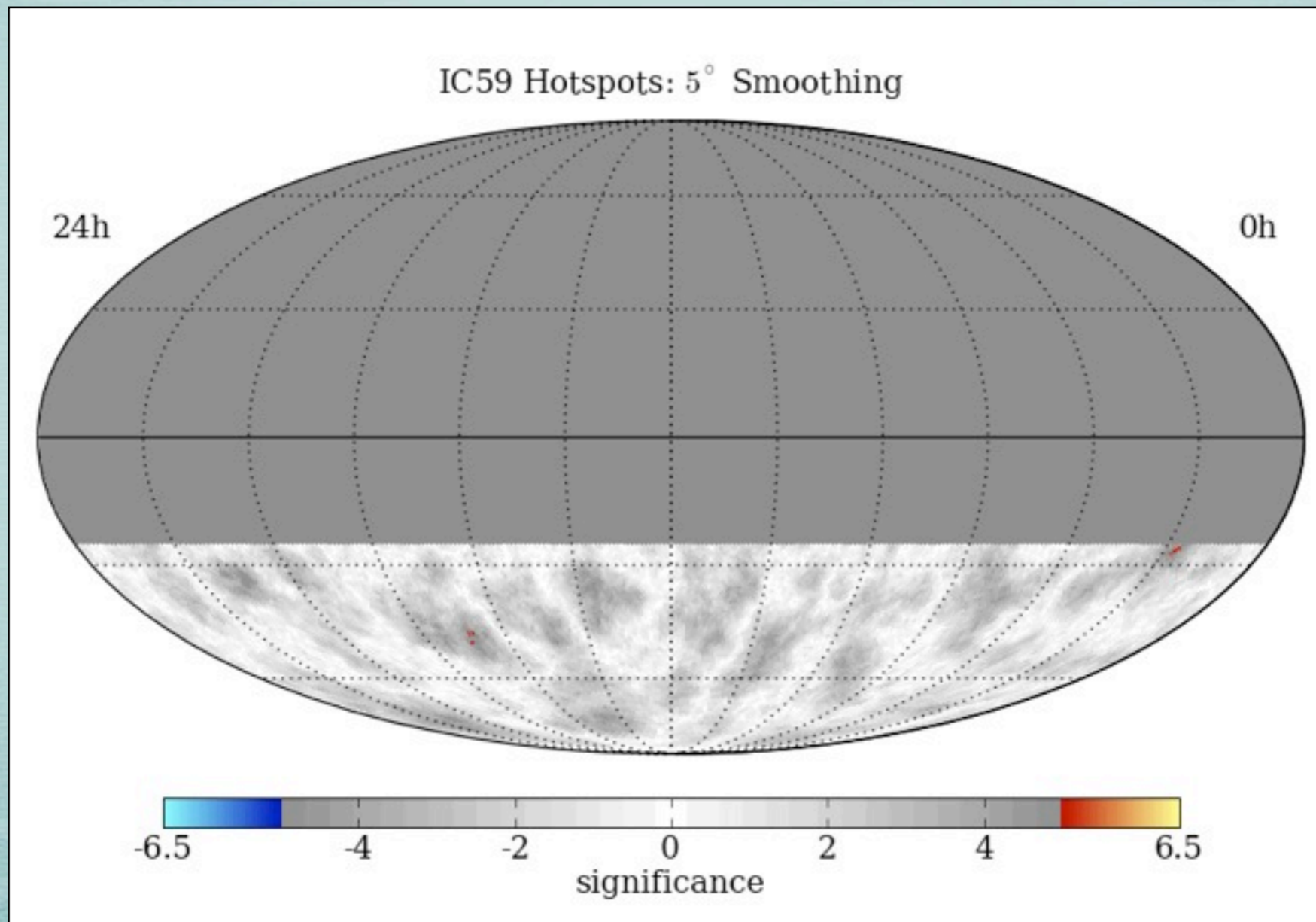
MAP SMOOTHING SCAN

Scan from 1 - 30° in smoothing
Different regions have different optimal angular smoothing
Significances are pre-trial



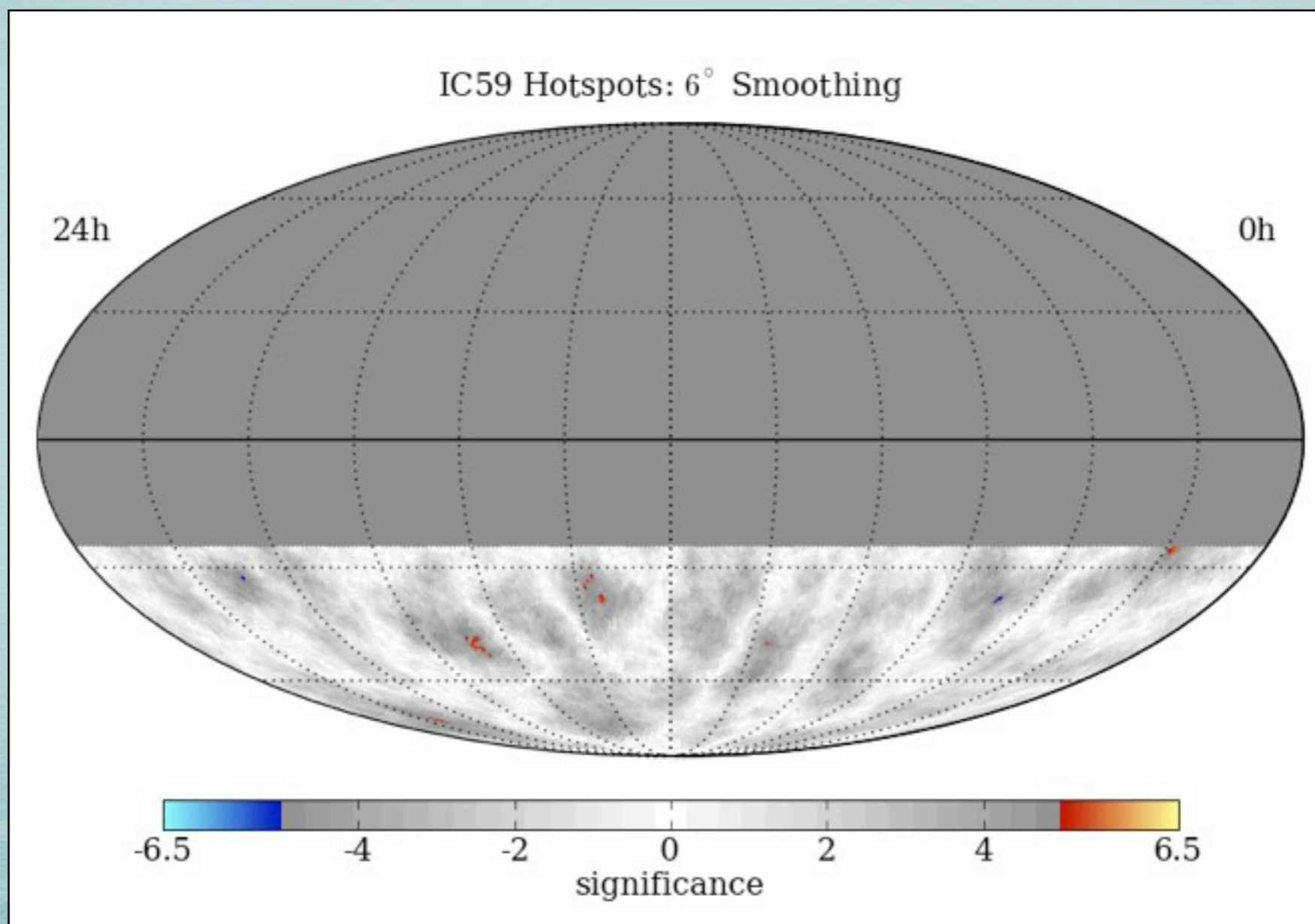
MAP SMOOTHING SCAN

Scan from 1 - 30° in smoothing
Different regions have different optimal angular smoothing
Significances are pre-trial



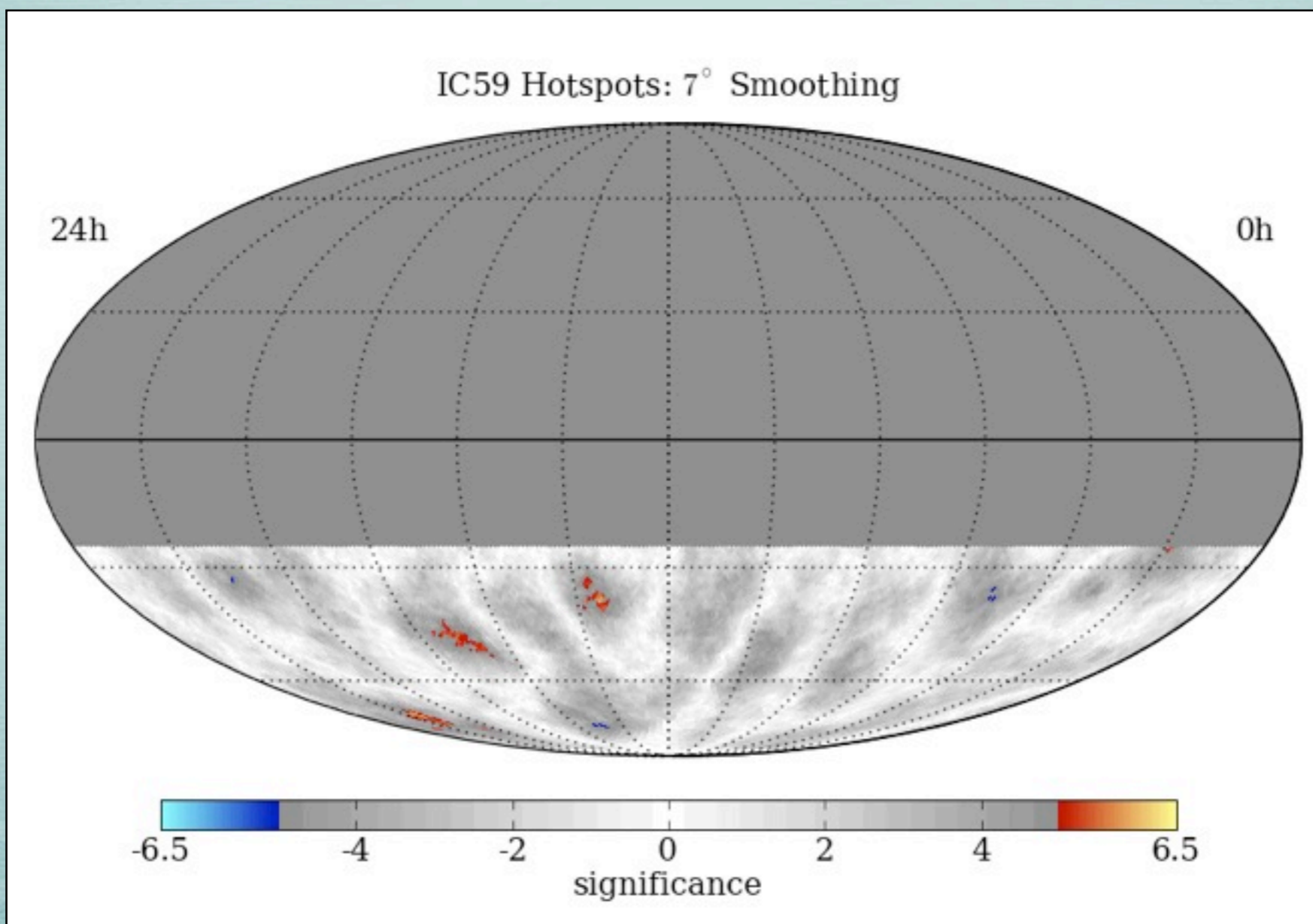
MAP SMOOTHING SCAN

Scan from 1 - 30° in smoothing
 Different regions have different optimal angular smoothing
 Significances are pre-trial



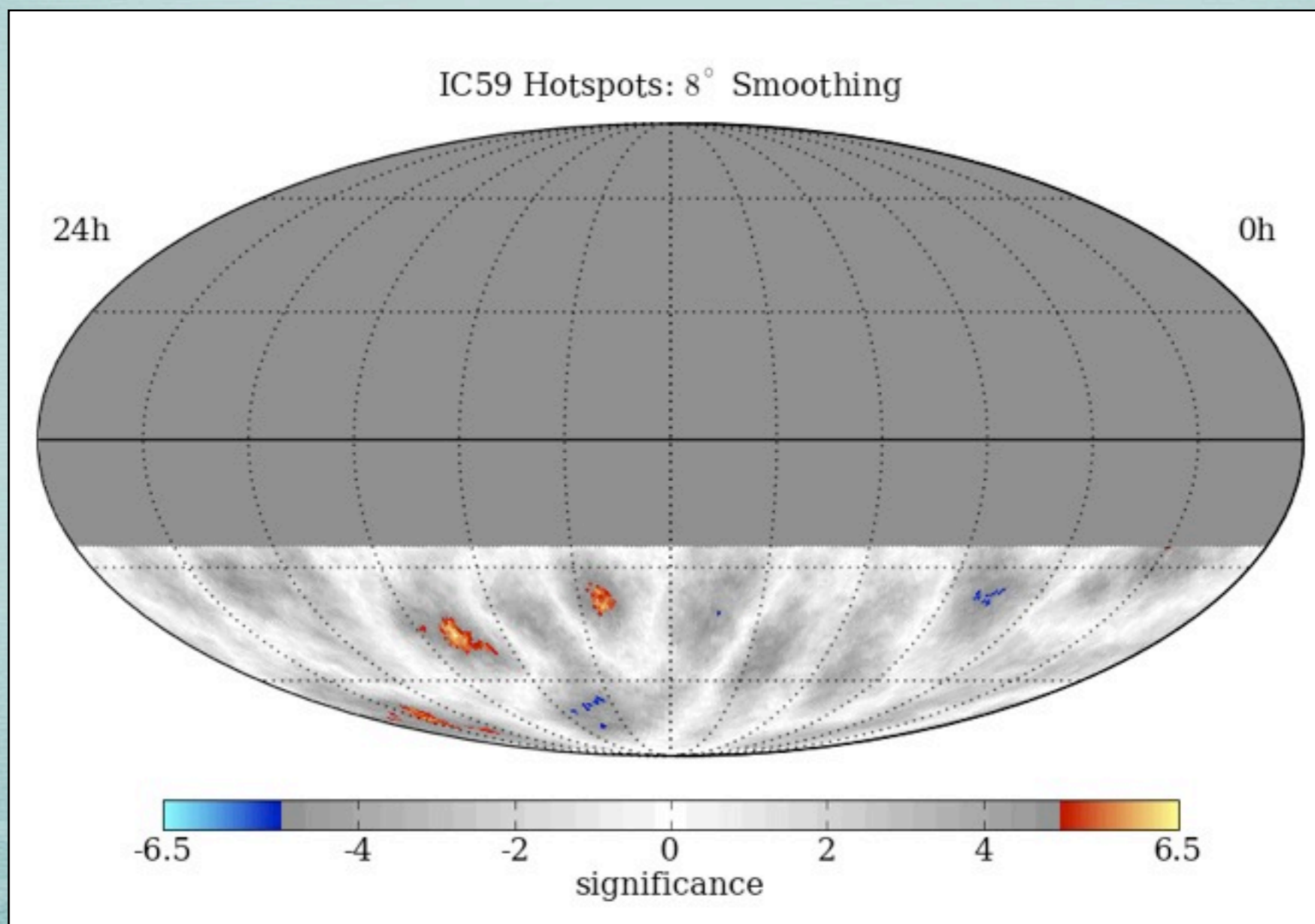
MAP SMOOTHING SCAN

Scan from 1 - 30° in smoothing
 Different regions have different optimal angular smoothing
 Significances are pre-trial



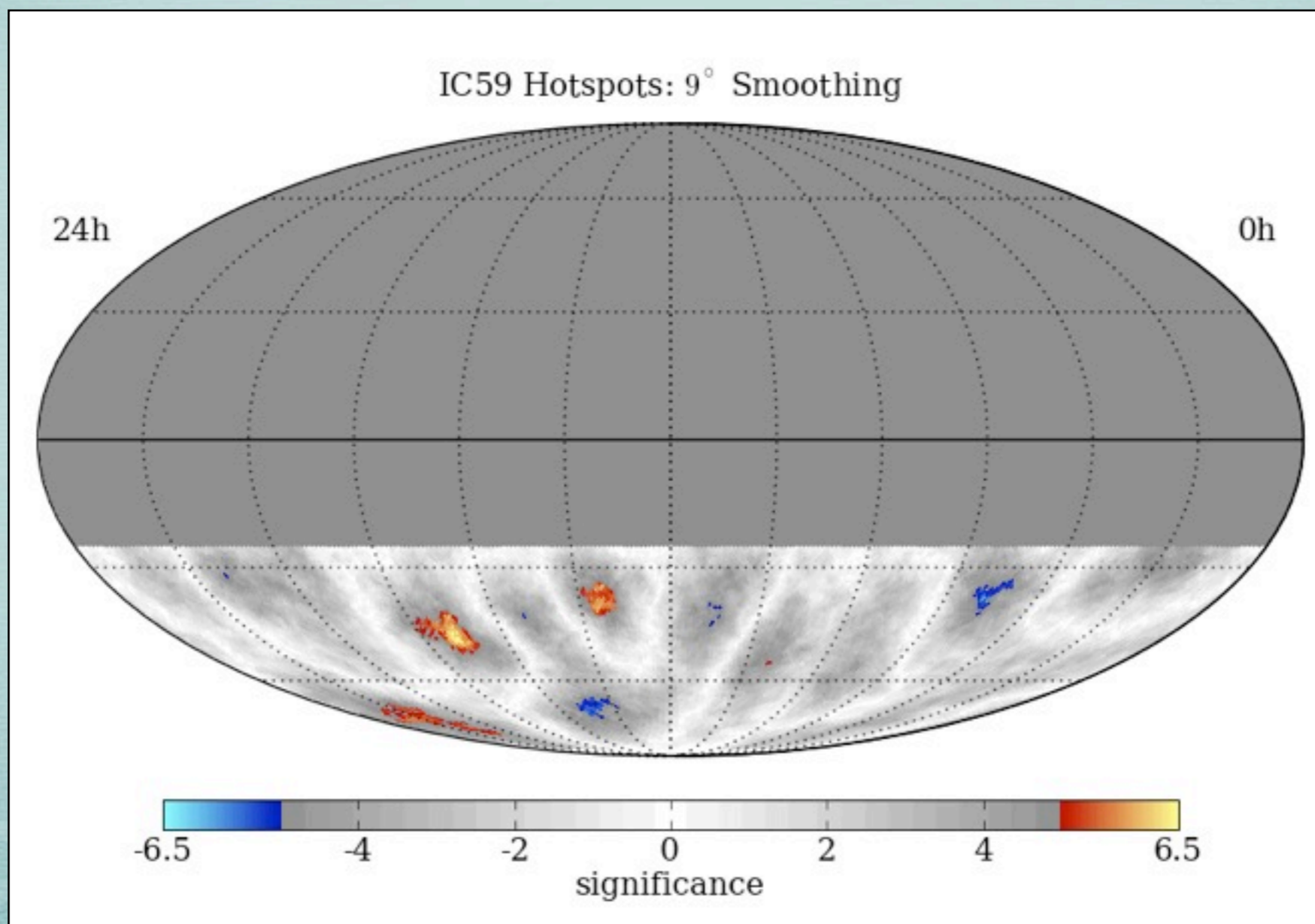
MAP SMOOTHING SCAN

Scan from 1 - 30° in smoothing
 Different regions have different optimal angular smoothing
 Significances are pre-trial



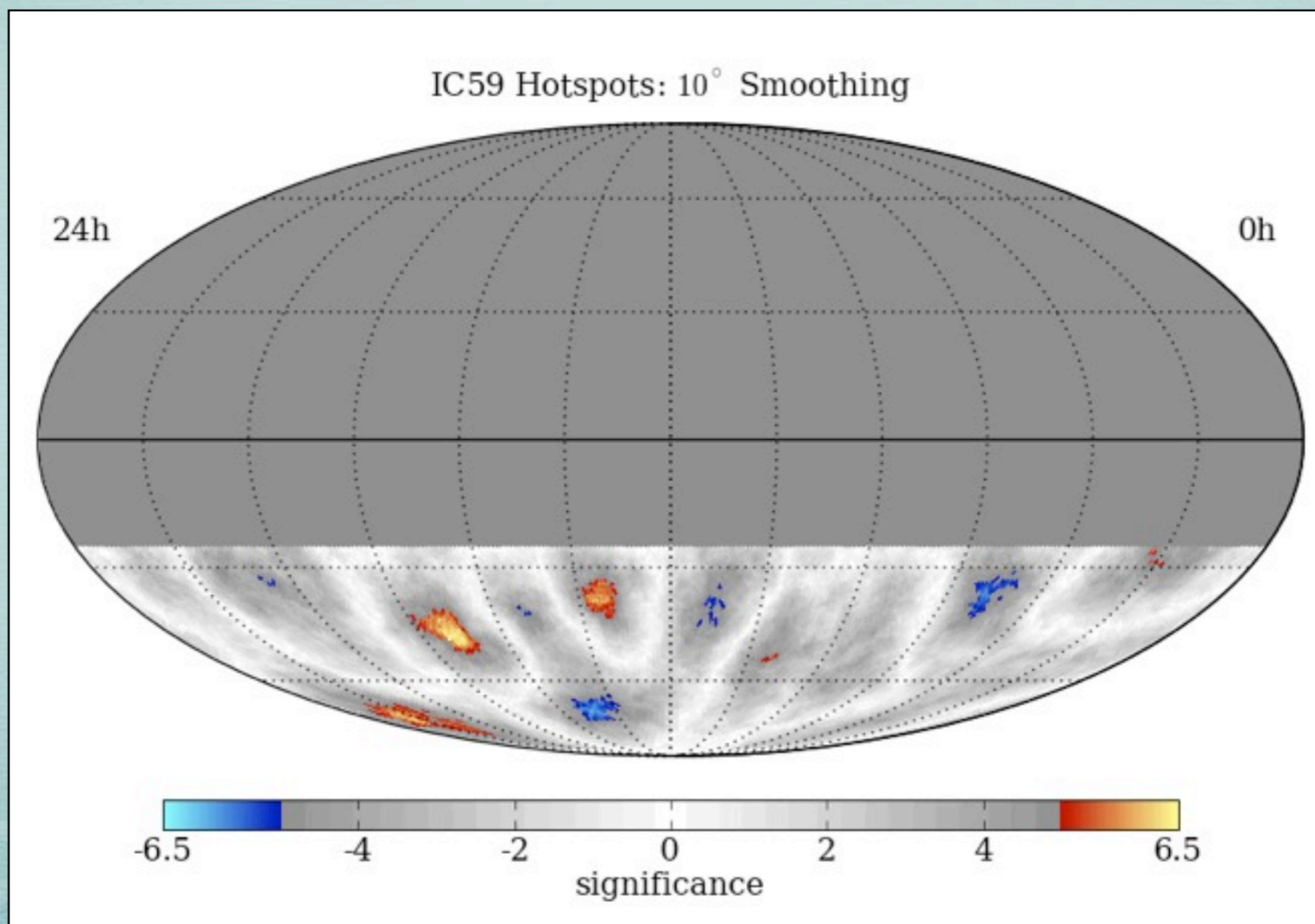
MAP SMOOTHING SCAN

Scan from 1 - 30° in smoothing
 Different regions have different optimal angular smoothing
 Significances are pre-trial



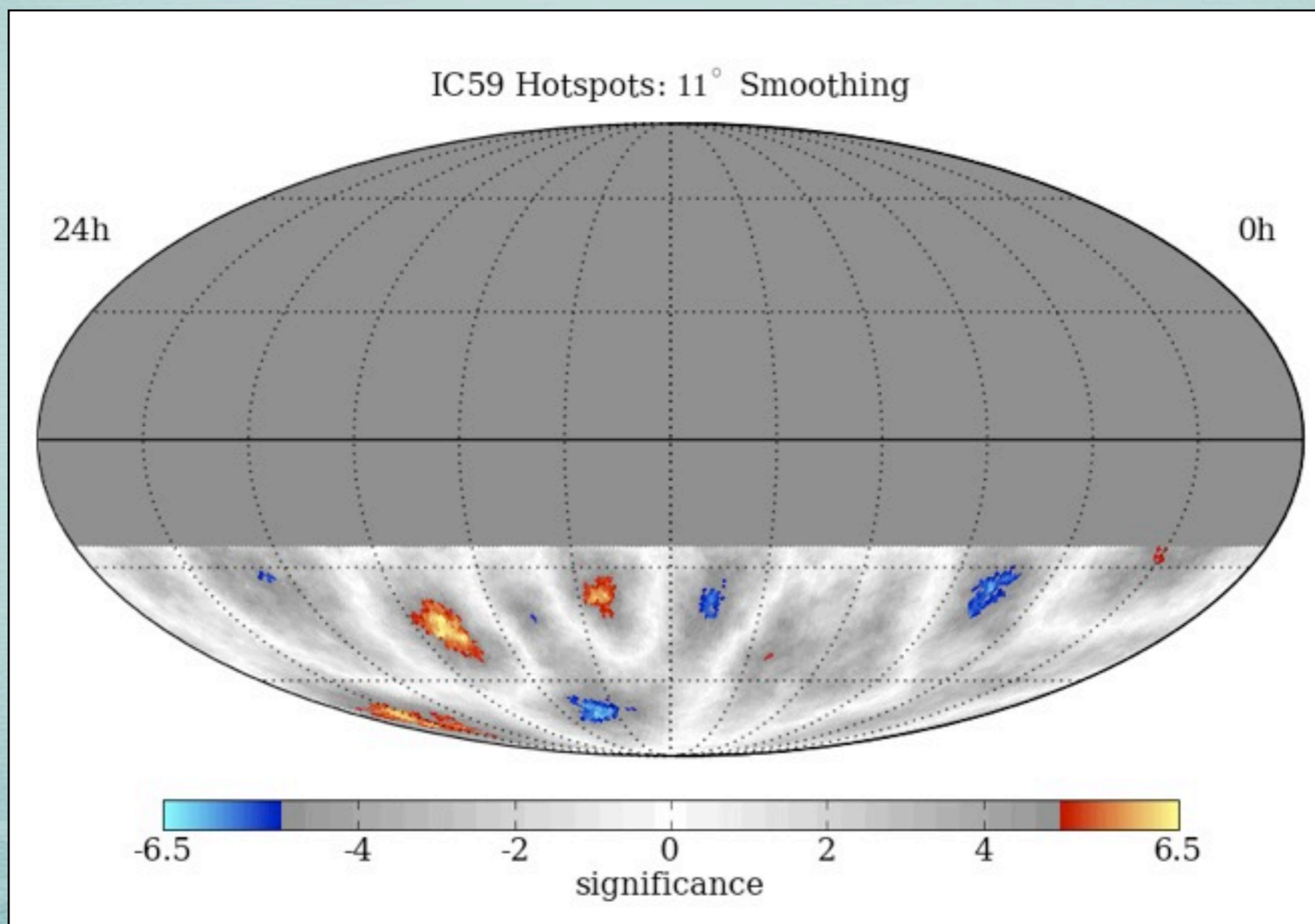
MAP SMOOTHING SCAN

Scan from 1 - 30° in smoothing
 Different regions have different optimal angular smoothing
 Significances are pre-trial



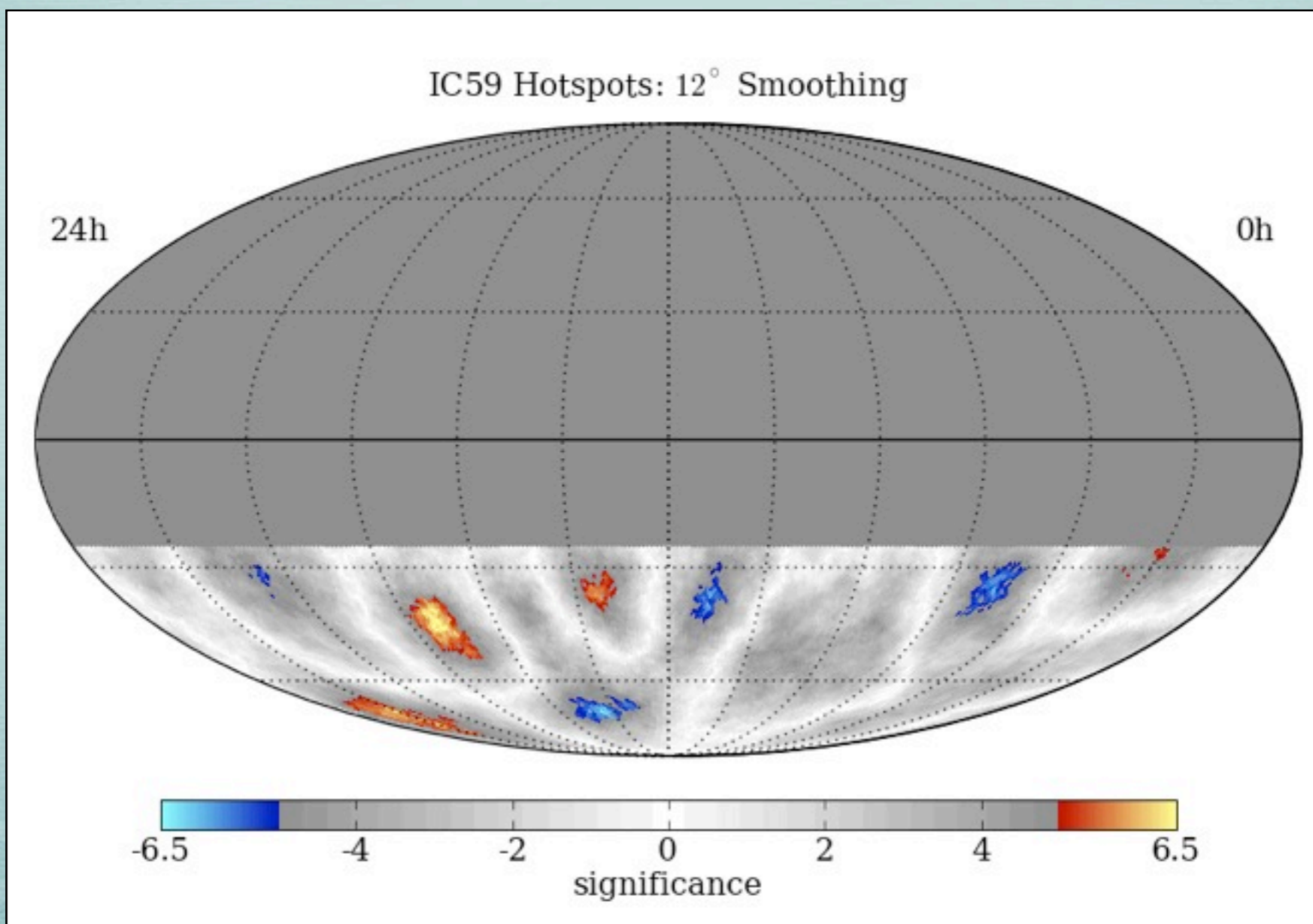
MAP SMOOTHING SCAN

Scan from 1 - 30° in smoothing
 Different regions have different optimal angular smoothing
 Significances are pre-trial



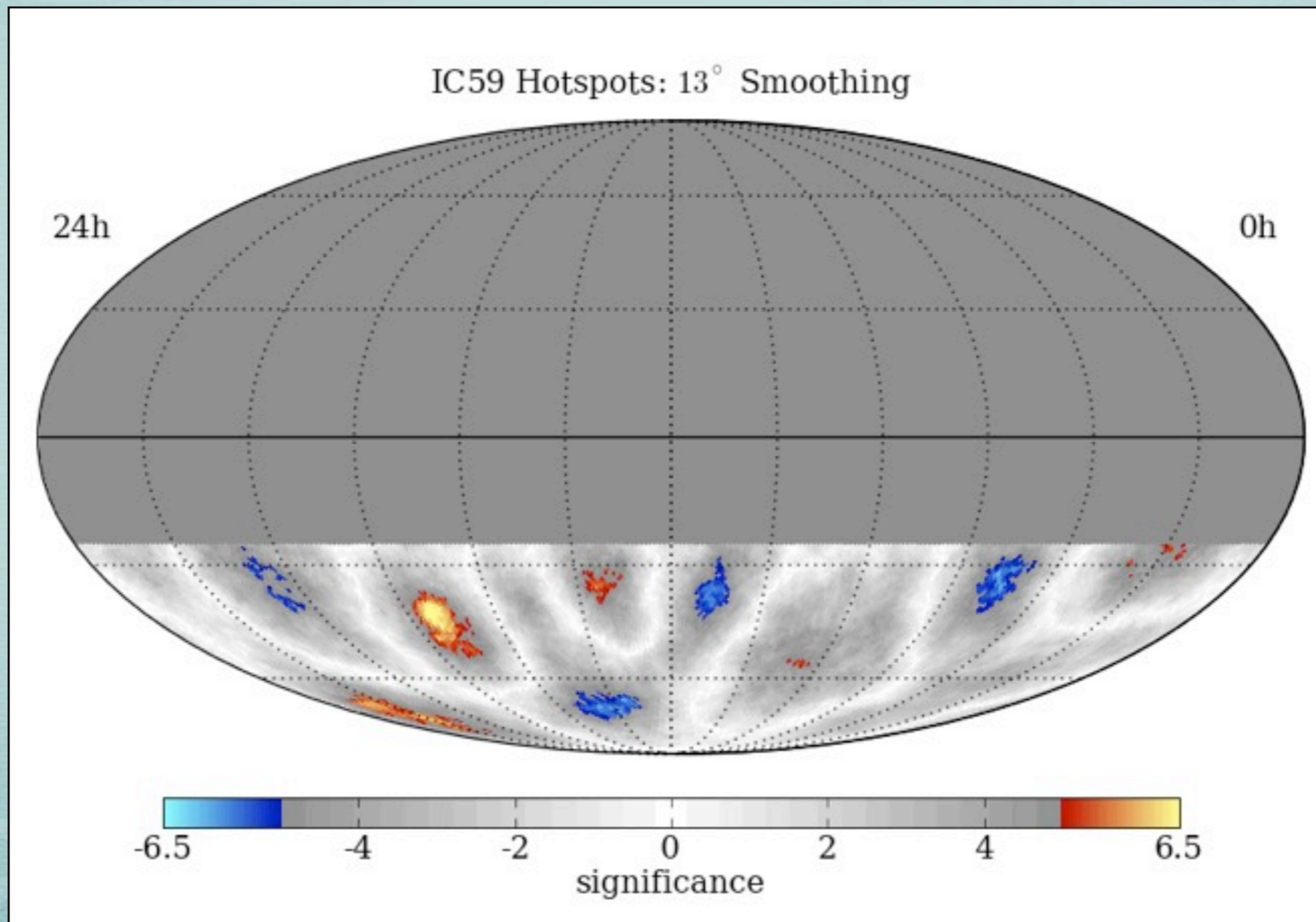
MAP SMOOTHING SCAN

Scan from 1 - 30° in smoothing
 Different regions have different optimal angular smoothing
 Significances are pre-trial



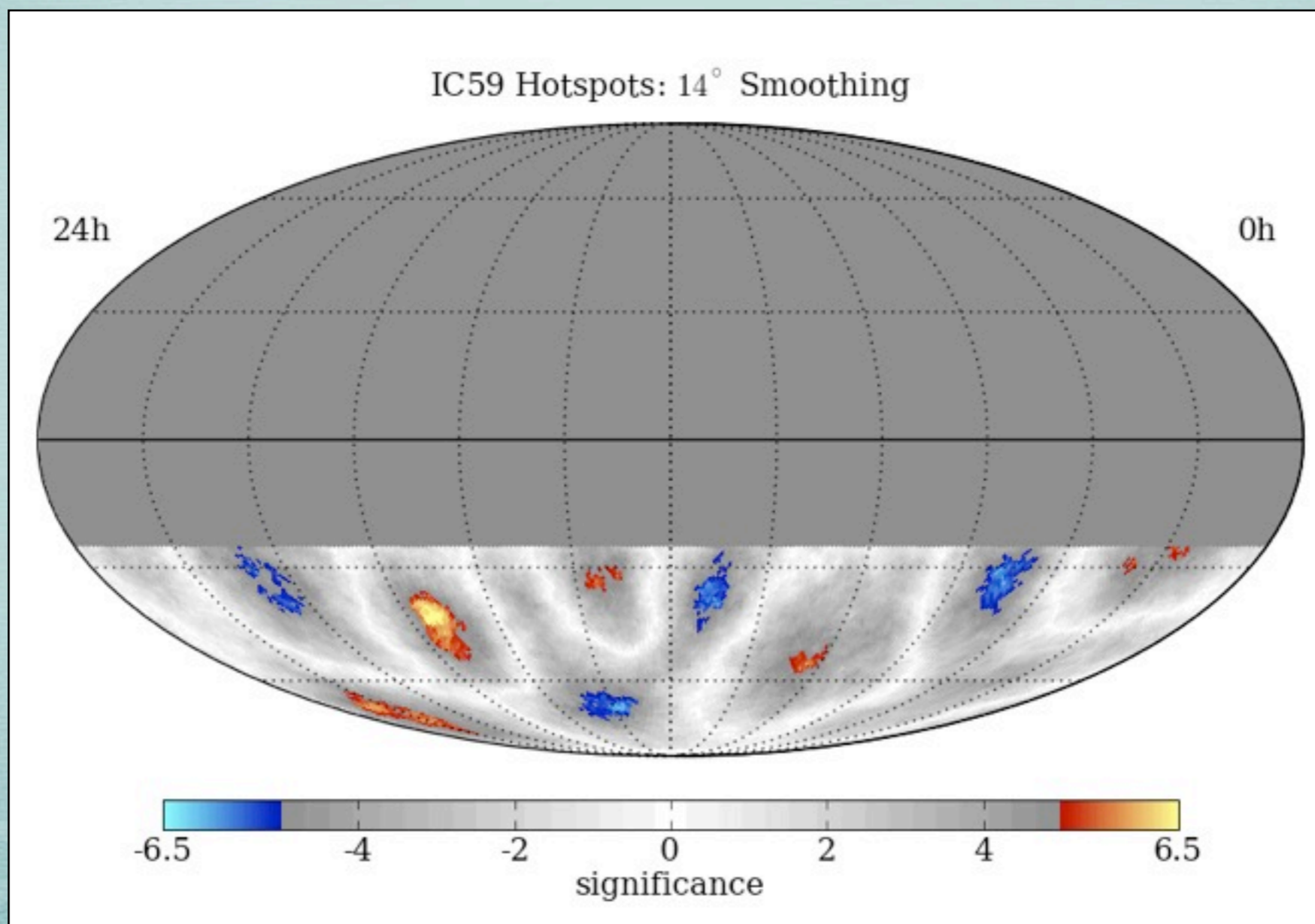
MAP SMOOTHING SCAN

Scan from 1 - 30° in smoothing
Different regions have different optimal angular smoothing
Significances are pre-trial



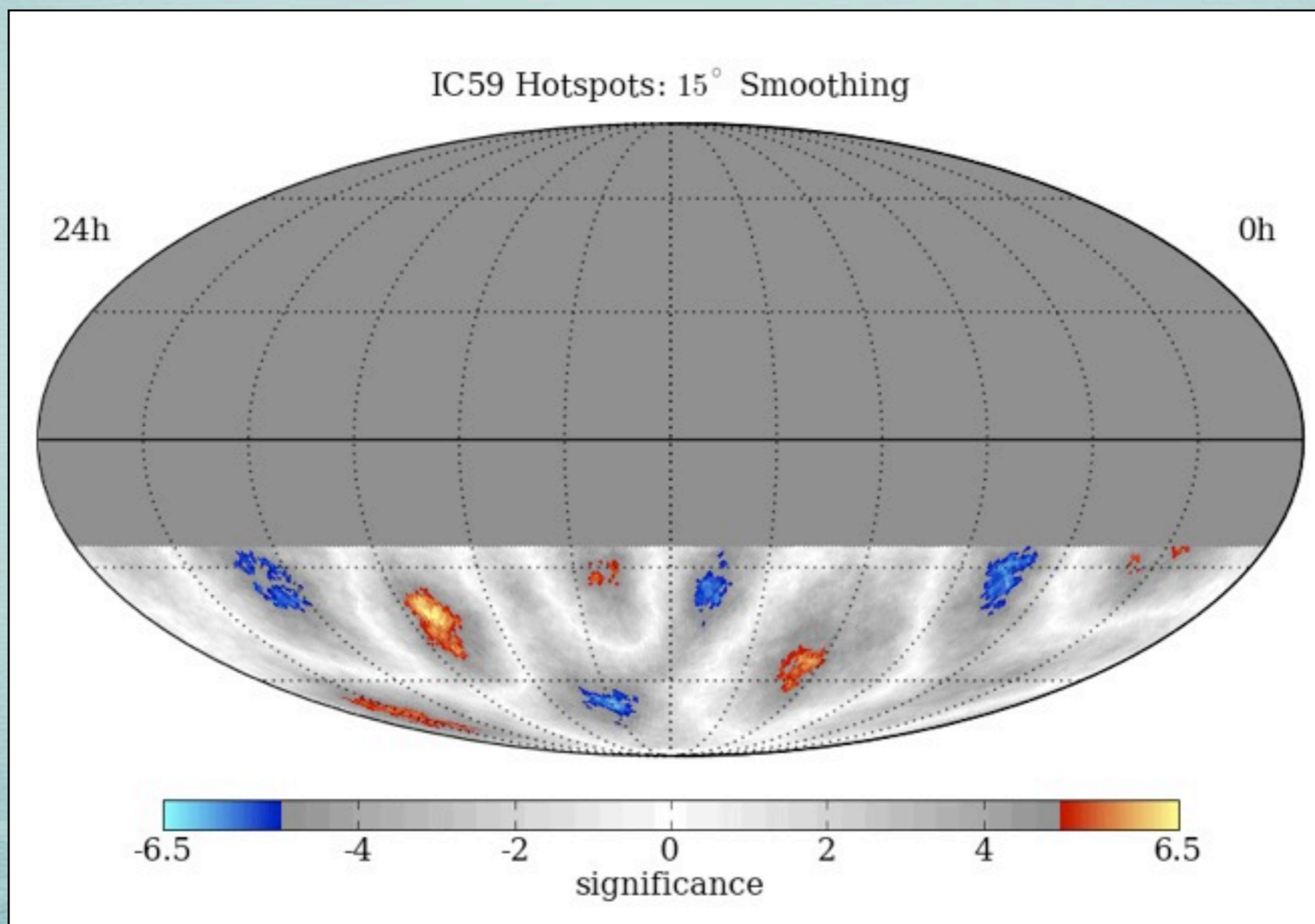
MAP SMOOTHING SCAN

Scan from 1 - 30° in smoothing
 Different regions have different optimal angular smoothing
 Significances are pre-trial



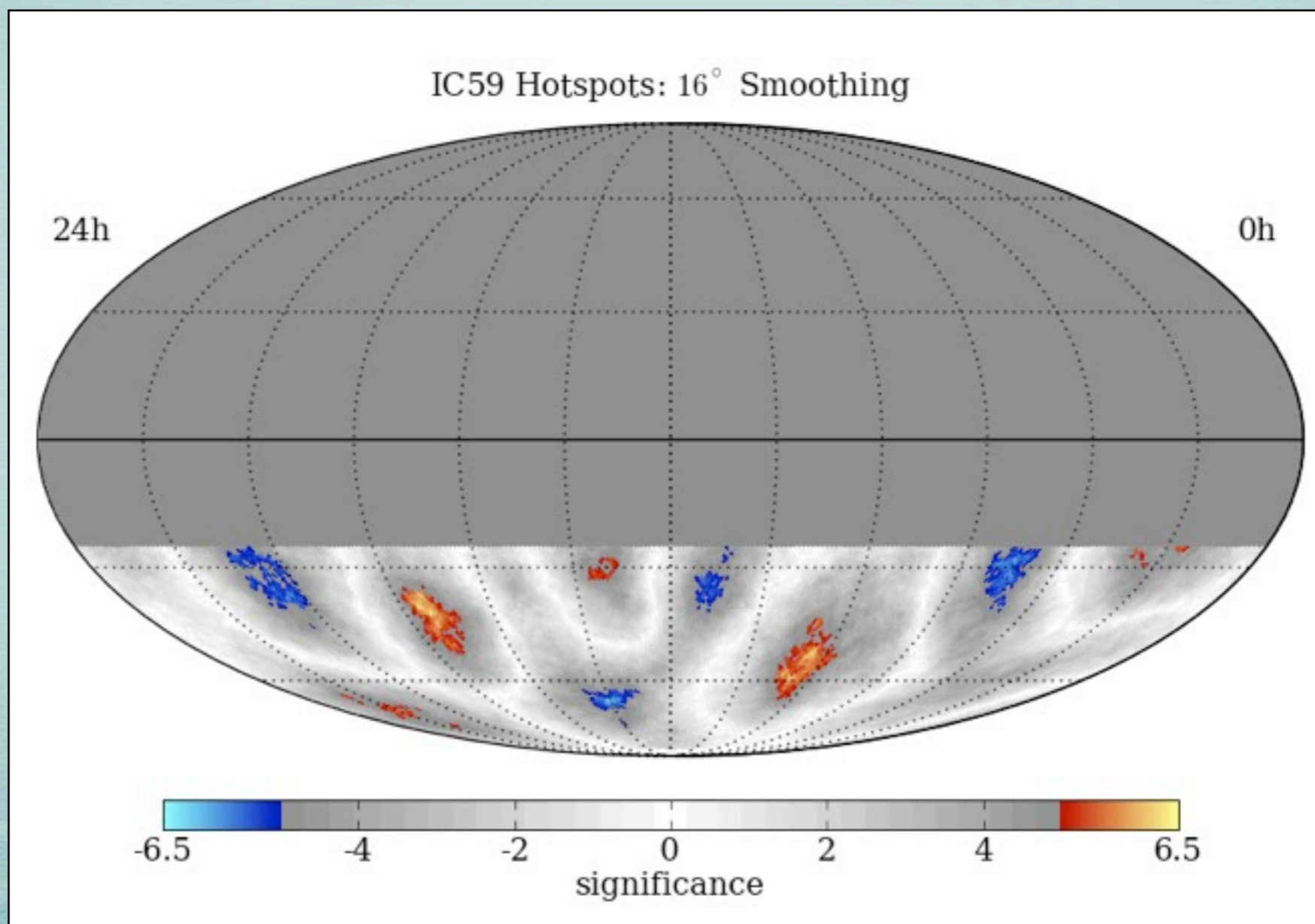
MAP SMOOTHING SCAN

Scan from 1 - 30° in smoothing
 Different regions have different optimal angular smoothing
 Significances are pre-trial



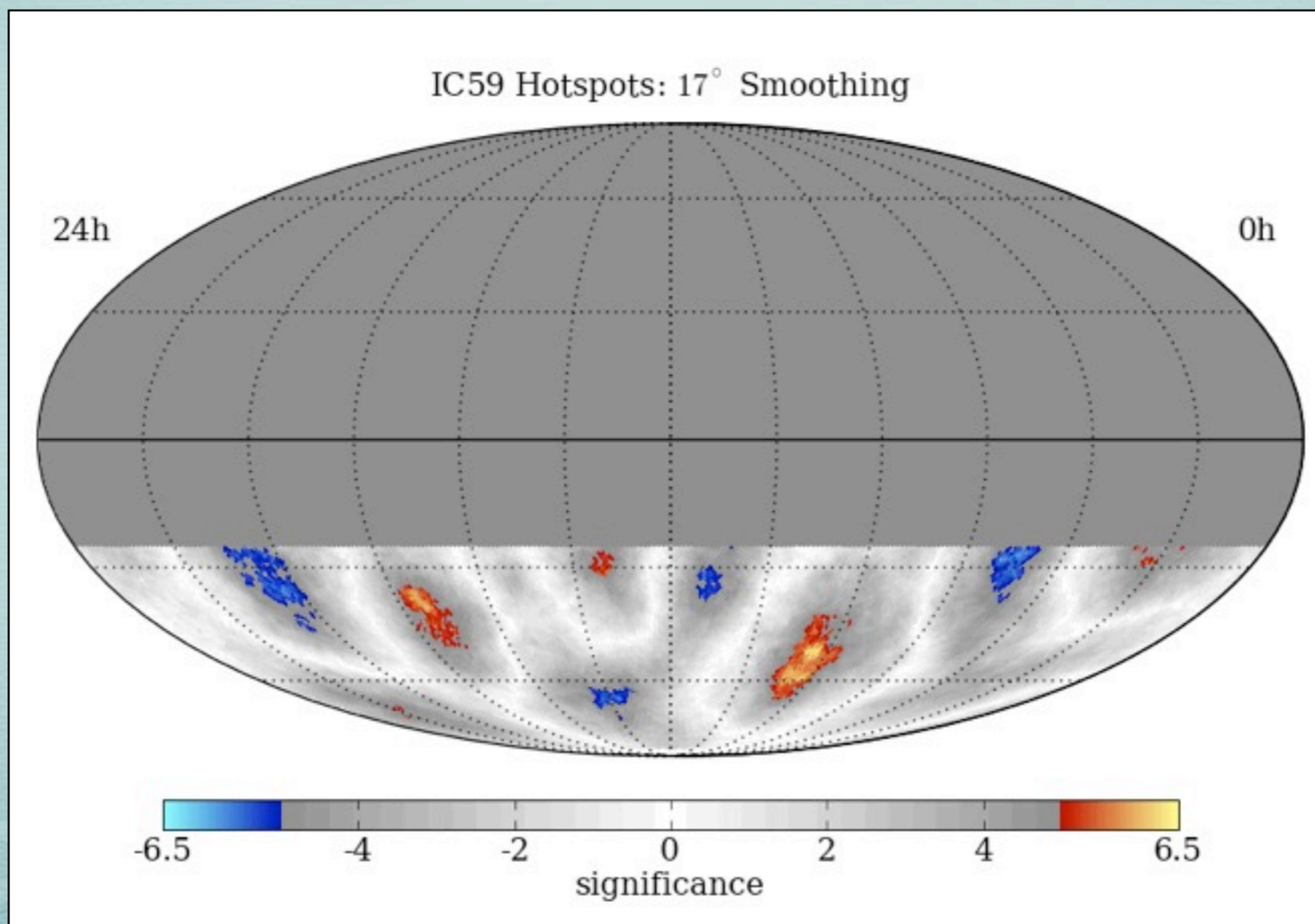
MAP SMOOTHING SCAN

Scan from 1 - 30° in smoothing
 Different regions have different optimal angular smoothing
 Significances are pre-trial



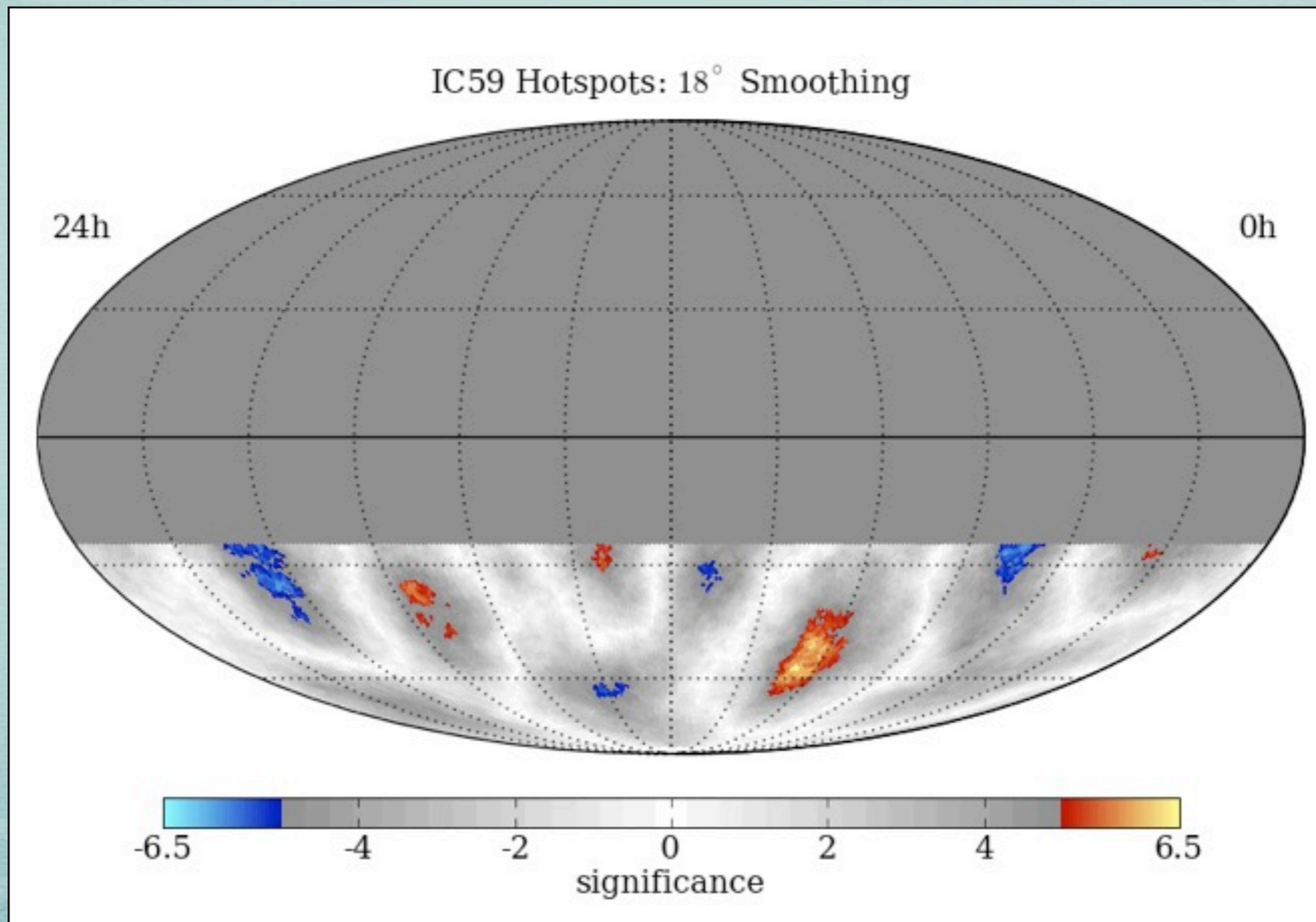
MAP SMOOTHING SCAN

Scan from 1 - 30° in smoothing
 Different regions have different optimal angular smoothing
 Significances are pre-trial



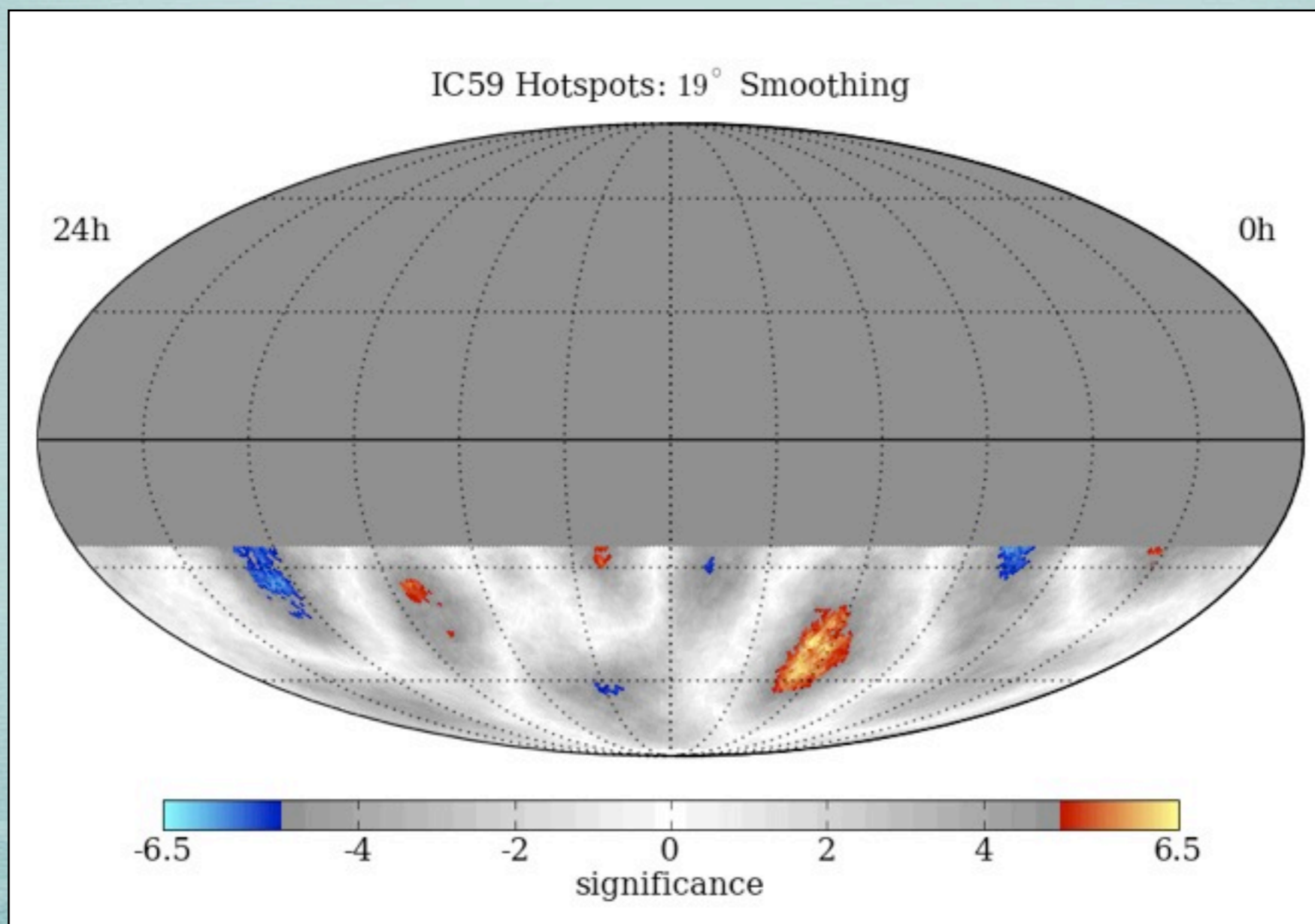
MAP SMOOTHING SCAN

Scan from 1 - 30° in smoothing
Different regions have different optimal angular smoothing
Significances are pre-trial



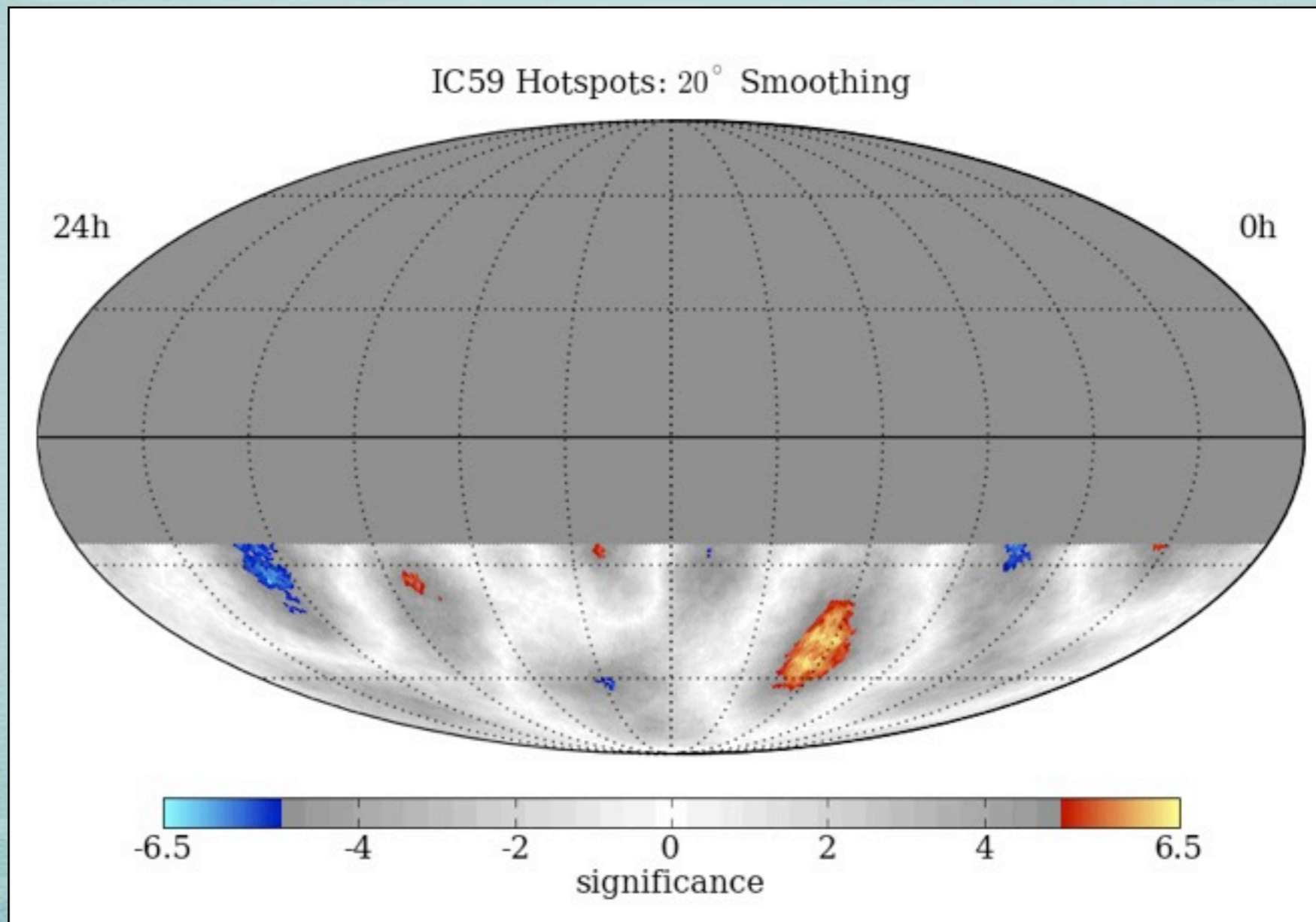
MAP SMOOTHING SCAN

Scan from 1 - 30° in smoothing
 Different regions have different optimal angular smoothing
 Significances are pre-trial



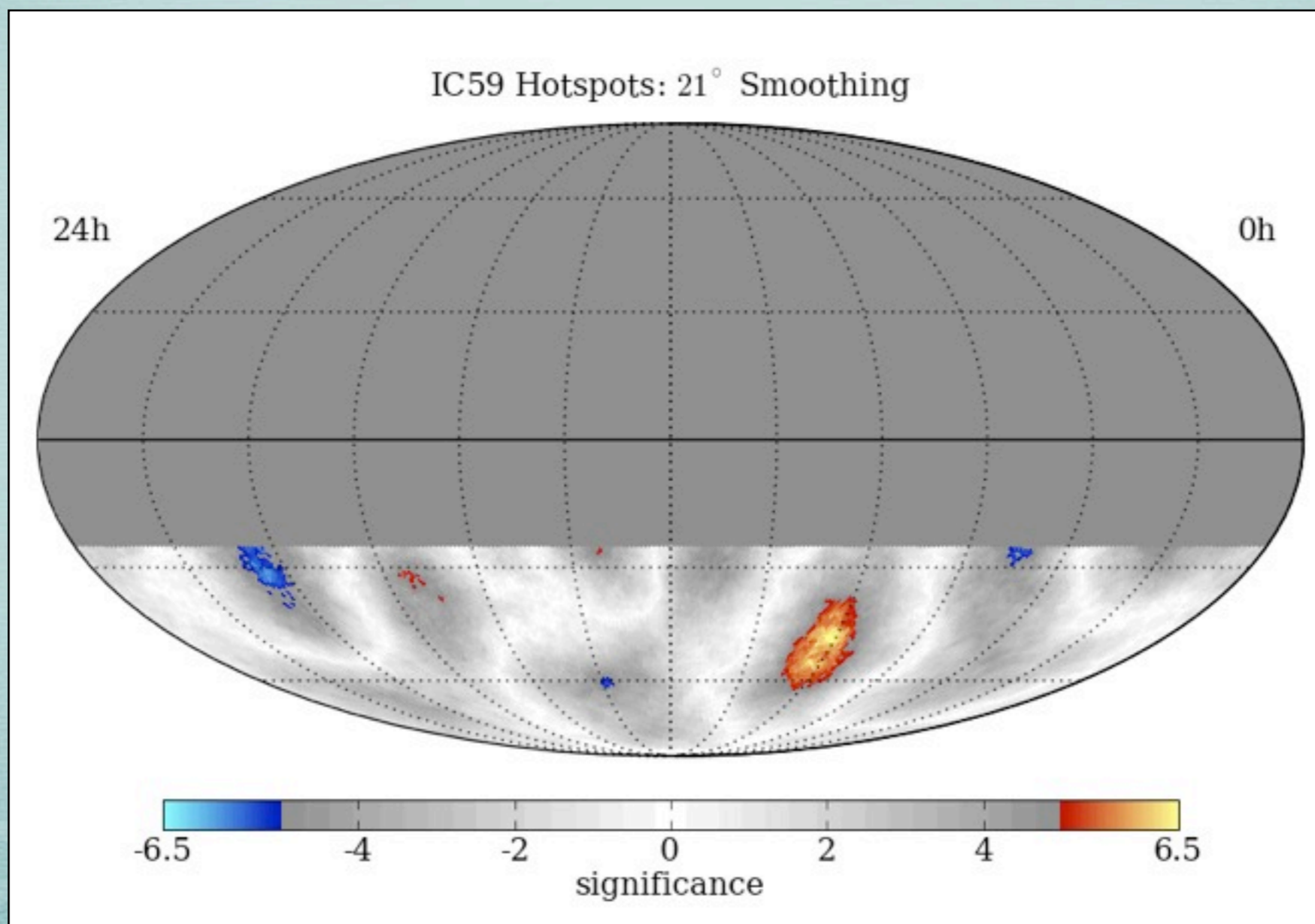
MAP SMOOTHING SCAN

Scan from 1 - 30° in smoothing
Different regions have different optimal angular smoothing
Significances are pre-trial



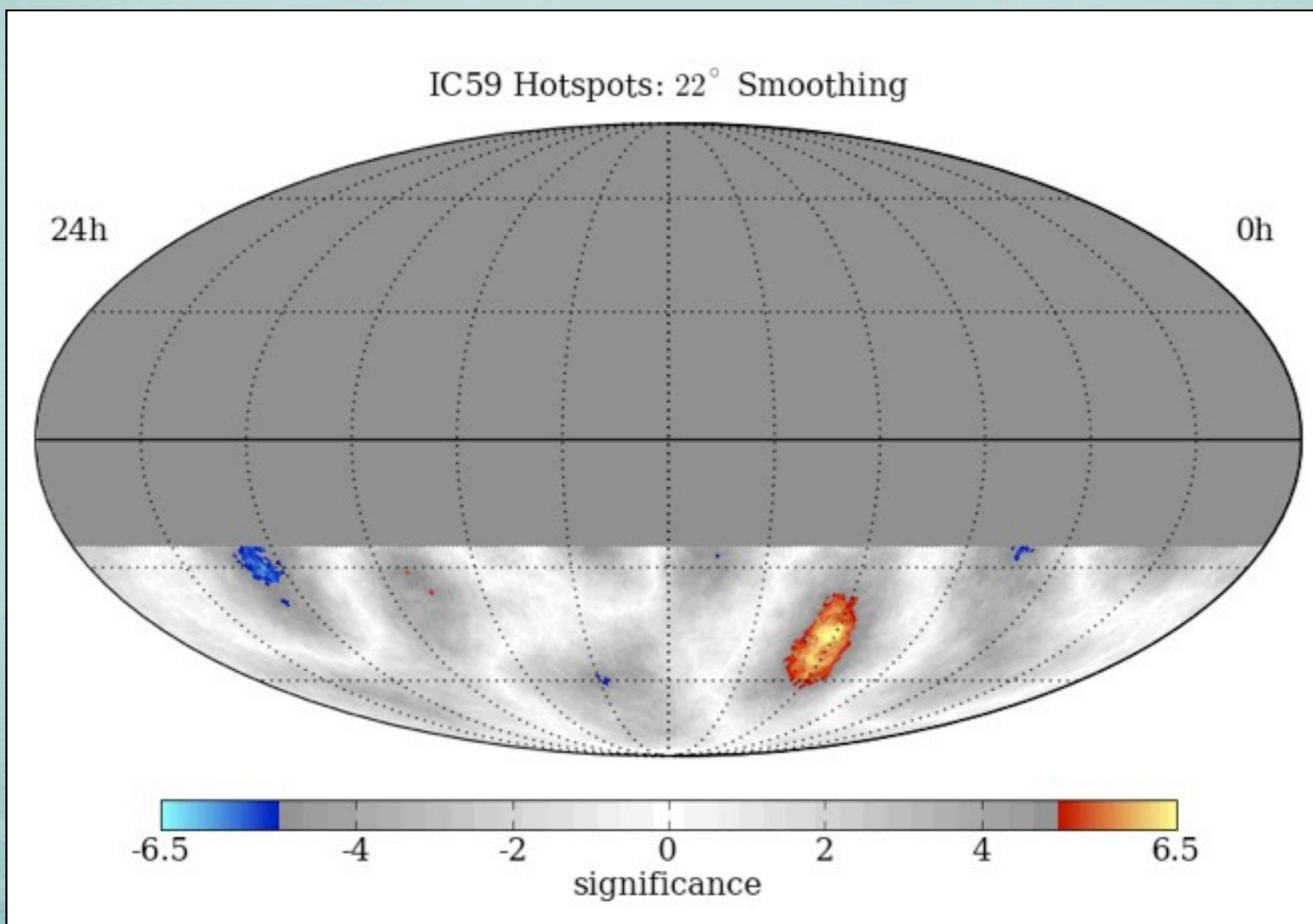
MAP SMOOTHING SCAN

Scan from 1 - 30° in smoothing
 Different regions have different optimal angular smoothing
 Significances are pre-trial



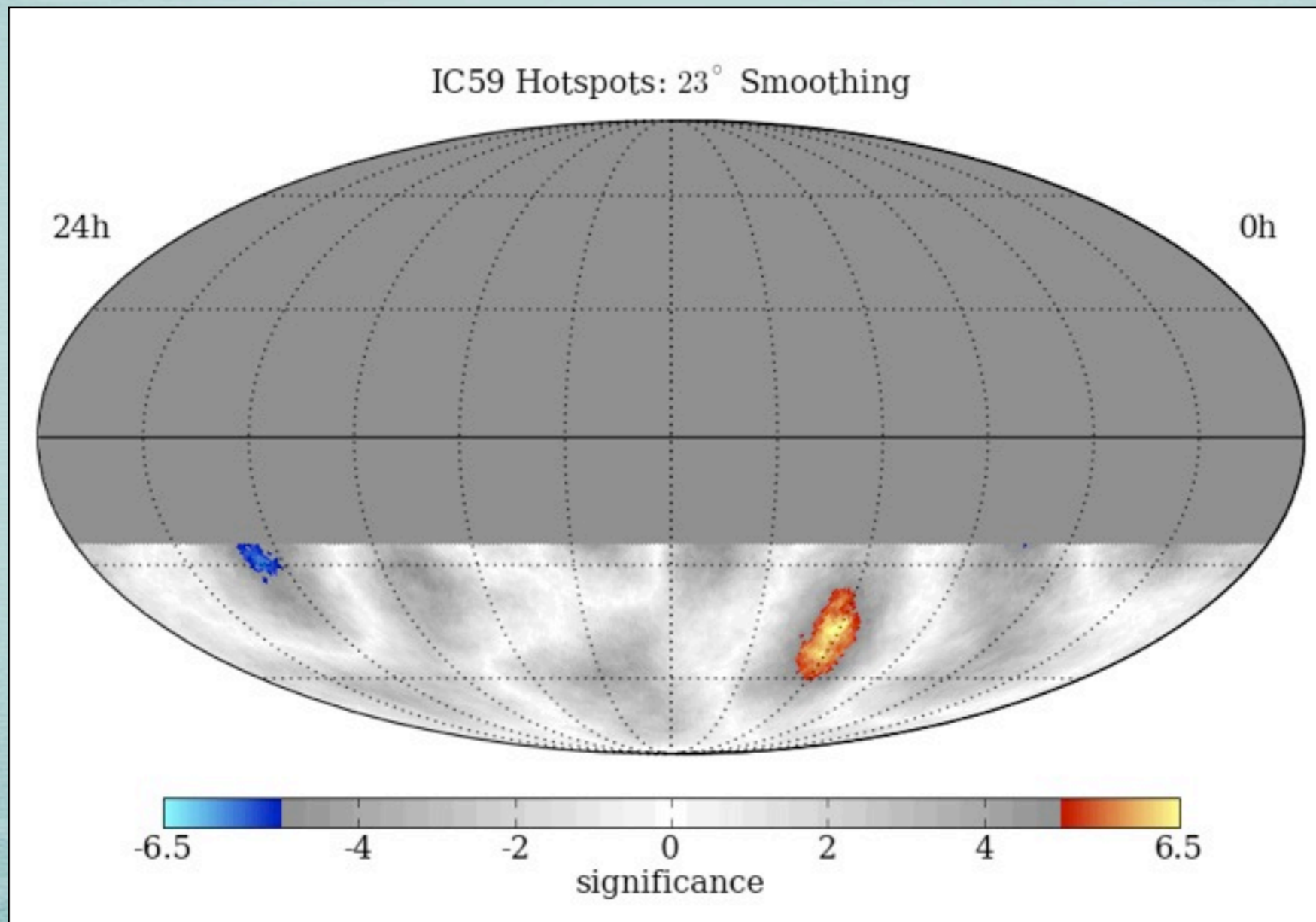
MAP SMOOTHING SCAN

Scan from 1 - 30° in smoothing
 Different regions have different optimal angular smoothing
 Significances are pre-trial



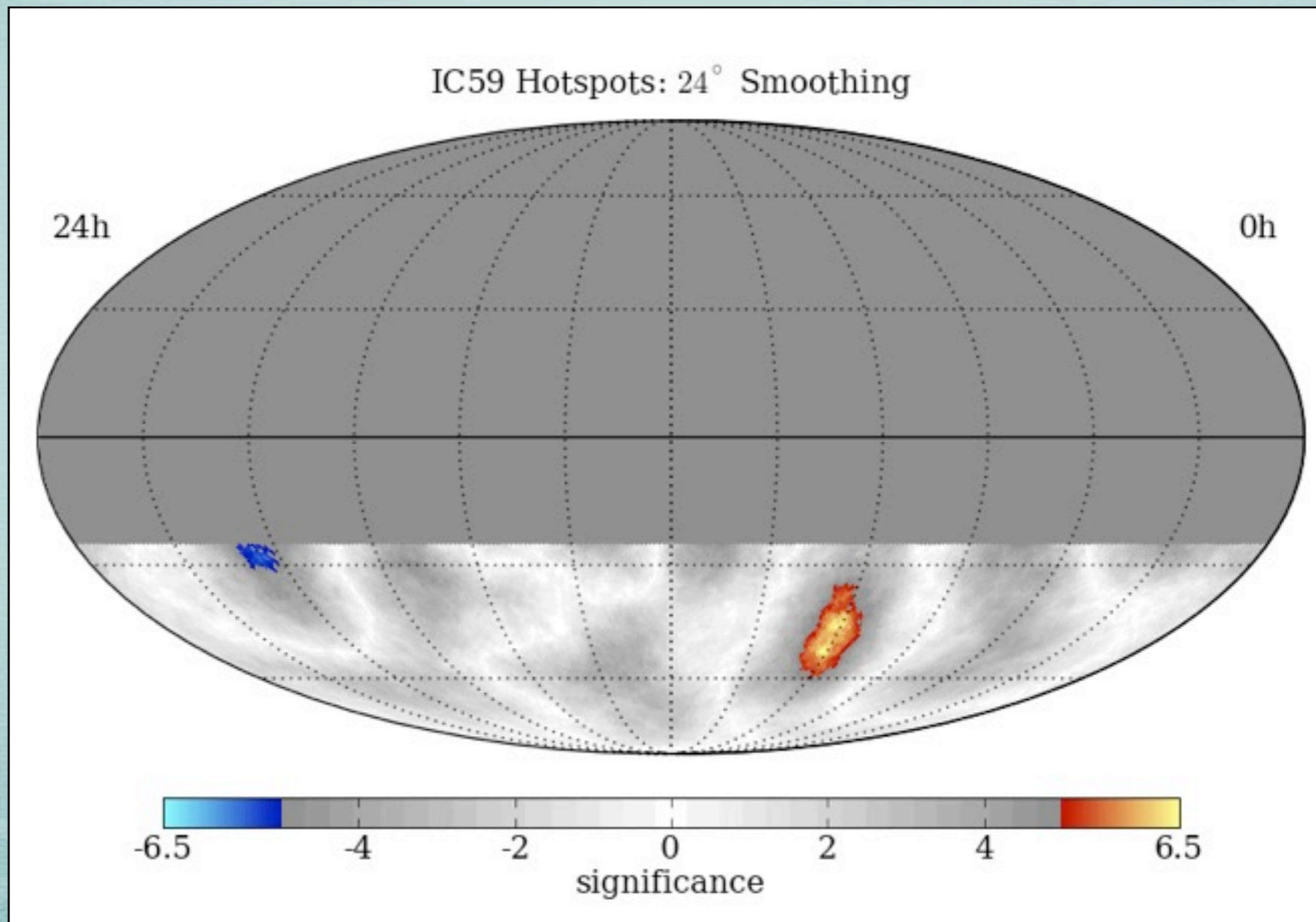
MAP SMOOTHING SCAN

Scan from 1 - 30° in smoothing
Different regions have different optimal angular smoothing
Significances are pre-trial



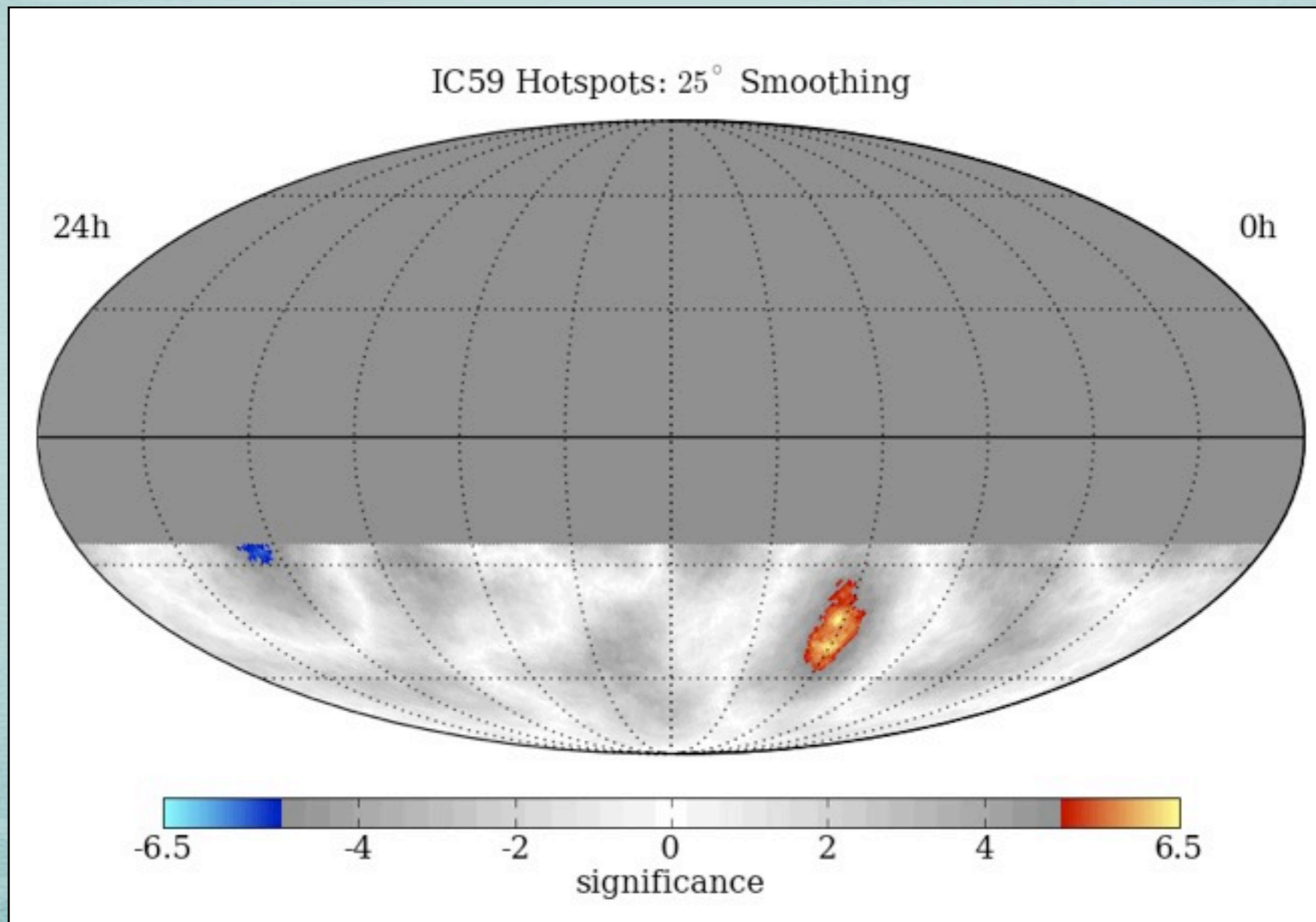
MAP SMOOTHING SCAN

Scan from 1 - 30° in smoothing
Different regions have different optimal angular smoothing
Significances are pre-trial



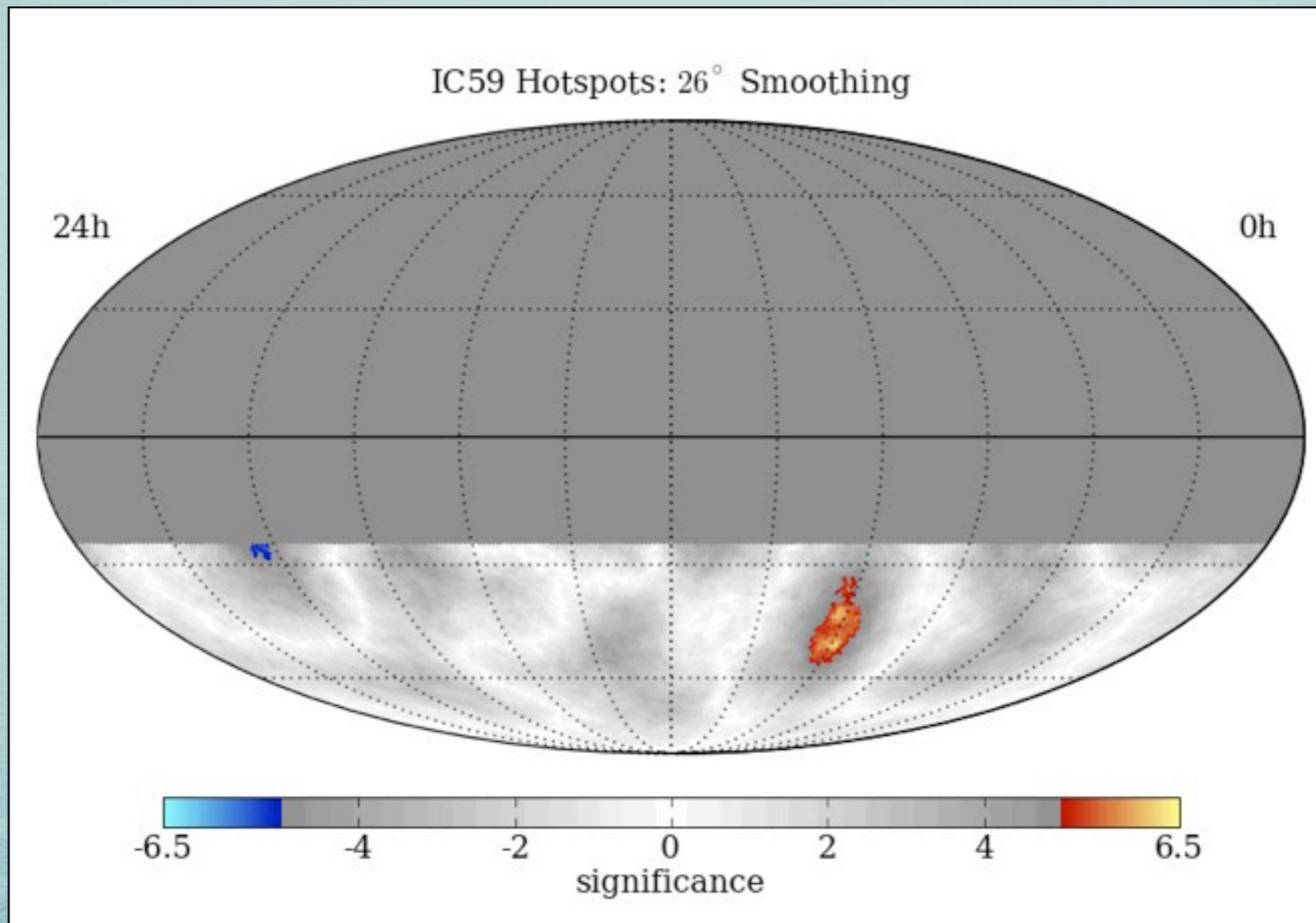
MAP SMOOTHING SCAN

Scan from 1 - 30° in smoothing
Different regions have different optimal angular smoothing
Significances are pre-trial



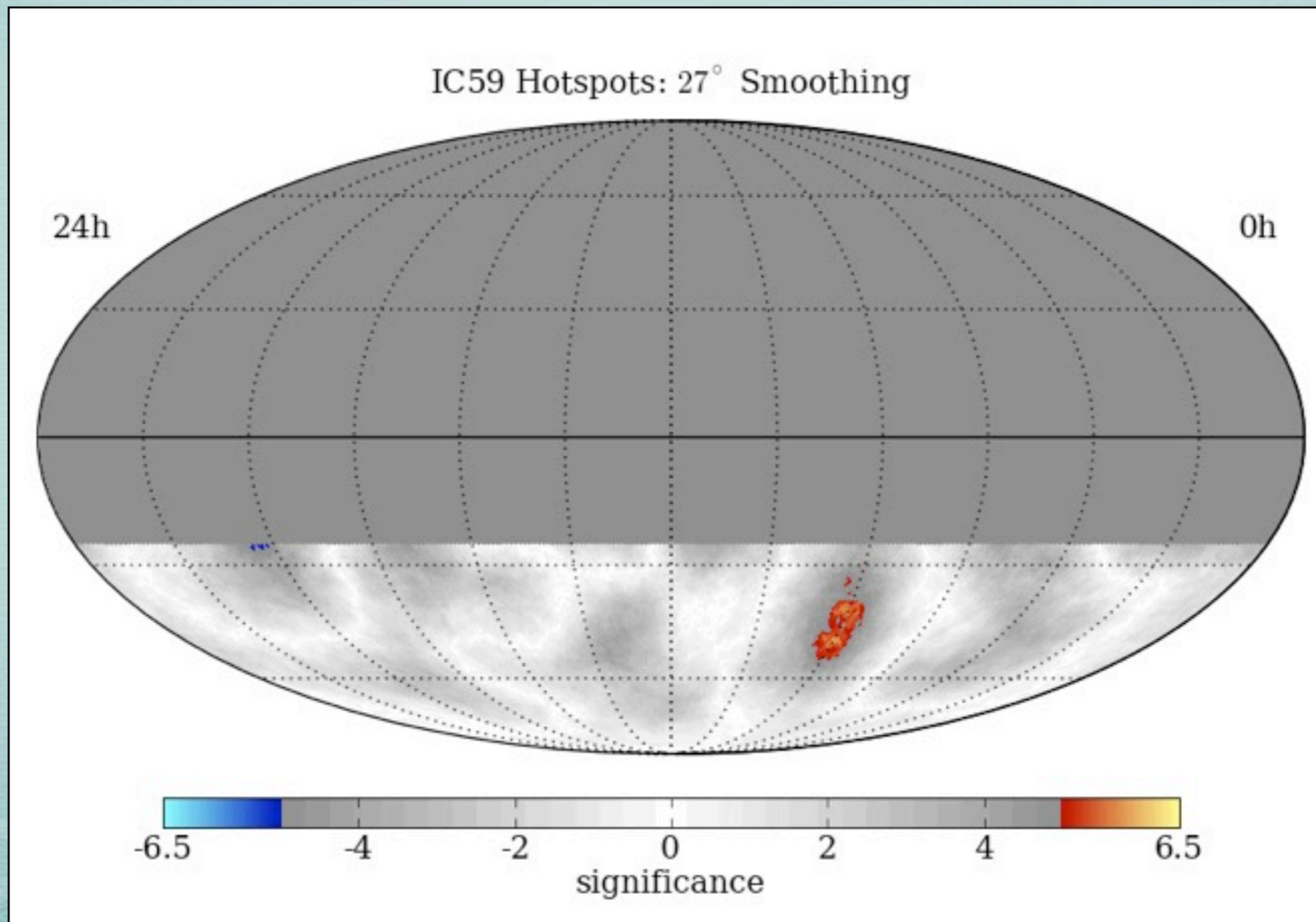
MAP SMOOTHING SCAN

Scan from 1 - 30° in smoothing
 Different regions have different optimal angular smoothing
 Significances are pre-trial



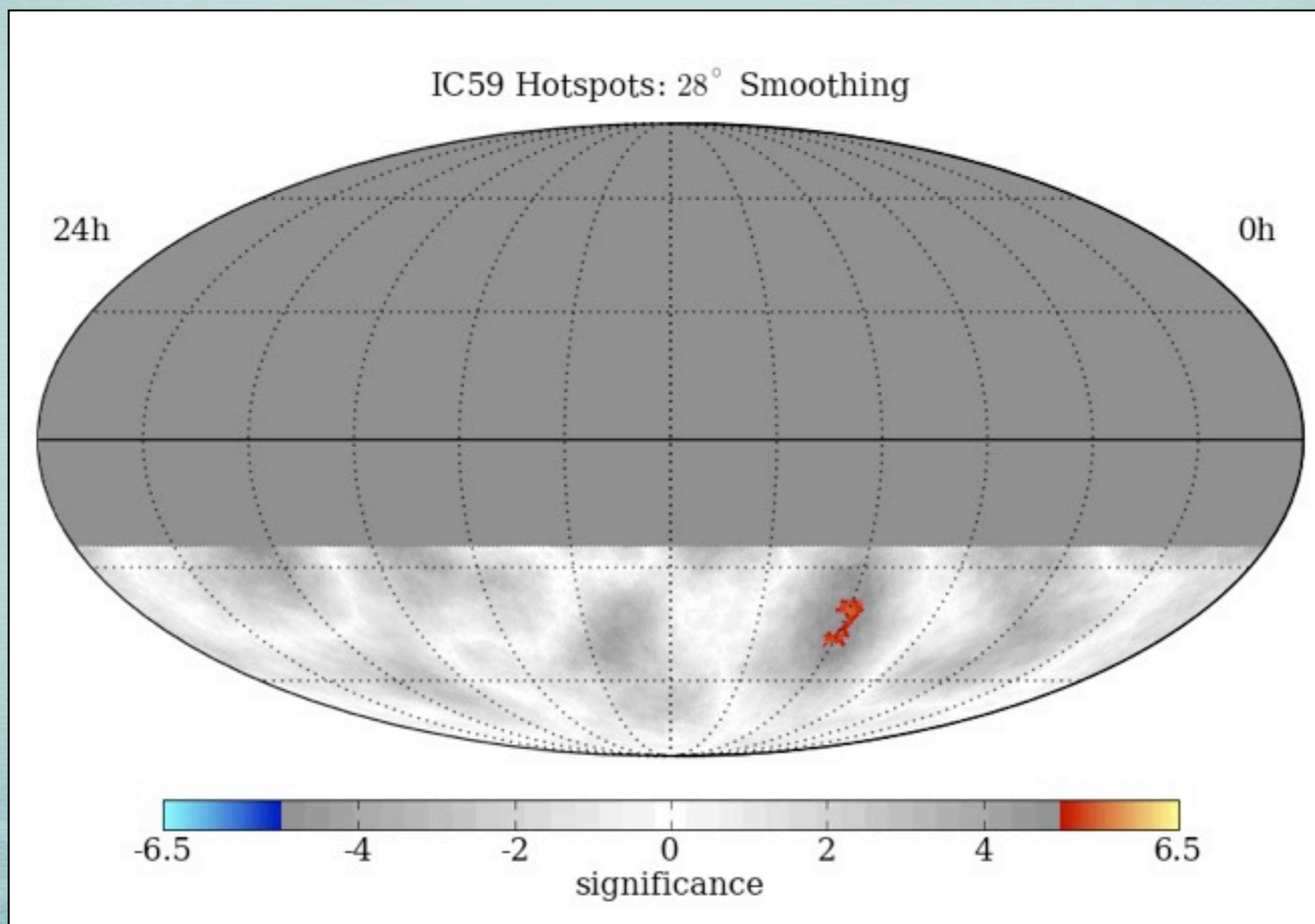
MAP SMOOTHING SCAN

Scan from 1 - 30° in smoothing
Different regions have different optimal angular smoothing
Significances are pre-trial



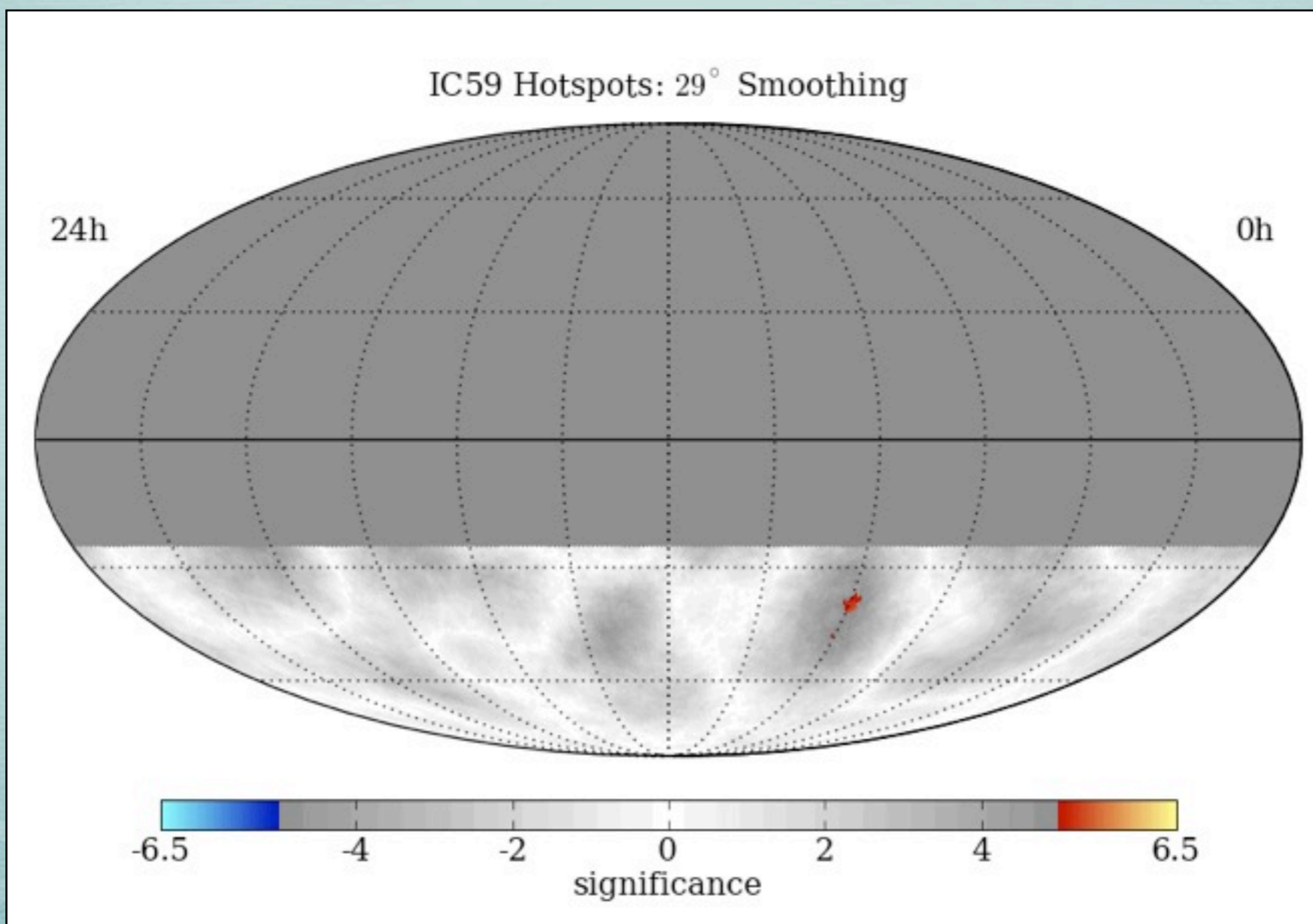
MAP SMOOTHING SCAN

Scan from 1 - 30° in smoothing
 Different regions have different optimal angular smoothing
 Significances are pre-trial



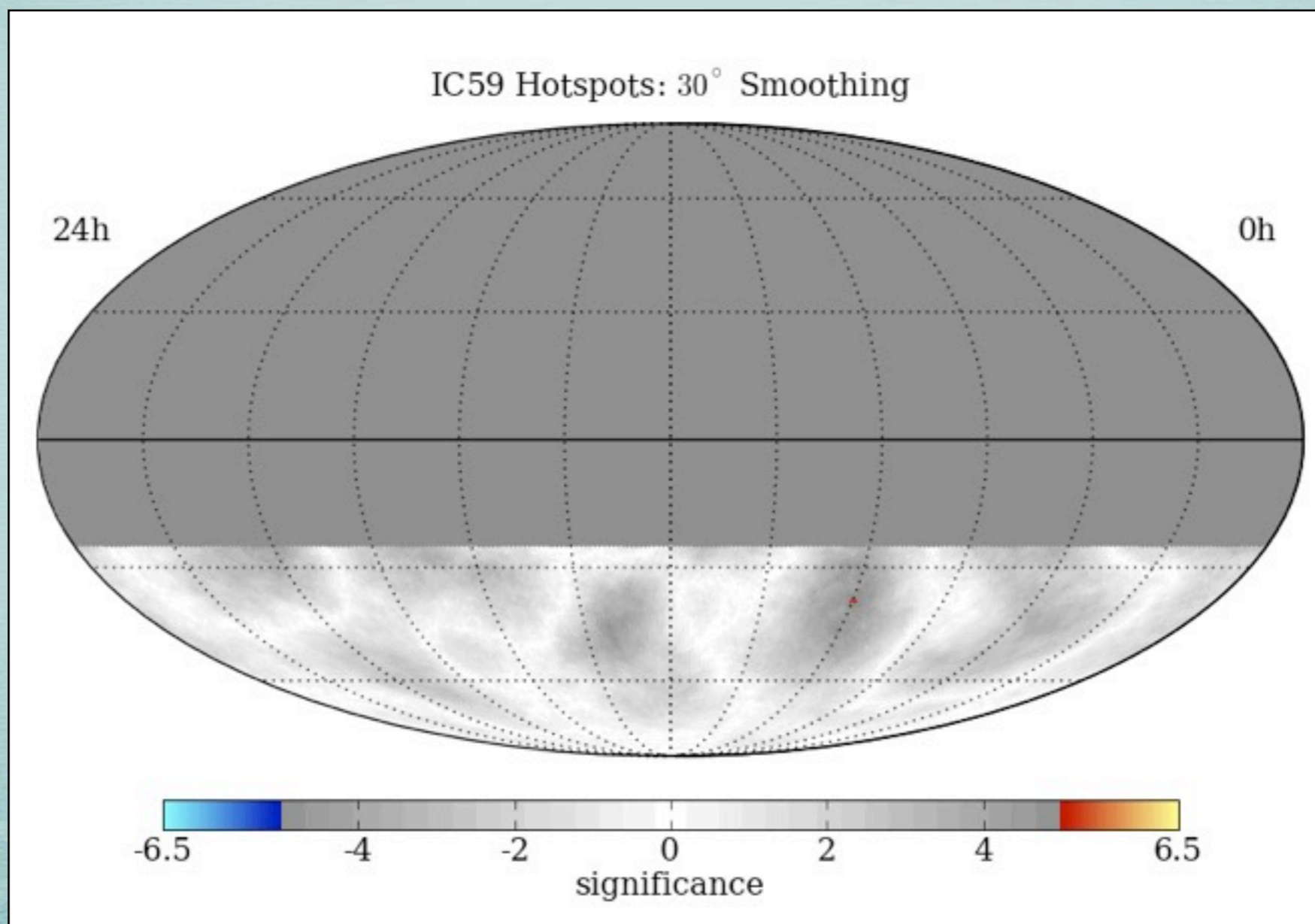
MAP SMOOTHING SCAN

Scan from 1 - 30° in smoothing
 Different regions have different optimal angular smoothing
 Significances are pre-trial



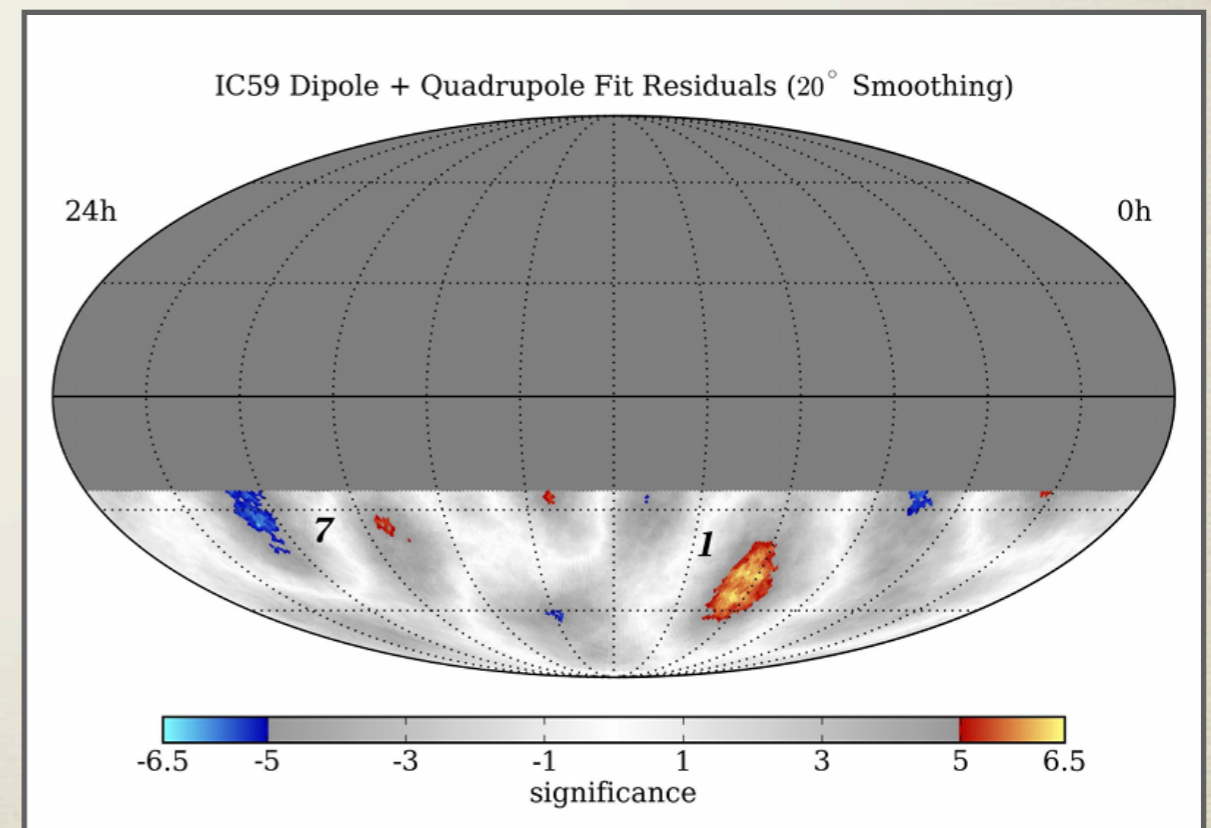
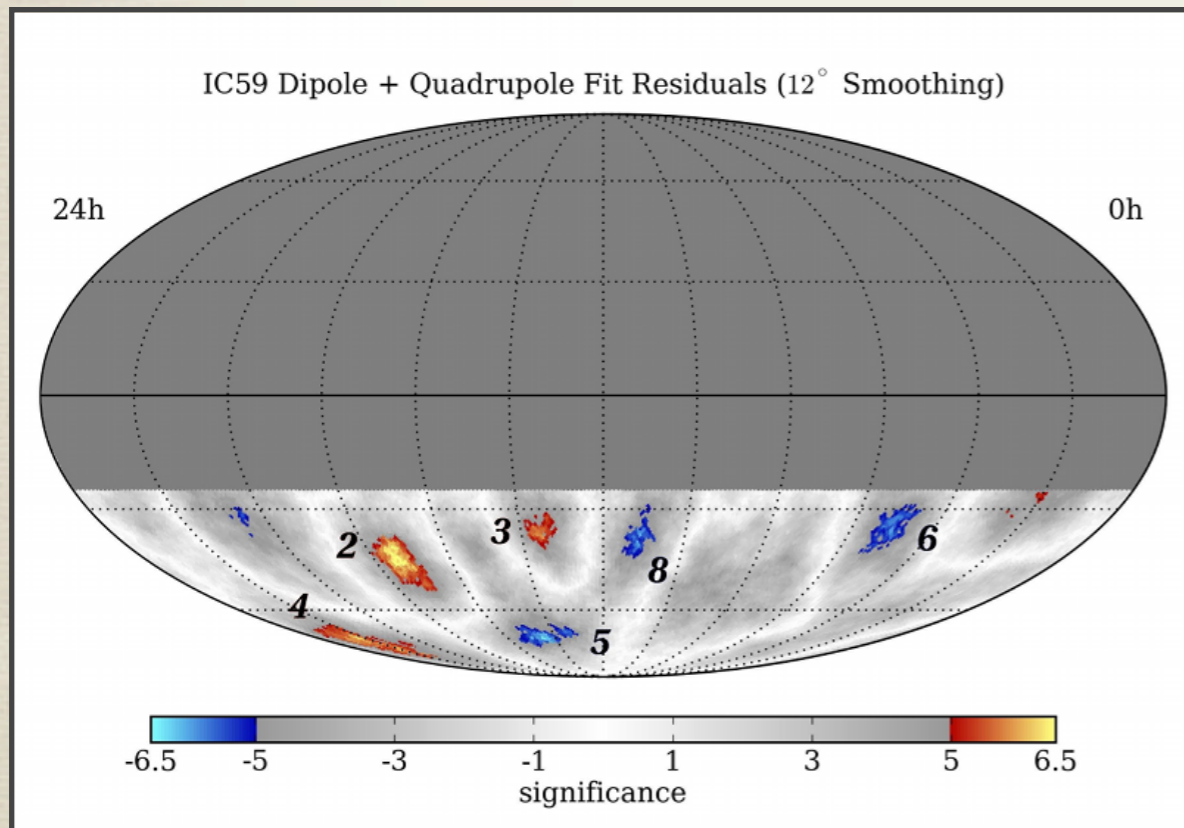
MAP SMOOTHING SCAN

Scan from 1 - 30° in smoothing
 Different regions have different optimal angular smoothing
 Significances are pre-trial



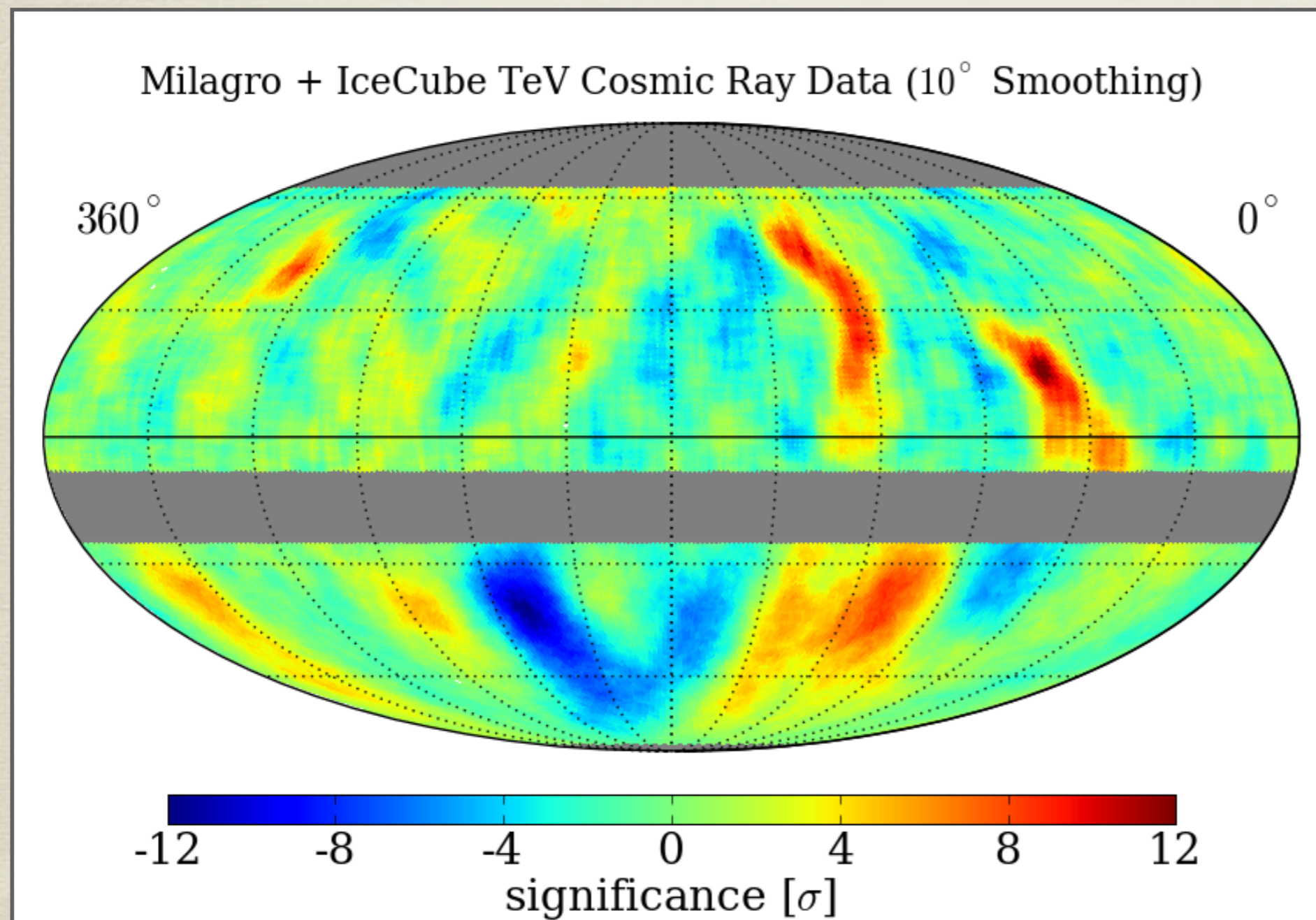
Identification of significant structures

region	right ascension	declination	optimal scale	peak significance	post-trials
1	$(122.4^{+4.1}_{-4.7})^\circ$	$(-47.4^{+7.5}_{-3.2})^\circ$	22°	7.0σ	5.3σ
2	$(263.0^{+3.7}_{-3.8})^\circ$	$(-44.1^{+5.3}_{-5.1})^\circ$	13°	6.7σ	4.9σ
3	$(201.6^{+6.0}_{-1.1})^\circ$	$(-37.0^{+2.2}_{-1.9})^\circ$	11°	6.3σ	4.4σ
4	$(332.4^{+9.5}_{-7.1})^\circ$	$(-70.0^{+4.2}_{-7.6})^\circ$	12°	6.2σ	4.2σ
5	$(217.7^{+10.2}_{-7.8})^\circ$	$(-70.0^{+3.6}_{-2.3})^\circ$	12°	-6.4σ	-4.5σ
6	$(77.6^{+3.9}_{-8.4})^\circ$	$(-31.9^{+3.2}_{-8.6})^\circ$	13°	-6.1σ	-4.1σ
7	$(308.2^{+4.8}_{-7.7})^\circ$	$(-34.5^{+9.6}_{-6.9})^\circ$	20°	-6.1σ	-4.1σ
8	$(166.5^{+4.5}_{-5.7})^\circ$	$(-37.2^{+5.0}_{-5.7})^\circ$	12°	-6.0σ	-4.0σ



Milagro + IceCube combined map

IceCube map contains all data from IC22, IC40 and IC59 data sets



Milagro map:

[Abdo, A. A., et al. 2008, Phys. Rev. Lett., 101, 221101]

- 2.2×10^{11} events
- direct integration (2 hr)
- 10° smoothing
- median energy **1 TeV**

IceCube map:

- 5.6×10^{10} events
- time scrambling (4 hr)
- 10° smoothing
- median energy **20 TeV**

Conclusions

- * **IceCube** detector was **completed in December 2010** and is now taking data in its final configuration (86 strings).
- * **Large scale anisotropy:**
 - ▶ Sidereal anisotropy at 20 TeV confirms previous observation.
 - ▶ First observation of sidereal anisotropy @ 400 TeV in southern hemisphere.
 - ▶ Indication of a persistence of anisotropy @ 400 TeV: evidence of a “dip”.
- * **Small and medium scale** structures:
 - ▶ Southern sky in TeV cosmic rays shows significant anisotropy across a wide range of angular scales (10-180 degrees).
- * **The origin of the anisotropy is still unknown.**